

International
Progress Report

IPR-01-15

Äspö Hard Rock Laboratory

Modelling of an in-situ failure test in the research tunnel at Olkiluoto

Jorma Autio

Erik Johansson

Petteri Somervuori

Saanio & Reikkola Consulting Engineers

December 1999

Svensk Kärnbränslehantering AB

Swedish Nuclear Fuel

and Waste Management Co

Box 5864

SE-102 40 Stockholm Sweden

Tel +46 8 459 84 00

Fax +46 8 661 57 19



Äspö Hard Rock
Laboratory

Report no.	No.
IPR-01-15	F19K
Author	Date
Autio, Johansson, Somervuori	99-12-19
Checked by	Date
Christer Svemar	
Approved	Date
Christer Svemar	02-01-28

Äspö Hard Rock Laboratory

Modelling of an in-situ failure test in the research tunnel at Olkiluoto

Jorma Autio
Erik Johansson
Petteri Somervuori
Saanio & Reikkola Consulting Engineers

December 1999

Keywords: Failure test, modelling of deformation, rock failure, numerical modelling

This report concerns a study which was conducted for SKB. The conclusions and viewpoints presented in the report are those of the author(s) and do not necessarily coincide with those of the client.

SAMMANFATTNING

Mikrosprickbildningen i de fullskaliga deponeringshålens väggar i forskningstunneln i Olkiluoto, Finland, har analyserats med hjälp av kvantitativ mikroskopi.

Undersökningens huvudsyften var utvärdering av inträngningsdjupet hos en epoxybaserad tätningssubstans som anbringats på bergväggarna samt grafisk sprickkaraktisering av den störda zonen med avseende på mineralogi och textur. Följande parametrar bestämdes från den yttre till den inre (minst påverkade) delen av störda zonen: specifika sprickarean, sprickorienteringen, sprickvidden och procentuella sprickvolymen; de olika förfarandena som användes för utvärdering förklaras i rapporten.

Olika mikroskopimetoder användes: polarisationsmikroskopi, fluorescensmikroskopi med reflekterat ljus, konfokal laserscanningsmikroskopi och scanningmikroskopi (med elektrondetektorer av sekundär och backscattertyp). Bildinformationen har kvantifierats med hjälp av stereoteknik och digital bildanalys. Alla sprickstudier har gjorts på s.k. "vertikala sektioner" vinkelrätt mot borrhållsväggarna. För undvikande av artefakter har motsvarande snitt för mikroskopi framställts med icke konventionell teknik.

De erhållna resultaten gav det överraskande beskedet att djupet hos den mest störda zonen begränsas till 1.5 till 2 mm medan viss, men mindre, störning konstaterades till 3-4 mm djup. Epoxysubstansens inträngningsdjup var 2-3 mm. De nybildade sprickorna med störst vidd (>5.5 mikrometer) befanns i huvudsak vara orienterade parallellt med hålväggen och representera mindre än 10 % av hela sprickmängden. Den specifika sprickarean, S_v , var mellan 0.06 m^{-1} i störzonen till 2-3 mm djup och 0.02 m^{-1} på djupet 5-6 mm. S_v minskade snabbt med ytterligare ökande avstånd från hålväggen och varierade här mellan 0.005 och 0.01 m^{-1} .

ABSTRACT

An in-situ failure test has been planned to be carried out in the Research Tunnel at Olkiluoto. The test involves creating an artificial stress field large enough to cause a failure. The general objective of the work is to assess the applicability of numerical modeling codes for studying rock failure and associated crack propagation. As the first step in the design phase the failure test was modeled in 3D by using Flac^{3D} code using preliminary input information. The main objective of the modeling was to evaluate the feasibility of the test. According to the modeling it is certain that an artificial stress large enough to cause failure can be created and the stress distribution on the stem section of the hole is quite uniform. A failure appears regardless of the material model and failure criteria used at a swelling pressure of well under 60 MPa. The failure takes place as tensile failure on the upper and lower surface of the test hole and as compressive/shear failure on the sides of the hole.

TABLE OF CONTENTS

SAMMANFATTNING	i
ABSTRACT	ii
TABLE OF CONTENTS	iii
LIST OF FIGURES	iv
LIST OF TABLES	iv
1 GENERAL	1
2 MODELLING - INPUT DATA	3
2.1 Geology and mineralogy	3
2.2 Strength and deformation properties	4
2.3 Test geometry	7
2.4 Constraining stresses	8
2.4.1 In situ stresses	8
2.4.2 Pressure exerted by the expanding agent	11
3 CONSTITUTIVE MATERIAL MODELS	13
4 FAILURE CRITERIA	15
5 RESULTS OF FLAC MODELLING	17
5.1 Preliminary FLAC ^{2D} modelling	17
5.2 Displacements of the centre hole before external loading	18
5.3 Elastic material model	19
5.4 Safety factors for the elastic material model and the Mohr-Coulomb strength criterion	23
5.5 Safety factors for the elastic material model employing Mogi's strength criterion	24
5.6 Safety factors for Mohr-Coulomb plastic material model	24
5.7 Safety factors for the strain-softening material model	25
6 CONCLUSIONS AND DISCUSSION	27
REFERENCES	35
APPENDICES	37

LIST OF FIGURES

- Figure 2.1-1. The Research Tunnel at Olkiluoto showing the full-scale experimental deposition holes.
- Figure 2.2-1. Strength properties of gneissic and homogeneous tonalite in the Research Tunnel (Johansson & Autio 1993).
- Figure 2.2-2. Strength properties of gneissic tonalite in the Research Tunnel (Johansson & Autio 1995). The values shown here include the Crack Damage and Crack Initiation stress determined from the stress-strain curve.
- Figure 2.2-3. Compressive strength of the gneissic tonalite shown in Figure 2.2-2 plotted as a function of tensile strength.
- Figure 2.2-4. The position of gneissic tonalite in Deere's classification system.
- Figure 2.3-1. Geometry used in modelling showing also the estimated horizontal tangential stress component acting perpendicular to the surface of test hole.
- Figure 2.4-1. Horizontal section of the Research Tunnel showing the direction of primary in-situ stresses and preliminary lay-out of the test.
- Figure 2.4-2. Magnitude of the maximum principal stresses around a full-scale deposition hole (Table 2.4-1) with respect to depth from the floor of the Research Tunnel.
- Figure 2.4-3. Contour plot of the maximum principal stresses around full-scale deposition holes. The angle between the principal in-situ stress and the tunnel axis is 90° .
- Figure 2.4-4. Expansion pressure of Betonamit with respect to reaction time for different hole diameters (according to Betonamit International AG, Liechtenstein).
- Figure 3-1. The three different constitutive material models: 1) Elastic, 2) Mohr-Coulomb and 3) Strain-softening.
- Figure 4-1. Mohr-Coulomb criterion types 1, 2 and 3 and their respective lines.
- Figure 4-2. Mogi's criterion lines estimated from a uniaxial compression test.
- Figure 5.1-1. The result of the 2D modelling showing the failure areas at a swelling pressure of 60 MPa.
- Figure 5.2-1. Diameter of a hole on the surface of the full scale hole as a function of the maximum in-situ stress. The σ_v component has been varied to assess the sensitivity of the result.
- Figure 5.3-1. Diagram showing slot length (L) and slot width (W).
- Figure 5.3-2. Contour plots of the maximum principal stress σ_1 at a swelling pressure of 60 MPa with the different slot dimensions.
- Figure 5.3-3. Contour plots of the maximum principal stress (σ_1) at swelling pressures of 30 and 40 MPa with a slot width of 1000 mm and length of 775 mm.
- Figure 5.3-4. Contour plots of the maximum principal stress (σ_1) at swelling pressures of 50 and 60 MPa with a slot width of 1000 mm and length of 775 mm.
- Figure 5.4-1. Safety factor plot for the elastic material model and Mohr-Coulomb failure criterion of type 3 at a swelling pressure of 50 MPa, slot width of 1000 mm and slot length of 775 mm.
- Figure 5.5-1. Safety factor plot for the elastic material model employing Mogi's failure criterion at a swelling pressure of 50 MPa, slot width of 1000 mm and slot length of 775 mm.

- Figure 6-1. The result of modelling swelling pressures of 30 MPa (top) and 40 MPa (bottom) using the Mohr-Coulomb material model with criterion of type 2, cohesion 26.6 MPa, friction angle 23.5° .
- Figure 6-2. The result of modelling swelling pressures of 30 MPa (top) and 40 MPa (bottom) using the Mohr-Coulomb material model with criterion of type 3, cohesion 40.5 MPa, friction angle 0° .
- Figure 6-3. Vertical section taken perpendicular to the axis of test hole showing the modelled failure areas.
- Figure 6-4. A vertical section taken parallel to the axis of the test hole showing state of stress (top) and state of failure (bottom), swelling pressure of 50 MPa with the Mohr-Coulomb material model of type 2 with cohesion 26.6 MPa and friction angle of 23.5° .
- Figure 6-5. A horizontal section taken parallel to the axis of the test hole, showing state of stress (top) and state of failure (bottom), swelling pressure of 50 MPa with the Mohr-Coulomb material model of type 2 with cohesion 26.6 MPa and friction angle of 23.5° .
- Figure 6-6. Sections 1 and 2 perpendicular to the test hole at positions shown in Figure 6-4 showing the states of failure, swelling pressure of 50 MPa with the Mohr-Coulomb material model of type 2 with cohesion 26.6 MPa and friction angle of 23.5° .
- Figure 6-7. Sections 3 and 4 perpendicular to the test hole at positions shown in Figure 6-4 showing the states of failure, swelling pressure of 50 MPa with the Mohr-Coulomb material model of type 2 with cohesion 26.6 MPa and friction angle of 23.5° .

LIST OF TABLES

- Table 2.2-1. Summary of the average rock mechanical properties of the gneissic tonalite in the Research Tunnel.
- Table 2.2-2. Compressive strength (UCS), Crack Initiation (CI) and Crack Damage (CD) strength of gneissic tonalite samples from the Research Tunnel (Johansson & Autio 1995).
- Table 2.4-1. Maximum principal stress σ_1 around a full-scale deposition hole with respect to depth from the tunnel floor. Estimates are based on numerical modelling using 3DEC-code. The two angles shown (90° and 45° , see Figure 2.4-1), were used to study the sensitivity of the model and specify the angle between the maximum principal stress and the tunnel axis.
- Table 3-1. Parameters used in the strain-softening model.

1 GENERAL

An failure test suitable for execution in the Research Tunnel at Olkiluoto has been designed to study the failure of rock in-situ. The test involves creating an artificial stress field large enough to cause failure. Failures in rock and rock mechanical properties related to the mechanical stability of rock intended for use as a deep underground repository for spent nuclear fuel in the Finnish bedrock have been the subject of previous studies from a variety of points of view.

The development of computers and associated modelling programs has led to a situation in which it is possible to model fracture propagation in three dimensional geometries by using programs such as the Particle Flow Code (PFC) by Itasca Consulting Group, Inc. (Minneapolis, USA). The sizes of such models are quite limited and most of methods of this type are today used for research purposes. Examples of the modelling work carried at URL (Pinawa, Canada) in the Mine-by-tunnel strongly imply that as computers become more efficient and the knowledge of methods and applications becomes wider, the modelling of fracture propagation around underground openings will become more feasible.

The general objective of an in-situ failure test is to assess the applicability of numerical modelling codes and methods to the study of rock failure and associated crack propagation. One of the main tasks in an in-situ failure test is to carry out the modelling of rock failure by using both a conventional method of modelling without fracture propagation and a more sophisticated method capable of modelling the fracture propagation process. The observed failure patterns and the results obtained from the computer model are compared and evaluated

The site planned for execution of the in-situ failure test is one of the experimental full-scale deposition holes in the Research Tunnel at Olkiluoto, which is a favourable location since the rock properties are already well known, the state of stress is low and will result in only minor deformation as a result of stress release, and because the extent of the excavation-disturbed zone adjacent to the walls of the full-scale holes is insignificant from the testing point of view.

The test program includes three phases: design, execution and analysis. After completion of the design phase the feasibility of the test will be evaluated before proceeding to the experimental (i.e. execution) phase. The first step in the design phase - the preliminary modelling of the failure test in three dimensions (3D) by using Flac^{3D} code (Itasca 1995b) - is reported in this paper.

The numerical modelling was based on the information about rock strength, in-situ stresses and other input data which was available at the time of modelling. In the course of the design phase the input data for modelling presented in this report will be studied in greater detail and further modelling will be carried out using more specific and accurate data.

2 MODELLING - INPUT DATA

2.1 Geology and mineralogy

The VLJ-repository has been excavated in an east-west striking tonalite formation surrounded by mica gneiss. The rock types found in the Research Tunnel are gneissic tonalite and pegmatite. The tonalite is usually slightly-foliated, medium-grained, massive and sparsely-fractured. Besides the gneissic tonalite, which is referred to as anisotropic tonalite or gneissic tonalite, a fine-grained, homogeneous tonalite variant is also met. Pegmatite is found as veins and is non-foliated, coarse-grained, massive and sparsely-fractured (Äikäs & Sacklén 1993).

The main rock type found in the full-scale holes is gneissic tonalite the dominant dip and dip direction being about 30° and 145° respectively. Minor sections consisting of pegmatite are also found. In addition, a small section consisting of homogeneous tonalite is found in full-scale hole Number 3 (see Fig. 2.1-1) between the pegmatite and anisotropic tonalite. The orientation of fractures in the Research Tunnel can be divided into four different groups. The set of steeply-dipping fractures (dip direction east-west) is dominant.

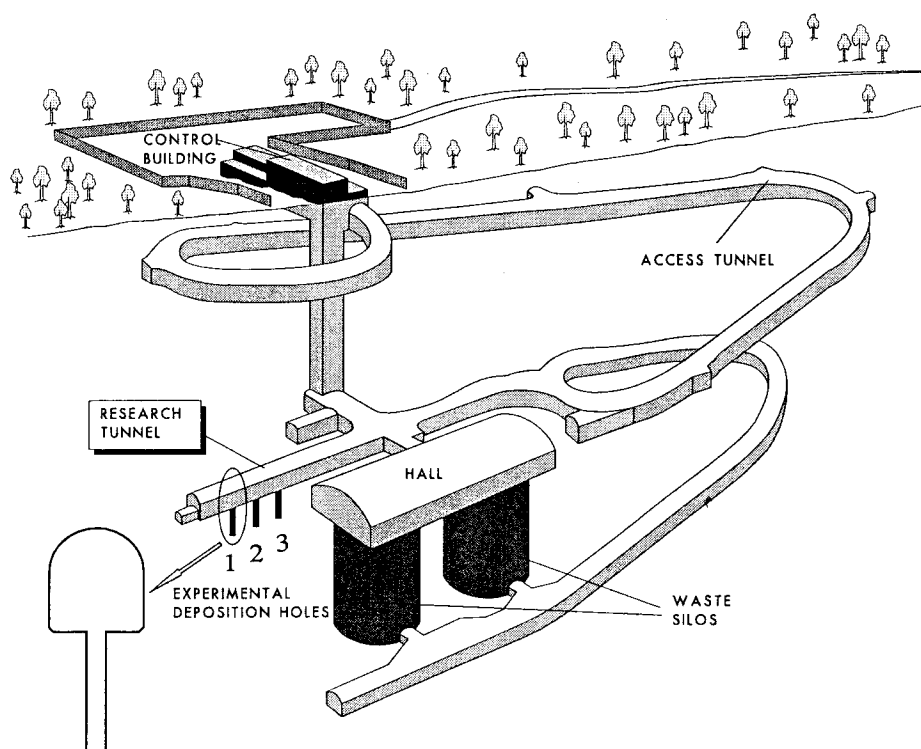


Figure 2.1-1. The Research Tunnel at Olkiluoto showing the full-scale experimental deposition holes.

The mineralogy of the gneissic tonalite was determined by Geological Survey of Finland. According to the microscopic thin section examination and point counting method used, the main minerals in the anisotropic tonalite are quartz (16.4%), plagioclase (37.2%), biotite (29.6%) and hornblende (11%), these four making up approximately 94% of the total content. This division of minerals is consistent with results obtained at an earlier date which are representative of a larger volume of rock in the Research Tunnel. The mafic minerals, especially the oblong grains of biotite and hornblende, are oriented. Grains are subhedral and the alteration to secondary minerals is insignificant.

The grain size of the quartz is 0.3-0.5 mm even though the size of the quartz clusters is 1-2 mm. The grain size of the plagioclase is larger, the largest grains observed being between 2 and 3 mm in size. The anorthic content of the plagioclase is 31-32%. Biotite occurs as clusters of flaky grains with a typical size between 1 and 3 mm.

2.2 Strength and deformation properties

A summary of the average strength and deformation is shown in Table 2.2-1 which is based on the results shown in Table 2.2-2 and Figures 2.2-1, 2.2-2, 2.2-3 and 2.2-4 which contain all the results currently available for the rock mechanical parameters of the gneissic tonalite given in (Johansson & Autio 1993 and Johansson & Autio 1995). The average measured value of compressive strength for gneissic tonalite, 80 MPa, is lower than that of typical granitic rocks and homogeneous tonalite (112 MPa). Gneissic tonalite, the most common form of tonalite in the Research Tunnel, exhibits compressive strength values that are clearly lower than that of the homogeneous tonalite which is encountered only in the upper part of borehole KR7. The tensile strength of the gneissic tonalite, 9 MPa, and its deformation properties (Young's modulus of 60 GPa) are typical values for granitic rocks. Measured values for tensile strength and Young's modulus of the homogeneous tonalite were 10 MPa and 66 GPa respectively.

Averages of all the measured values presented in Tables 2.2-1 and 2.2-2 were used as inputs for the modelling work: Young's modulus 58.3 GPa, Poisson's ratio 0.25, uniaxial compressive strength 81 MPa, tensile strength 8.4 MPa and density 2804 kg/m³. The rock was assumed to be isotropic at this point although it was evident that some degree of anisotropy caused by the distinct gneissic structure would appear in closer studies. The rock around the full-scale holes is sparsely fractured.

Table 2.2-1. Summary of the average rock mechanical properties of the gneissic tonalite in the Research Tunnel.

Peak strength (MPa)	Tensile strength (MPa)	Young's modulus (GPa)	DRI value	CAI value	Quartz content (%)	Joint freq. pcs/m
80	9	60	55	3.8	15-20	1.0

STRENGTH PROPERTIES OF TONALITE

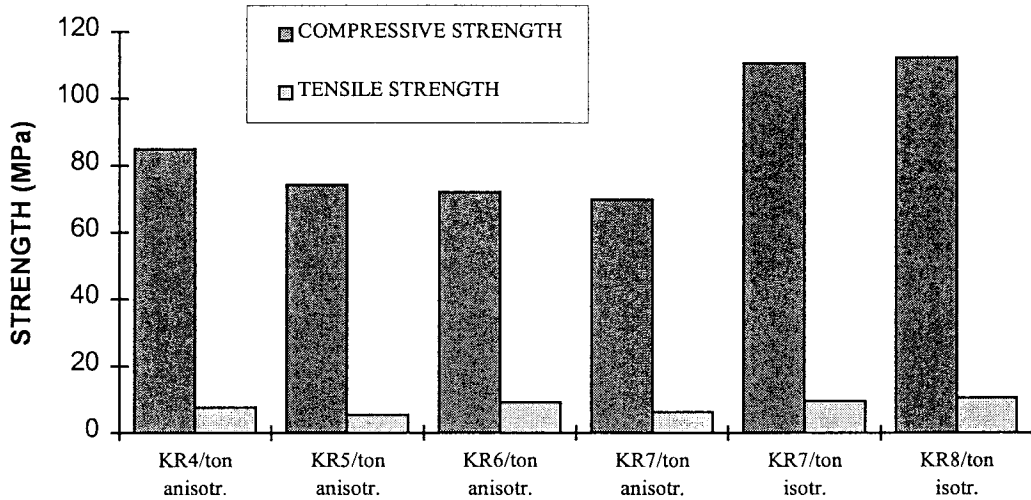


Figure 2.2-1. Strength properties of gneissic and homogeneous tonalite in the Research Tunnel (Johansson & Autio 1993).

OLKILUOTO, RESEARCH TUNNEL

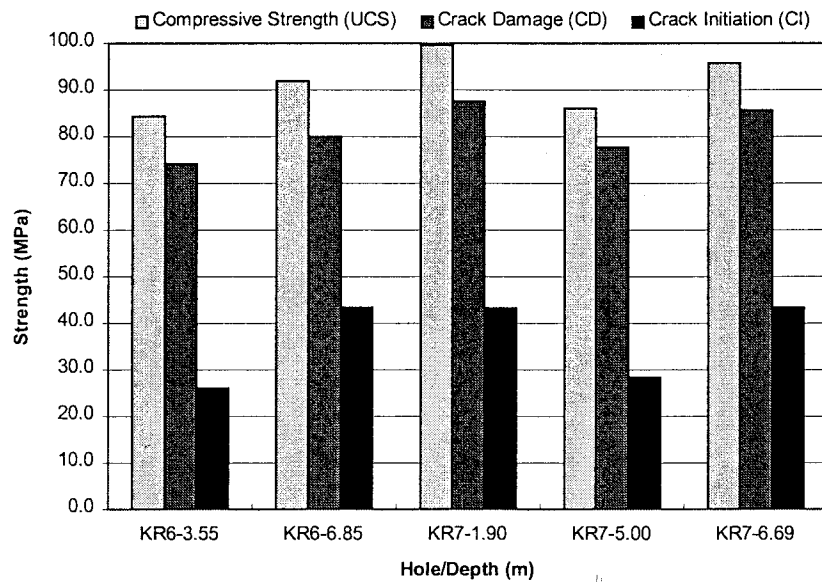


Figure 2.2-2. Strength properties of gneissic tonalite in the Research Tunnel (Johansson & Autio 1995). The values shown here include the Crack Damage and Crack Initiation stress determined from the stress-strain curve.

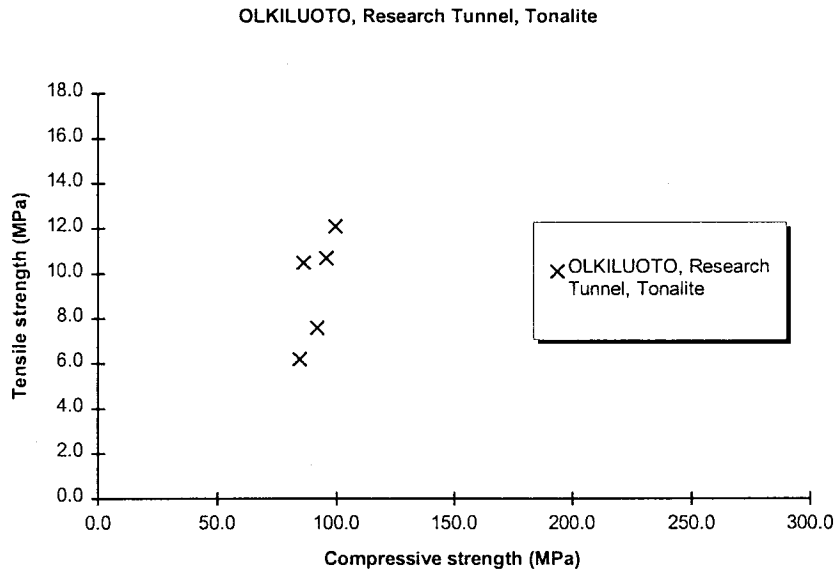


Figure 2.2-3. Compressive strength of the gneissic tonalite shown in Figure 2.2-2 plotted as a function of tensile strength.

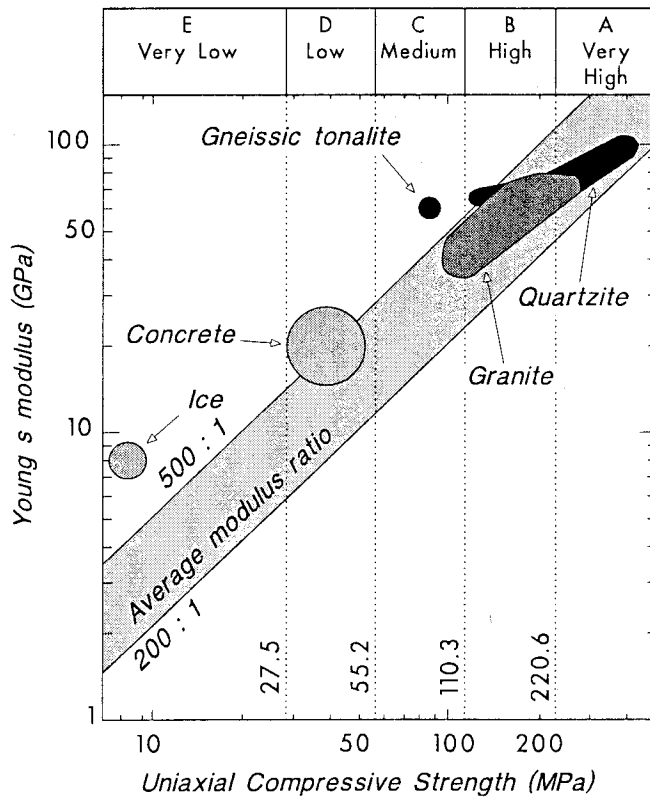


Figure 2.2-4. The position of gneissic tonalite in Deere's classification system.

Table 2.2-2. Compressive strength (UCS), Crack Initiation (CI) and Crack Damage (CD) strength of gneissic tonalite samples from the Research Tunnel (Johansson & Autio 1995).

Property Test sample	Compr. strength (MPa)	Tensile strength (MPa)	Crack Initiation		Crack Damage	
			(CI) (MPa)	(% of UCS)	(CD) (MPa)	(% of UCS)
VLJ- KR6- 3.55 m	84.4	6.2	26.1	23.0	74.2	87.8
VLJ- KR6- 6.85 m	91.9	7.6	43.4	35.0	80.0	87.0
VLJ- KR7- 1.90 m	99.6	12.1	43.3	32.2	87.6	88.0
VLJ- KR7- 5.00 m	86.1	10.5	28.4	24.4	77.7	90.3
VLJ- KR7- 6.69 m	95.8	10.7	43.4	33.6	85.7	89.5
<i>average</i>	91.6	9.4	36.9	29.6	81.0	88.5

2.3 Test geometry

The geometry used in the modelling consisted of a horizontally-oriented hole with identical slots positioned vertically above and below it, see Figure 2.3-1. The diameter and length of the central hole were set at 200 mm and 500 mm respectively. The distance from the axis of the borehole to the closest surface of each slot was set at 350 mm. Three different widths and depths of slot were modelled to establish the effect of slot dimensions on the resultant stress distribution. In the first model the width was set at 500 mm and the depth at 300 mm, in the second model the width was 1000 mm and the depth 500 mm, and in the third model the width was 1000 mm and the depth was 775 mm. The thickness of the slot was 50 mm. The depth of the center hole was assumed to be in the depth range from 3.5 to 4.5 m from the tunnel floor.

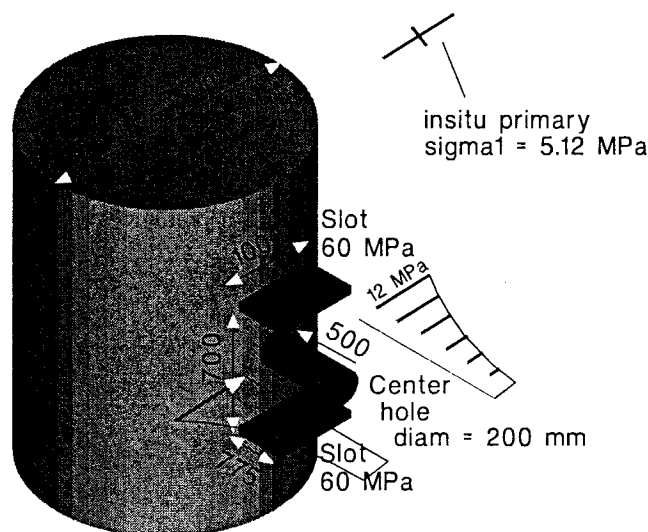


Figure 2.3-1. Geometry used in modelling showing also the estimated horizontal tangential stress component acting perpendicular to the surface of test hole.

2.4 Constraining stresses

2.4.1 In situ stresses

According to stress measurements (Kuula & Johansson 1991, Nykyri et al. 1991) carried out before the construction of the VLJ-repository and the Research Tunnel the state of in-situ stress at the VLJ-repository and in the area of the Research Tunnel is low. Measured values of the maximum in-situ stress averaged from 5 to 6 MPa at the level of the repository. A value of 5.1 MPa was estimated for the σ_1 stress (horizontal) and 2.4 MPa for the σ_2 stress (horizontal) (Kuula & Johansson 1991). The calculated vertical stress (σ_3) of 1.9 MPa was assumed to be caused by gravity (Kuula & Johansson 1991). Results obtained from the monitoring of rock displacement during and after construction of the repository are consistent with these stress measurements (Nykyri et al. 1994). Stress orientation is shown in Figure 2.4-1.

The constraining in-situ stresses used for the modelling (in Chapters 5.3-5.7) were:

$$\begin{aligned}\sigma_1 &= \sigma_H = 5.1 \text{ MPa} \\ \sigma_2 &= \sigma_h = 2.4 \text{ MPa} \\ \sigma_3 &= \sigma_v = 1.9 \text{ MPa}\end{aligned}$$

The stress environment in the vicinity of the full-scale deposition holes differs from the in-situ stress because it is affected by both the full-scale hole and the existence of the Research Tunnel situated directly above it.

From both the modelling and the experimental points of view it is beneficial to have both uniform and symmetrical stress conditions in the test area. The vertical stress component perpendicular to the test hole shall be generated artificially and can be controlled. The stress component acting parallel to the axis of the test hole is the smallest stress component and approaches zero at the surface of the full-scale hole. Therefore from the experimental point of view the horizontal tangential stress component around the full-scale hole which is directed perpendicular to the axis of test hole is of most importance and discussed here.

The stress conditions adjacent to the full-scale holes was first calculated using Kirsh's equation for the tangential stress around a circular 2D opening. This does not include the effect of Research Tunnel and assumes that the length of the full-scale hole is infinite. This calculation gave a maximum tangential stress adjacent to the surface of the opening of 12 MPa at a depth of 4 cm (Analytical solution in Figure 2.4-2). At a depth of 32 cm the stress was about 8 MPa and at a depth of 90 cm the stress was about 6 MPa.

The stress conditions around the full-scale holes was then modelled by using numerical 3DEC code (Itasca 1994). For practical purposes, the geometry of the Research Tunnel (width 7 m and height 7.5 m) was simplified to more closely resemble the proposed deposition tunnel (width 3.3 m and height 4.6 m). For this reason, the actual effect of the Research Tunnel on stress conditions is larger (about 20% at the maximum) than the results given by modelling.

The results of the modelling are presented in Table 2.4-1 and Figure 2.4-2. This shows the magnitude of the principal stress on the surface of the full-scale hole with respect to depth from the tunnel floor. Figure 2.4-3 shows the distribution of principal stresses. The real stresses adjacent to the surface of the full-scale hole are higher because the element model used for the surface section was quite coarse. For this reason, the maximum principal stress at the surface is estimated to be 0.5-1.0 MPa higher than the value given by the model.

According to the cross-sectional contour plots, the stress conditions around the full-scale hole are close to two dimensional at a depth of 3.5 to 4.5 m from the tunnel floor. At this depth range neither the Research Tunnel nor the bottom of the full-scale hole appear to have significant effect on the stresses adjacent to the surface of the full-scale hole.

On the basis of the evaluation it was estimated that the tangential maximum stress around the full-scale holes should be close to 12 MPa at a depth ranging from 3.5 to 4.5 m. It was assumed that the stress follows Kirsch's equation and decreases to the in-situ level at a depth of 2 m from the surface of full-scale hole. The in-situ stresses shall be measured later to verify these preliminary estimates.

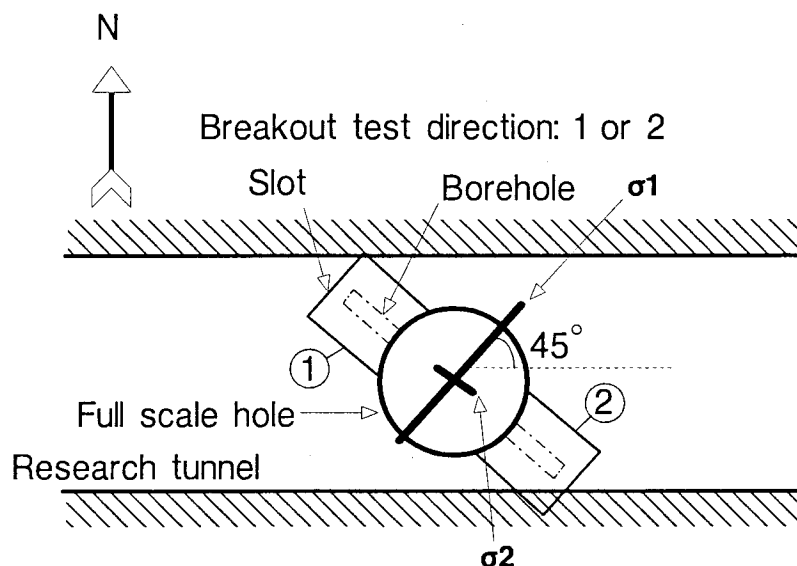


Figure 2.4-1. Horizontal section of the Research Tunnel showing the direction of primary in-situ stresses and preliminary lay-out of the test.

Table 2.4-1. Maximum principal stress σ_1 around a full-scale deposition hole with respect to depth from the tunnel floor. Estimates are based on numerical modelling using 3DEC-code. The two angles shown (90° and 45° , see Figure 2.4-1), were used to study the sensitivity of the model and specify the angle between the maximum principal stress and the tunnel axis.

Depth from the tunnel floor (m)	Stress σ_1 at angle 45° (MPa)	Stress σ_1 at angle 90° (MPa)
0.0	14.6	15.1
0.5	14.4	14.9
1.0	13.6	14.1
1.5	13.4	13.9
2.0	13.3	13.8
2.5	12.9	13.4
3.0	12.3	12.8
3.5	11.7	12.2
4.0	11.3	11.8
4.5	11.0	11.5
5.0	10.9	11.4
5.5	11.1	11.6
6.0	10.7	11.2
6.5	10.3	10.8
7.0	10.1	10.6

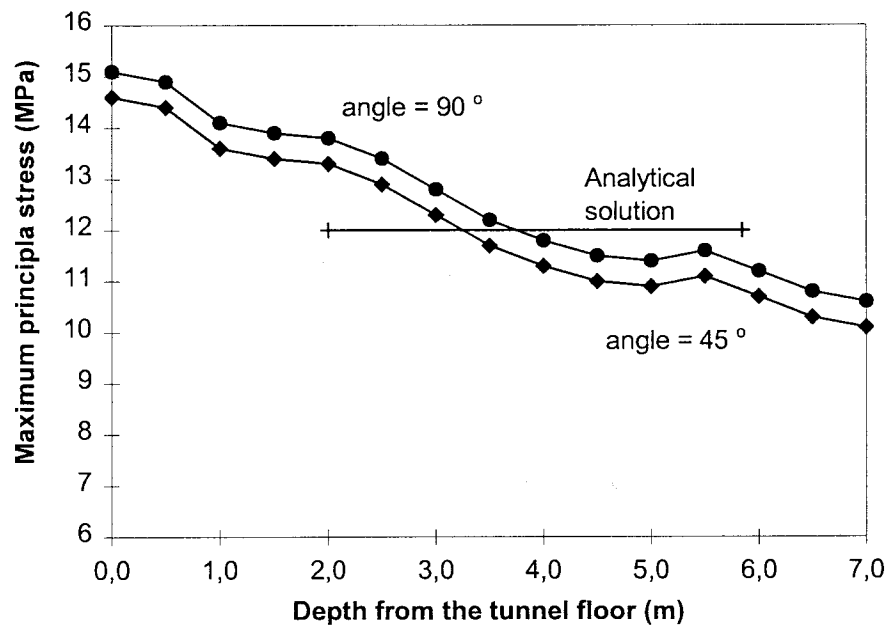


Figure 2.4-2. Magnitude of the maximum principal stresses around a full-scale deposition hole (Table 2.4-1) with respect to depth from the floor of the Research Tunnel.

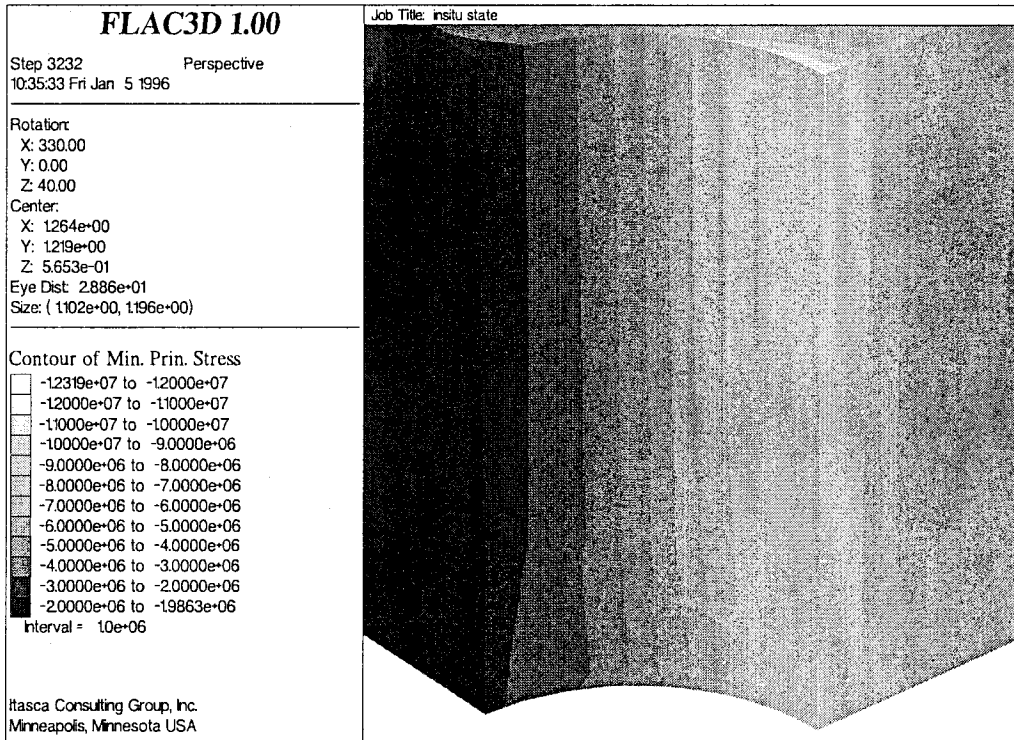


Figure 2.4-3. Contour plot of the maximum principal stresses around full-scale deposition holes. The angle between the principal in-situ stress and the tunnel axis is 90°.

2.4.2 Pressure exerted by the expanding agent

The stress around the centre hole is created by filling the slots shown in Figure 2.3-1 with expansive agent. The reacting material in the expanding agent is free calcium oxide CaO_{free} , which reacts with water to produce calcium hydroxide $\text{Ca}(\text{OH})_2$. The calcium hydroxide reacts with other substances and the resulting reaction volume is higher than the volume occupied by the original materials. If the resultant swelling is restricted, as is the case in a restricted space, pressure is generated. The expanding agent is sold in Finland under two different commercially-registered names - Betonamit and Demex. The swelling pressure with respect to time for Betonamit in a hole is shown in Figure 2.4-4 (hole diameters 20, 30 and 40 mm).

Different pressures caused by introducing an expanding agent into the slots were modelled to establish the minimum pressure level which would cause failure. The input pressures used (see Figure 2.3-1) were from 20 or 30 MPa up to 60 MPa at 10 MPa steps. It was assumed that a slot expansion pressure of at least 50 MPa could be achieved in the failure test.

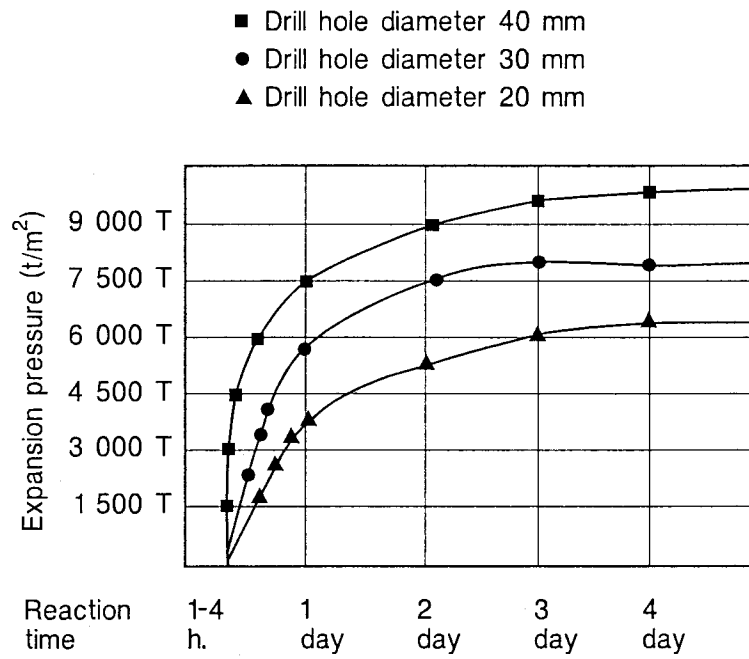


Figure 2.4-4. Expansion pressure of Betonamit with respect to reaction time for different hole diameters (according to Betonamit International AG, Liechtenstein).

3 CONSTITUTIVE MATERIAL MODELS

Three different types of material models (see Fig. 3-1) were used; 1) Elastic, 2) Mohr-Coulomb and 3) Strain-softening. The rock material models used were isotropic and no fractures were included in the model.

The following values (see Chapter 2.2 and Tables 2.2-1 and 2.2-2) were used as inputs for the elastic material model: Young's modulus 58.3 GPa, Poisson's ratio 0.25.

The material parameters used in the strain-softening model (Table 3-1) were chosen heuristically on the basis of typical values previously determined for similar types of rock and from the stress-strain curves for gneissic tonalite. As the objective was to conceptualise the strain-softening behaviour, the results achieved by modelling should be considered as preliminary.

The parameters used in the strain-softening model, cohesion, friction and dilatation, are defined as functions of the total plastic strain. Once plastic yield begins, the program keeps track of the total plastic strain and determines the current values of cohesion, friction and dilatation which correspond to this strain (Itasca 1995a). The cohesion, friction and dilatation are defined as a piecewise linear function of the total plastic strain. A detailed description of the model can be found in Itasca 1995a.

Table 3-1. Parameters used in the strain-softening model.

Plastic strain (%) e^{ps}	Cohesion (MPa)	Friction (degrees)	Calculated residual σ_c (MPa)
0.00	26.6	23.5	81
0.01	24.6	21.5	67
0.02	22.6	19.5	58
0.03	20.6	17.5	51

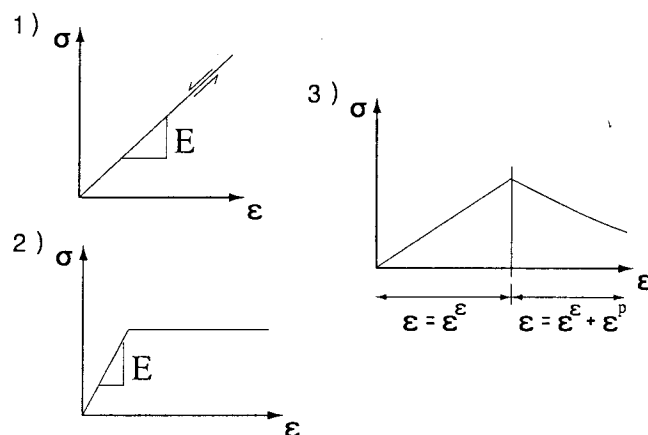


Figure 3-1. The three different constitutive material models: 1) Elastic, 2) Mohr-Coulomb and 3) Strain-softening.

4 FAILURE CRITERIA

The failure criteria used when calculating safety factors for the elastic analysis were Mohr-Coulomb and Mogi's polyaxial strength criterion (Haimson & Song 1995). Values of cohesion and friction angle for the Mohr-Coulomb criterion were estimated on the basis of results of uniaxial compression tests and Brazilian tensile tests. The criterion was estimated using three different types of subcriteria. These are shown as the lines marked 1, 2 and 3 (referred later as types 1, 2, and 3) in Figure 4-1 which correspond to cohesion and friction angle values of 12.7 MPa and 55°, 26.6 MPa and 23.5° and 40.5 MPa and 0° respectively. The Line 1 in Figure 4-1 was obtained by fitting it to the tensile strength and uniaxial compressive strength and follows the Mohr-Coulomb yield envelope at lower stresses. The Line 3 describes material with limited tensile strength and which strength is determined by cohesion only. Line 2 describes material between Lines 1 and 3 which strength follows the Mohr-Coulomb envelope at higher compressive strengths as seen in Figure 4-1. Mogi's polyaxial criterion includes both minimum and intermediate stresses (Haimson & Song 1995). The parameters for the criterion - see Equation (1) and (2) below where f is a nearly-linear function - were estimated on the basis of uniaxial compression and the corresponding tensile strengths, see Fig. 4-2.

$$\tau_{oct} = f_1(\sigma_2^m) \quad (1)$$

$$\frac{1}{3} \sqrt{(\sigma_1 - \sigma_2)^2 + (\sigma_2 - \sigma_3)^2 + (\sigma_3 - \sigma_1)^2} = f_1 \left[\frac{1}{2} (\sigma_1 + \sigma_3) \right] \quad (2)$$

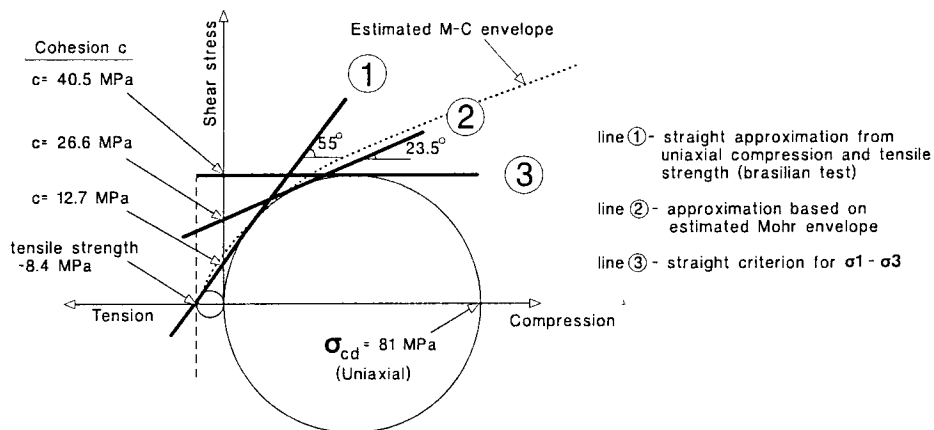


Figure 4-1. Mohr-Coulomb criterion types 1, 2 and 3 and their respective lines.

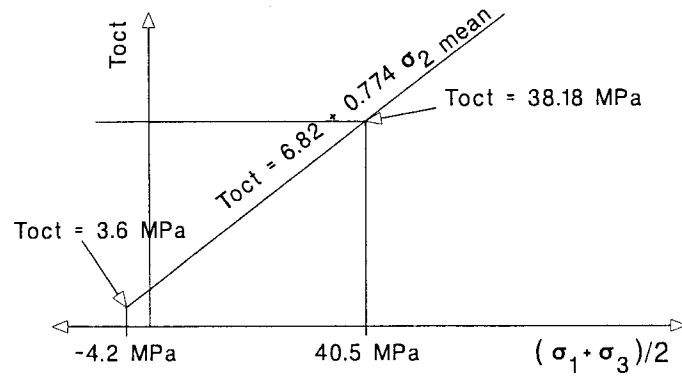


Figure 4-2. Mogi's criterion lines estimated from a uniaxial compression test.

5 RESULTS OF FLAC MODELLING

5.1 Preliminary FLAC^{2D} modelling

Preliminary evaluation of the test was carried out by using Flac^{2D} code. Two different geometries were compared, the final geometry chosen with horizontal slots and an alternative with vertical slots (see Appendix 2). It was concluded that the design with horizontal slots is preferable because of the more favourable ratio between vertical and horizontal stresses around the test hole. The result of the 2D modelling showing the failure areas at a swelling pressure of 60 MPa is presented in Figure 5.1-1 and in more detail in Appendix 1.

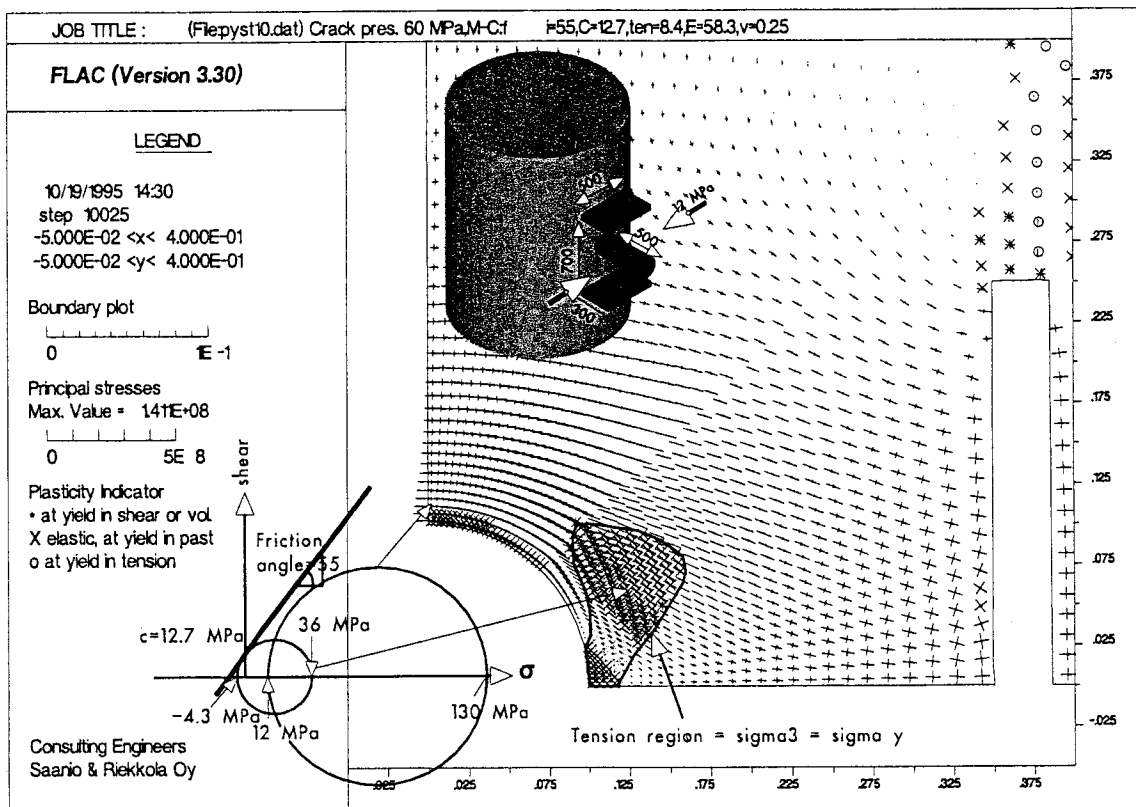


Figure 5.1-1. The result of the 2D modelling showing the failure areas at a swelling pressure of 60 MPa.

5.2 Displacements of the centre hole before external loading

Displacements in the rock caused by the boring of the central hole before making the slots were modelled using the Flac^{3D} program. The main objective was to obtain a rough idea of the deformation of the rock caused by boring of the center hole in order to assess the applicability of different stress measurement techniques. An elastic material model was used ($E=58.3$ GPa, $\nu=0.25$). Three different alternatives were used as input for the in-situ stresses σ_H - σ_h - σ_v : 1) 2.56-1.21-1 MPa; 2) 5.12-2.42-1 MPa; and 3) 10.24-4.84-1 MPa. These stress values were used only to estimate the deformation of the rock caused by the boring of the center hole before making the slots. The results of the modelling are shown in Appendices 49, 50 and 51 for these three stress combinations. A summary of the effect -of the in-situ stresses on the diameter of the central hole is shown in Figure 5.2-1. The diameter of the hole (100 mm) is reduced by from 10 to almost 60 micrometres, depending on the magnitude of the maximum principal stress.

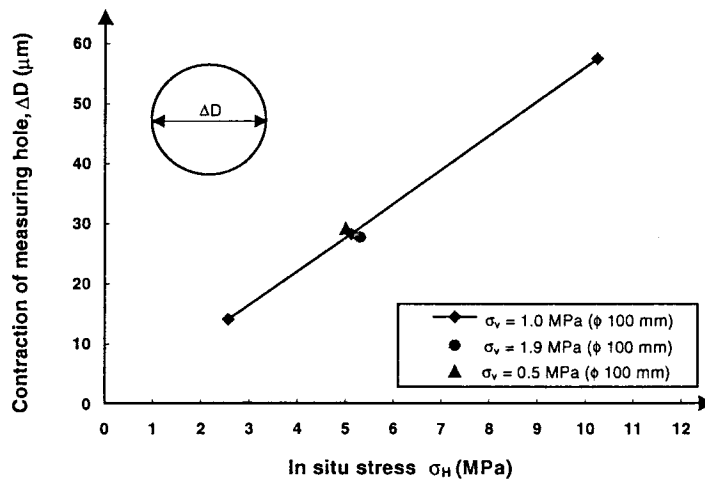


Figure 5.2-1. Diameter of a hole on the surface of the full scale hole as a function of the maximum in-situ stress. The σ_v component has been varied to assess the sensitivity of the result.

5.3 Elastic material model

This analysis was performed by using Flac^{3D} on an elastic material model and the following combinations of slot length (L) and width (W) (see Fig. 5.3-1):

- $L = 500 / W = 500$
- $L = 500 / W = 1000$
- $L = 775 / W = 1000$

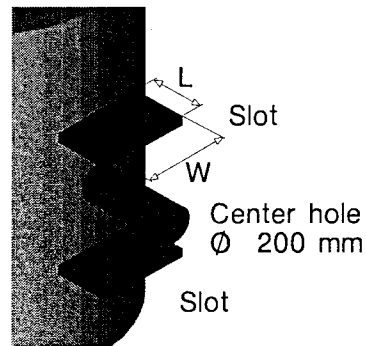
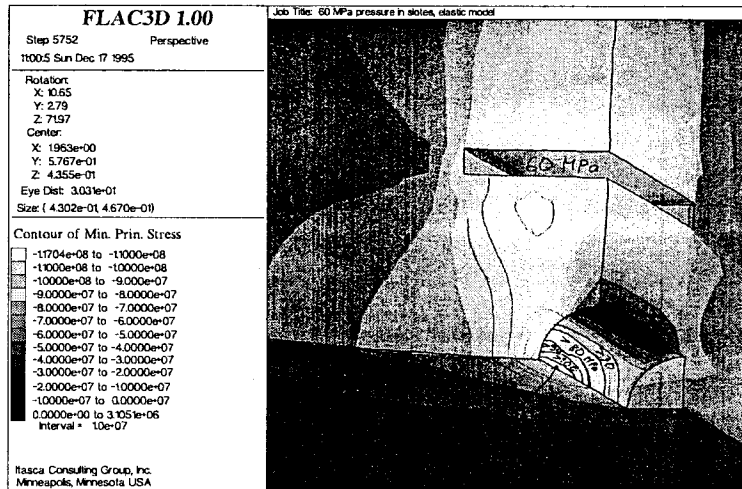
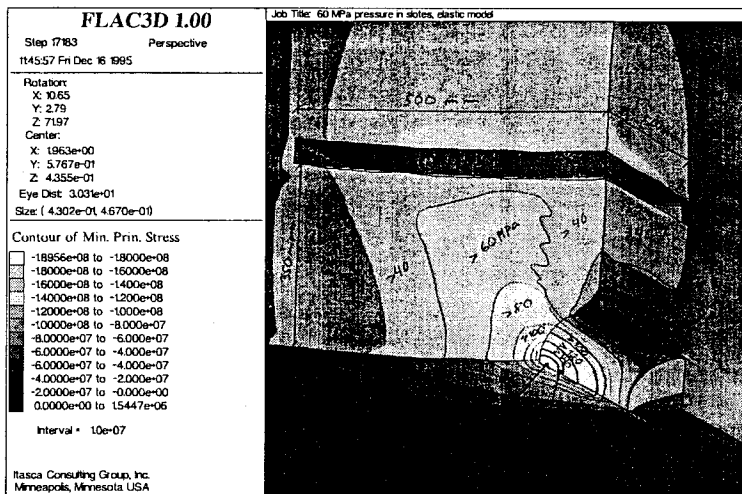


Figure 5.3-1. Diagram showing slot length (L) and slot width (W).

a)
 Slot :
 width 500 mm
 length 500 mm



b)
 Slot :
 width 1000 mm
 length 500 mm



c)
 Slot :
 width 1000 mm
 length 775 mm

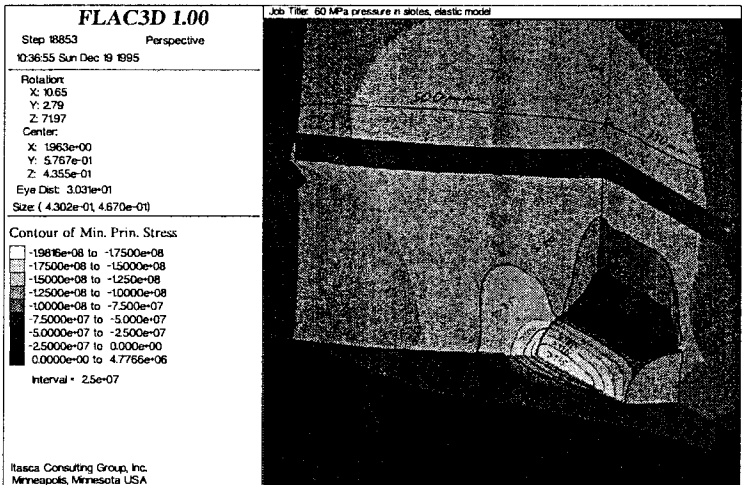


Figure 5.3-2. Contour plots of the maximum principal stress σ_1 at a swelling pressure of 60 MPa with the different slot dimensions.

The principal stress plots resulting from the modelling are presented in Appendices 9-15. The maximum tangential stress predicted for the surface of the test holes at a swelling pressure of 60 MPa imposed on the surfaces of the slots was 117 MPa (Appendix 9) with a slot length of 500 mm and width of 500 mm. Using a slot width of 1000 mm, the corresponding figures predicted for tangential stress were 189 MPa with a slot length of 500 mm (Appendix 10) and 198 MPa with a slot length of 775 mm (Appendix 15), see Figure 5.3-2.

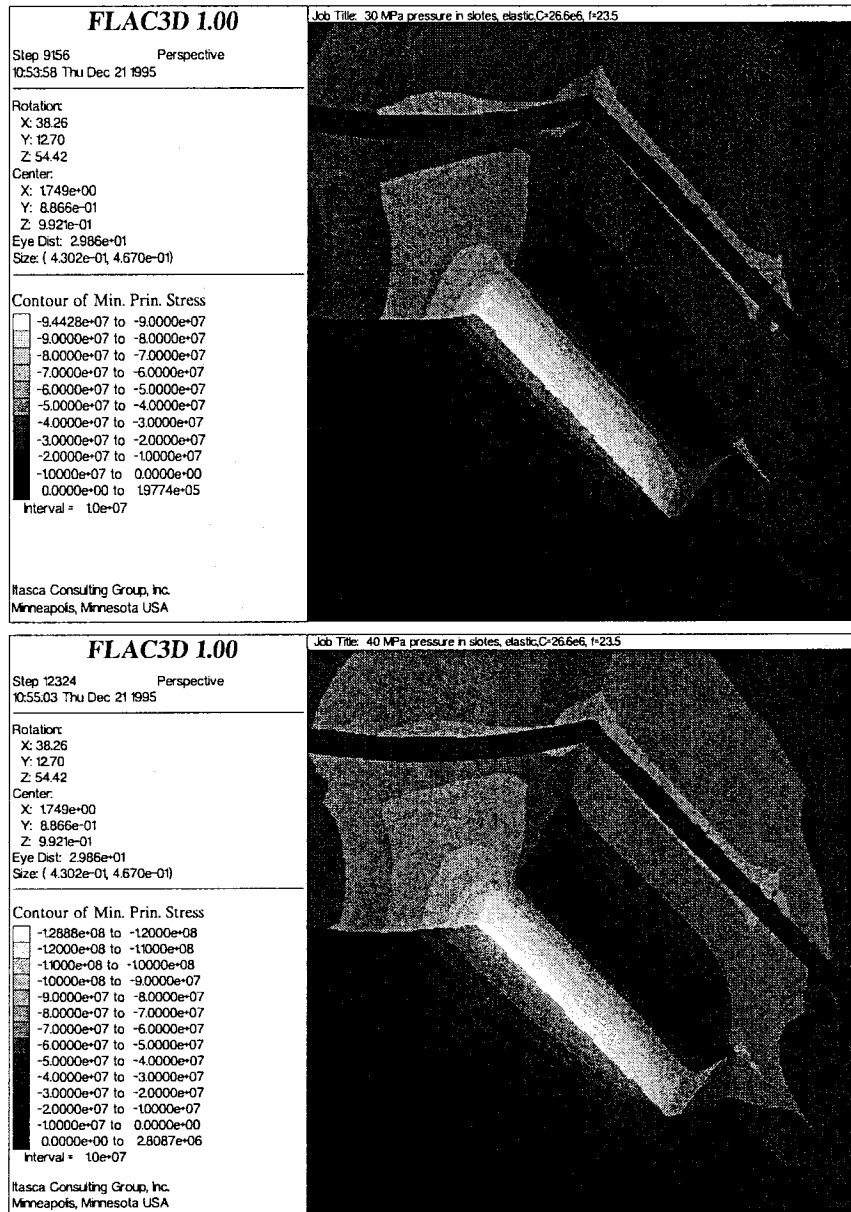


Figure 5.3-3. Contour plots of the maximum principal stress (σ_1) at swelling pressures of 30 and 40 MPa with a slot width of 1000 mm and length of 775 mm.

On the basis of the results achieved in the modelling, a slot of width 1000 mm and length 775 mm was assessed as being the most suitable for the tests. These slot dimensions resulted in maximum tangential stresses of 94, 129, 164 and 198 MPa at slot pressures of 30, 40, 50 and 60 MPa, see Figure 5.3-3 and 5.3-4. The points of maximum tangential stress were located adjacent to the face of the full-scale deposition hole.

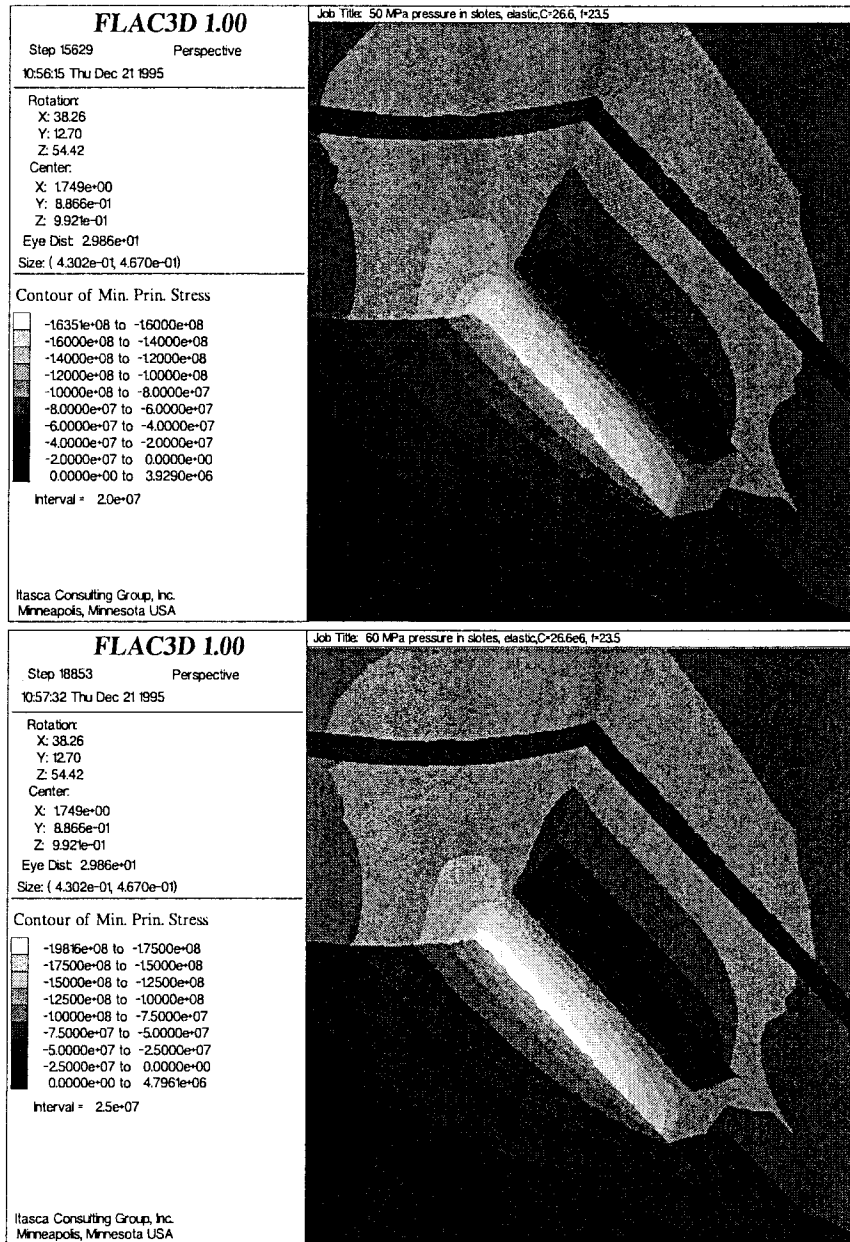


Figure 5.3-4. Contour plots of the maximum principal stress (σ_1) at swelling pressures of 50 and 60 MPa with a slot width of 1000 mm and length of 775 mm.

5.4 Safety factors for the elastic material model and the Mohr-Coulomb strength criterion

Safety factors were used to assess the possibility of failure. The results of failure assessment using the Mohr-Coulomb failure criterion are presented in Appendices 17 - 20. The safety factors employed were based on Mohr-Coulomb criteria types 1, 2, 3 (presented as cases 1, 2 and 3 in the Appendices) and were calculated for the elastic material model at slot pressures of 30, 40, 50 and 60 MPa, see Figure 5.4-1.

Tensile failure and crack propagation is initiated at the end of the slots when the pressure in the slot exceeds the strength of the rock. In all cases borehole failure begins once the slot pressure reaches a value of 30 MPa. Both compressive and tensile failure modes are predicted. Compressive failure (the term “compressive failure” is used here to define a failure at the surface caused by high tangential compressive stress) is clearly largest when the type 3 Mohr-Coulomb criterion is used (cohesion 40.5 MPa, friction angle 0°). In all three cases it can be seen that the depth of failure is greatest on the face of the full-scale deposition hole. With a Mohr-Coulomb criterion of type 1 (cohesion 12.7 MPa and friction angle 55°) the failure is very narrow and shear failure of the sidewall starts to take place at a slot pressure of 40 MPa (Appendices 26, 27 and 28).

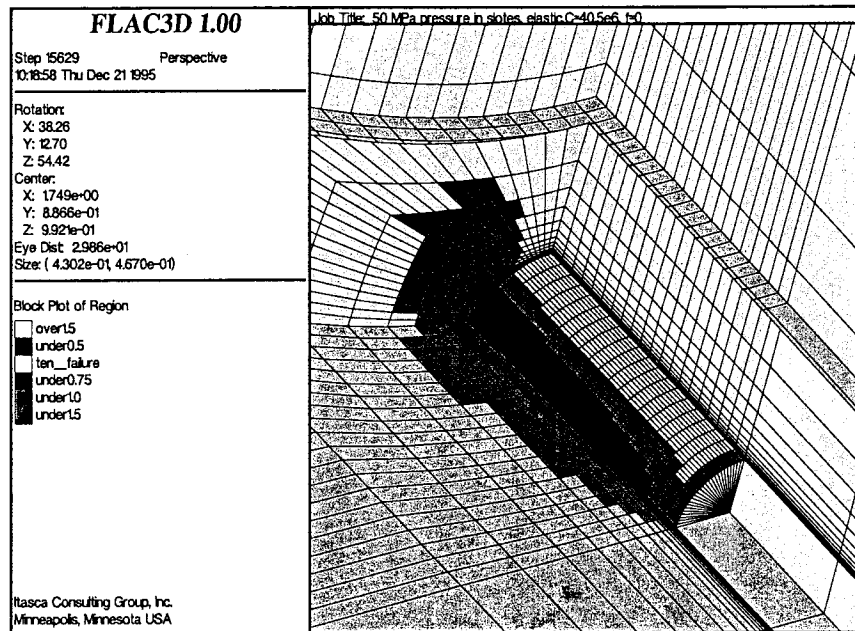


Figure 5.4-1. Safety factor plot for the elastic material model and Mohr-Coulomb failure criterion of type 3 at a swelling pressure of 50 MPa, slot width of 1000 mm and slot length of 775 mm.

5.5 Safety factors for the elastic material model employing Mogi's strength criterion

The results of failure assessment in the form of safety factors using the elastic material model and Mogi's failure criterion are presented in Appendices 29 - 32, see Figure 5.5-1. The results obtained are comparable with the already described Mohr-Coulomb case when employing criterion type 1. Tensile failure is initiated once the slot pressure reaches 30 MPa. When the slot pressure is 40 MPa, failure on the face of the full-scale deposition hole begins. Shear failure of the sidewall occurs when the slot pressure is 50 MPa.

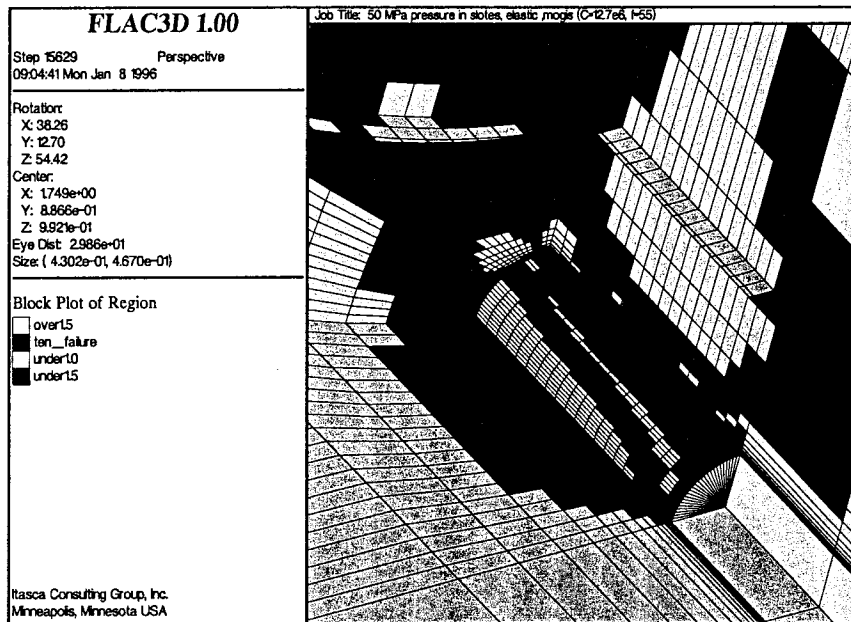


Figure 5.5-1. Safety factor plot for the elastic material model employing Mogi's failure criterion at a swelling pressure of 50 MPa, slot width of 1000 mm and slot length of 775 mm.

5.6 Safety factors for Mohr-Coulomb plastic material model

The results of failure assessment in the form of block state plots using the Mohr-Coulomb plastic material model (see Figure 4-1 for the constitutive material model) are presented in Appendices 33 - 44, see Figure 5.6-1. The plots show the locations in which blocks have failed according to the Mohr-Coulomb criterion, which has the same basis as the criteria employed when calculating safety factors for the elastic material model in Section 5.4. Failure zones are clearly larger when using criterion types 1 and 2 than type 3 of the Mohr-Coulomb criterion (see lines 1, 2 and 3 in Figure 4-1). The mechanism of failure is the same as that predicted by the elastic material models.

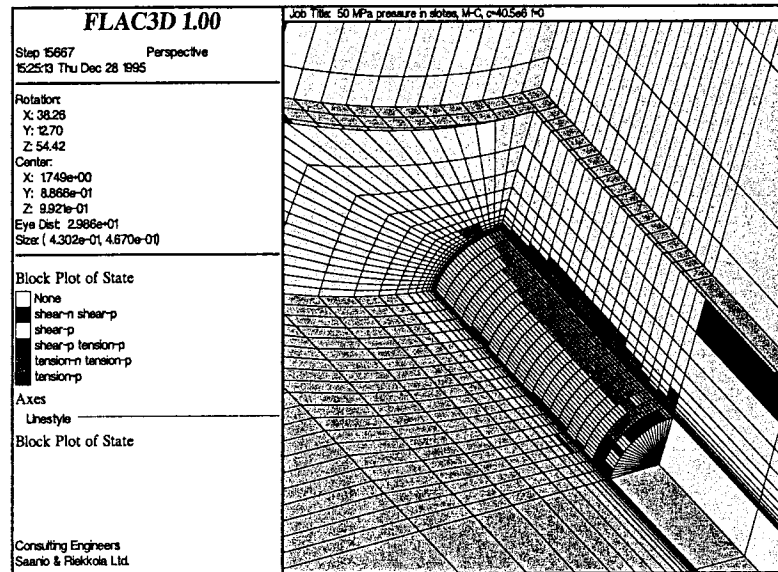


Figure 5.6-1. Safety factor plot for the Mohr-Coulomb plastic material model at a swelling pressure of 50 MPa, slot width of 1000 mm and slot length of 775 mm.

5.7 Safety factors for the strain-softening material model

The results of failure assessment in the form of block state plots using the strain-softening material model are presented in Appendices 45 - 48, see Figure 5.7-1. In this case, the failure predicted is more extensive than when using the other models. The thickness of the failure zone is 250-300 mm at a slot pressure of 60 MPa.

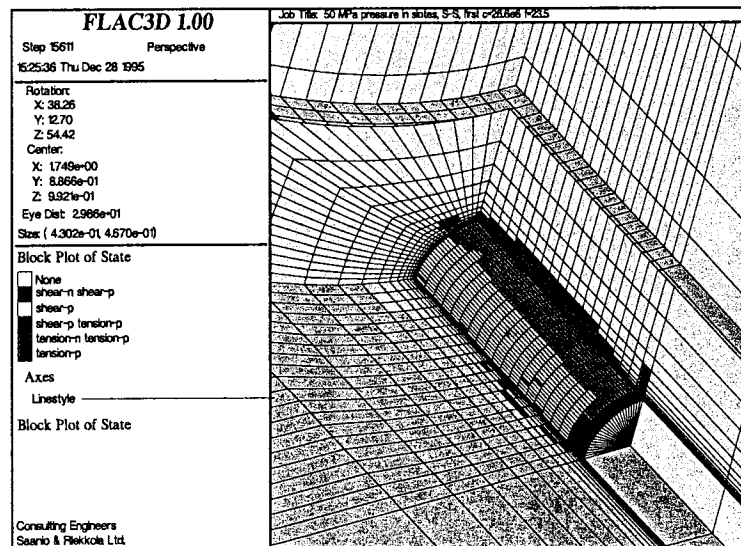


Figure 5.7-1. Block plot state for the strain-softening material model at a swelling pressure of 50 MPa, slot width of 1000 mm and slot length of 775 mm.

6 CONCLUSIONS AND DISCUSSION

Test geometry

Comparison of the predicted stress fields around the test hole resulting from the use of different slot sizes showed that the largest slot size (width 1000 mm / length 775 mm) resulted in significantly higher stresses and a more uniform stress field. Further enlargement of the slots would be impractical from an experimental point of view and a slot size of width 1000 mm and length 775 mm was assessed as being the most suitable for the test. The maximum tangential compressive stress developed around the borehole was 198 MPa at a slot pressure of 60 MPa and this was taken as the highest stress which could be achieved with an adequate degree of certainty. It was noted that even at a swelling pressure of 40 MPa, the maximum principal stresses at the surface of the hole exceed the uniaxial compressive strength of the rock. It is therefore certain that a swelling pressure high enough to cause failure can be achieved in the experiment and that the stress distribution on the stem section of the hole is reasonably two dimensional and uniform.

Models

Modelling using the elastic material model with Mohr-Coulomb failure criteria of type 2 and 3; the Mohr-Coulomb plastic material model with failure criteria of type 2 and 3, Mogi's failure criteria and the strain-softening material model gave very similar results at swelling pressures between 30 and 40 MPa. Slight differences could be seen in the extent of the failed areas but the main features observed were very similar.

As they had not been determined experimentally, the parameters used in the strain-softening model were of a tentative nature and this result is therefore considered to be the most unreliable. If the parameters could be used with greater confidence, the strain-softening model would be a suitable method for the modelling of progressive failure because the strength of the modelled material is reduced as failure takes place.

The parameters employed with Mogi's criterion were estimated from the results of uniaxial compression and Brazilian tests and the predicted safety factors should therefore only be comparable with modelling which employs the Mohr-Coulomb type 1 criterion. The magnitudes of the stress components σ_2 and σ_3 were of the same order and therefore the difference between results obtained using the Mohr-Coulomb criterion of type 1 and Mogi's criterion should be small.

Failure prediction

Modelling results obtained using the elastic material model and Mohr-Coulomb failure criteria of types 2 and 3; the Mohr-Coulomb material model and failure criteria of type 2 and 3; and Mogi's failure criterion and the strain-softening material model all predict

similar areas for initial failure. Regardless of the material model and criteria employed, failure appears at a swelling pressure of well below 60 MPa, in some cases at a swelling pressure as low as 30 MPa. The forms in which failure is predicted to take place are tensile failure on the upper and lower surfaces of the test hole and compressive/shear failure on the side surfaces. The results of modelling using swelling pressures of 30 and 40 MPa with the Mohr-Coulomb material model (type 2) with cohesion 26.6 MPa and friction angle of 23.5° (Appendices 41, 42, 43 and 44) and the same model (type 3) with cohesion of 40.5 MPa and friction angle 0° (Appendices 37, 38, 39 and 40) shown in Figure 6-1 and 6-2 are considered to be a satisfactory representation of the areas of failure surrounding the test hole. Figure 6-3 is a vertical section taken perpendicular to the axis of the test hole which shows the modelled failure areas.

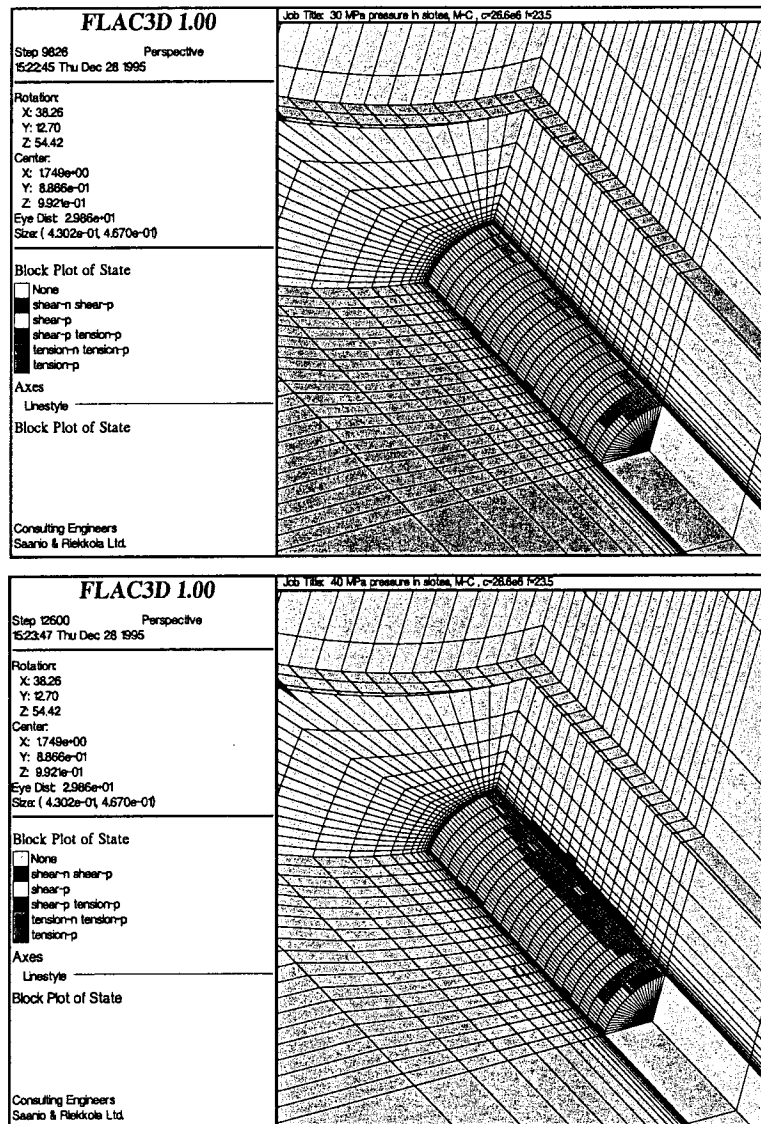


Figure 6-1. The result of modelling swelling pressures of 30 MPa (top) and 40 MPa (bottom) using the Mohr-Coulomb material model with criterion of type 2, cohesion 26.6 MPa, friction angle 23.5° .

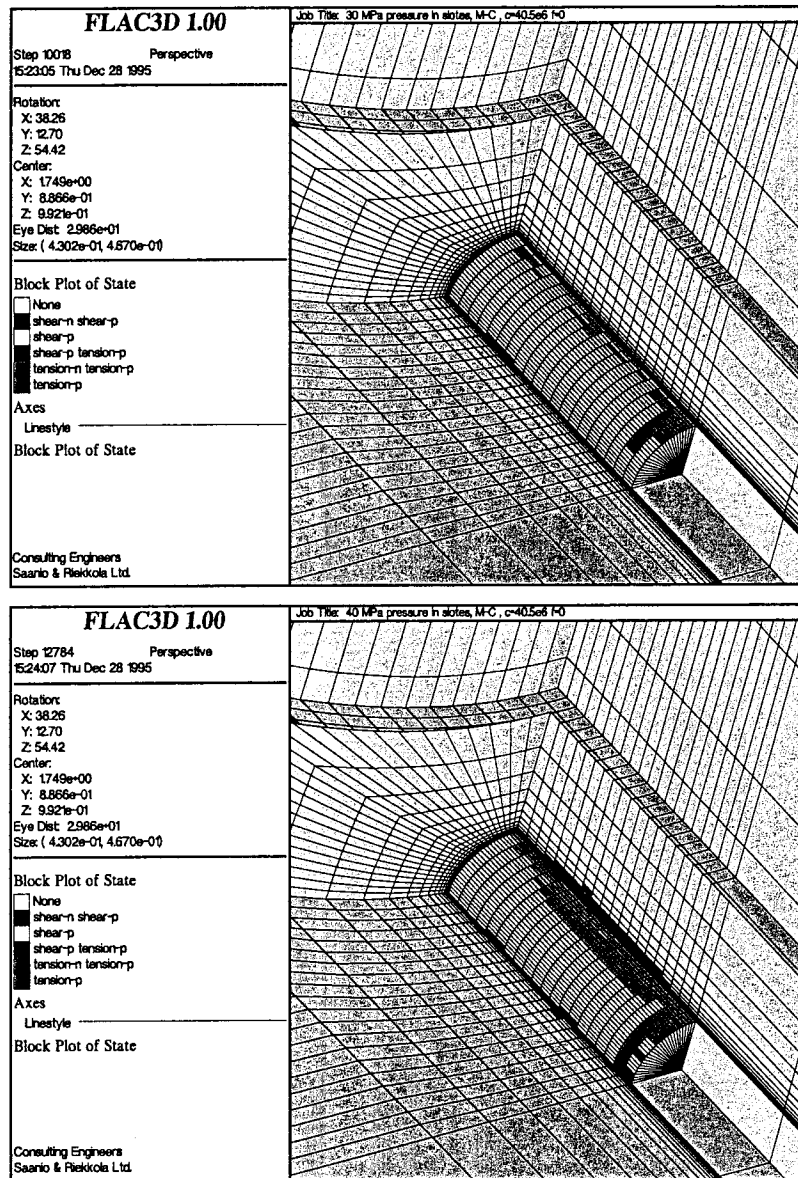


Figure 6-2. The result of modelling swelling pressures of 30 MPa (top) and 40 MPa (bottom) using the Mohr-Coulomb material model with criterion of type 3, cohesion 40.5 MPa, friction angle 0° .

The results of modelling using swelling pressure of 50 MPa with the Mohr-Coulomb material model with cohesion 26.6 MPa and friction angle of 23.5° , which is considered to be a satisfactory representation of the deformation surrounding the test hole, are shown in Figure 6-4. A vertical section taken parallel to the axis of the test hole is shown in Figure 6-4 and a horizontal section in Figure 6-5. The sections perpendicular to the test hole at positions shown in Figure 6-4 are shown in Figure 6-6 and 6-7.

None of the models used are directly applicable to the study of crack propagation and therefore modelling results obtained at levels of stress significantly higher than the failure level are considered to be unreliable.

In spite of the fact that the material models used in modelling were isotropic and there were evident inaccuracies in the estimated in-situ stresses some conclusion can be drawn concerning the feasibility of the test. The main results predicted by the modelling work described are:

- that failure will occur around the test hole,
- that failure will be initiated at relatively low swelling pressure levels (technically),
- that the areas in which failure will take place are on the top, bottom and sides of the holes (see Figure 6-1 and 6-2),
- that failure will also take place at the corners of the slots, and
- that failure on the surface of the full-scale deposition hole and at the corners of the slots will cause local unloading and stress re-distribution.

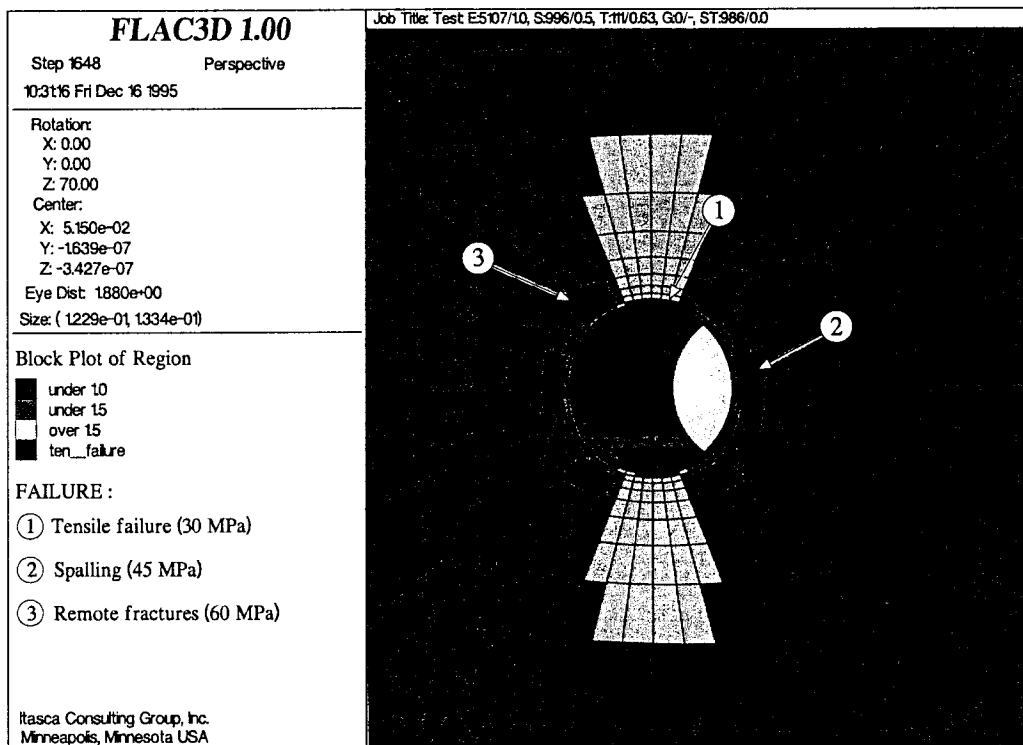


Figure 6-3. Vertical section taken perpendicular to the axis of test hole showing the modelled failure areas.

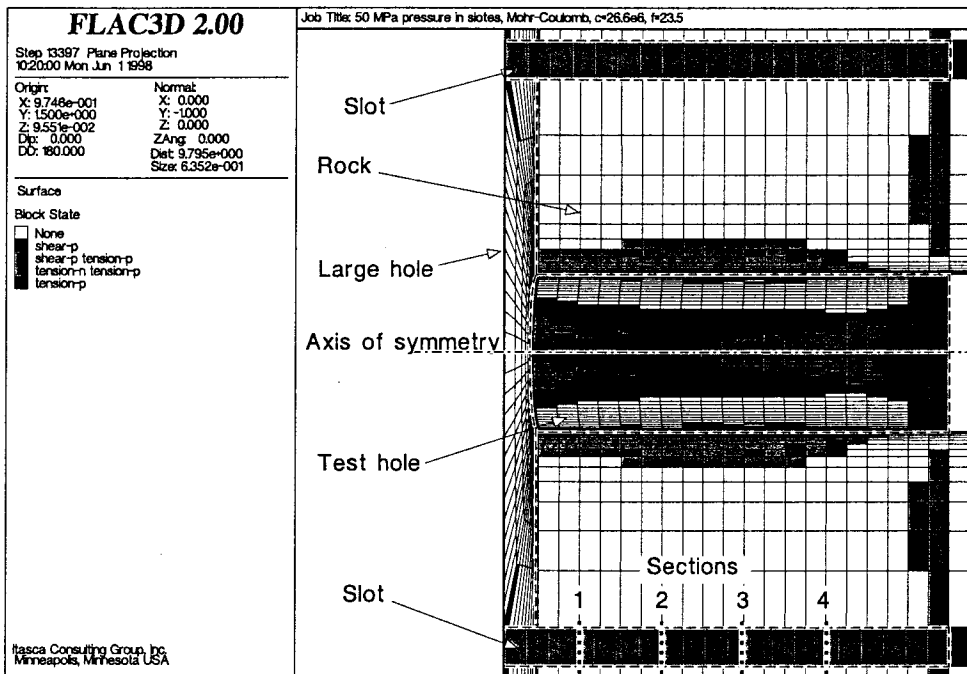
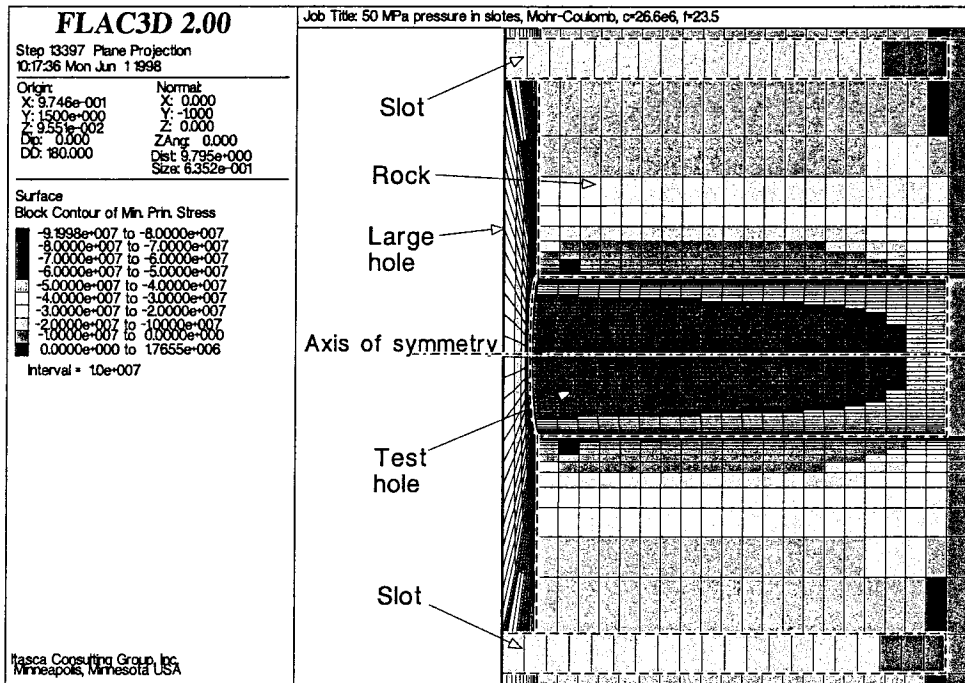


Figure 6-4. A vertical section taken parallel to the axis of the test hole showing state of stress (top) and state of failure (bottom), swelling pressure of 50 MPa with the Mohr-Coulomb material model of type 2 with cohesion 26.6 MPa and friction angle of 23.5°.

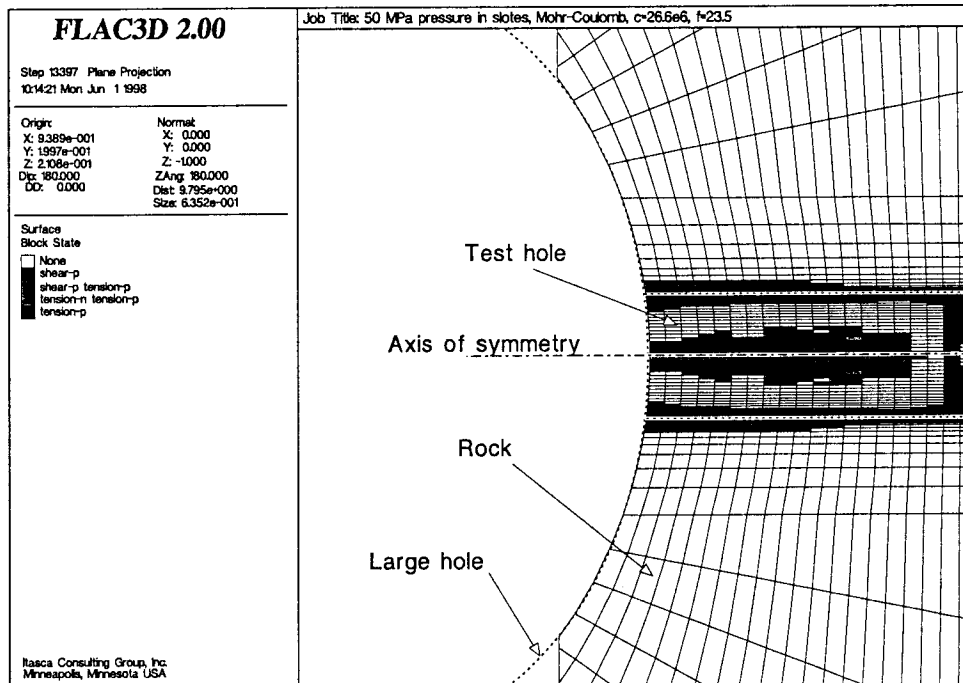
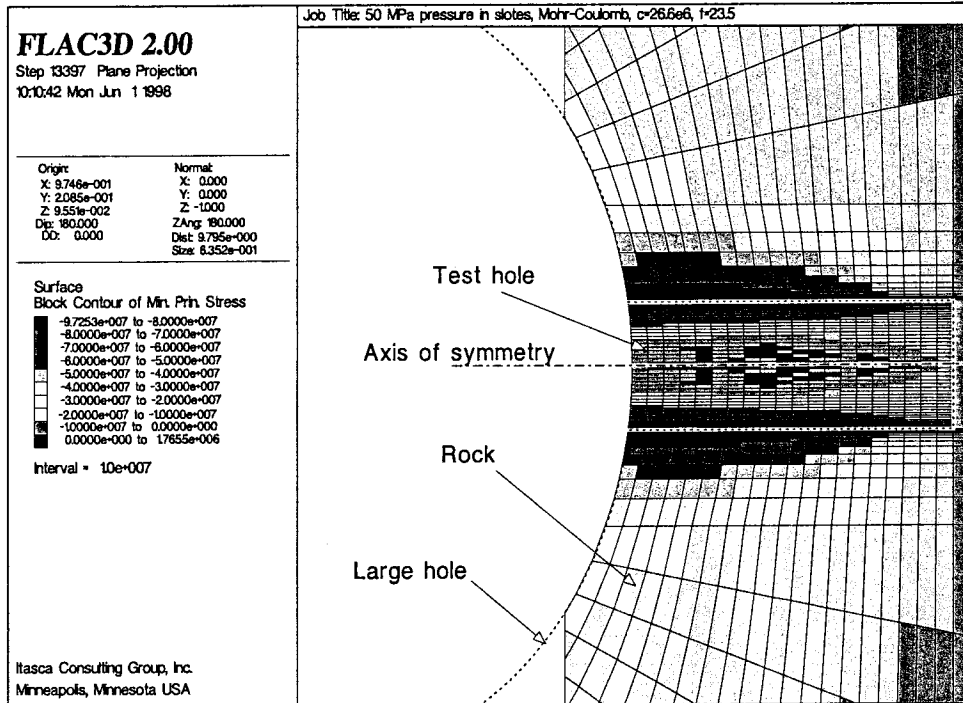
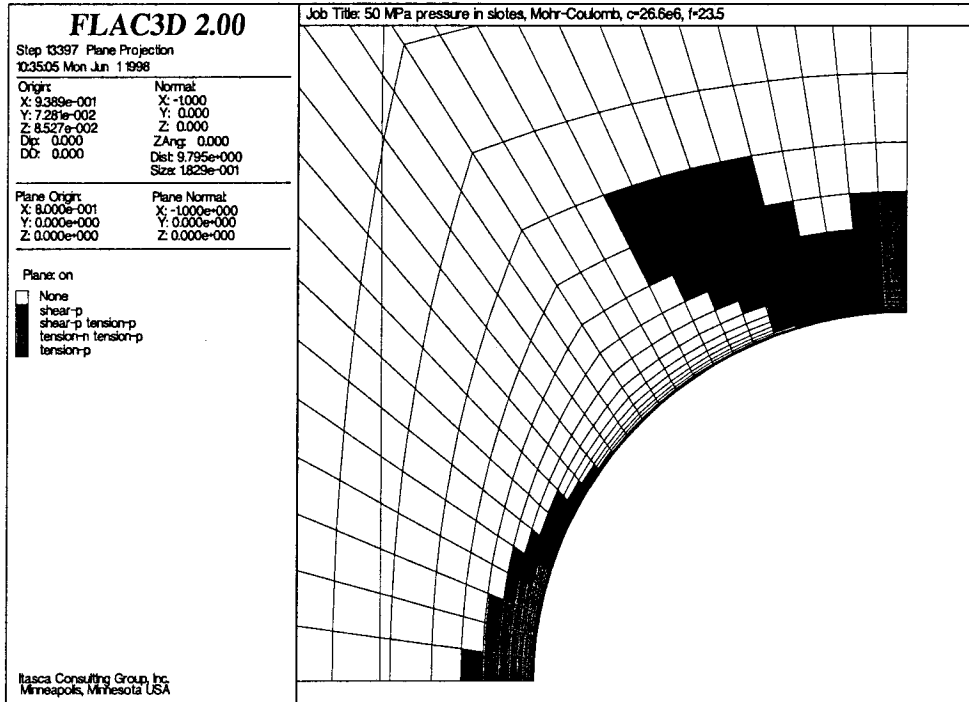


Figure 6-5. A horizontal section taken parallel to the axis of the test hole, showing state of stress (top) and state of failure (bottom), swelling pressure of 50 MPa with the Mohr-Coulomb material model of type 2 with cohesion 26.6 MPa and friction angle of 23.5°.

Section 1



Section 2

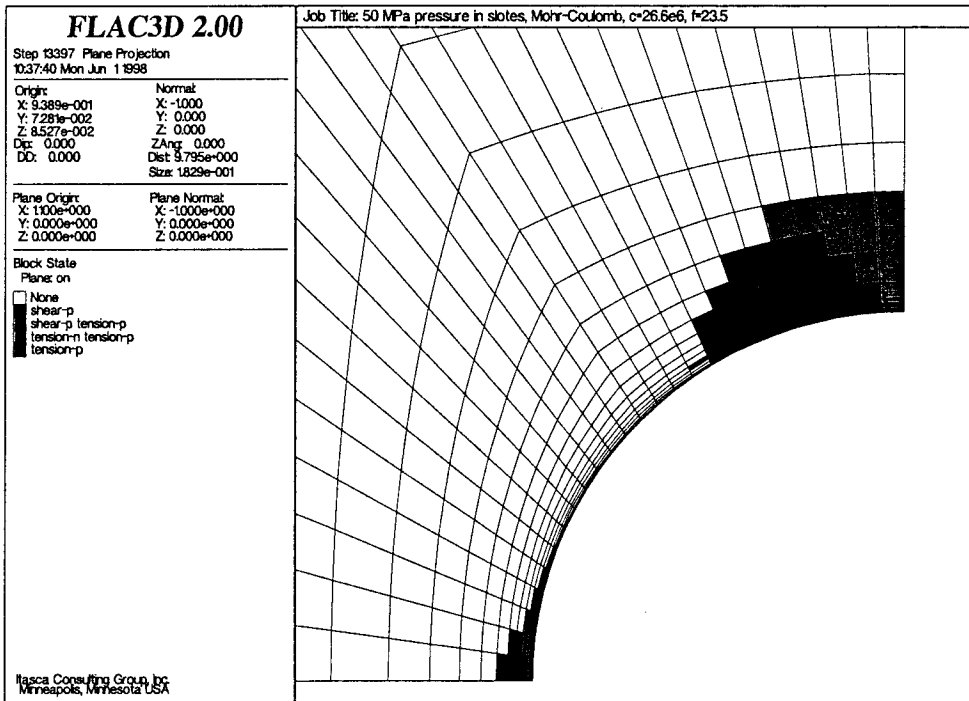
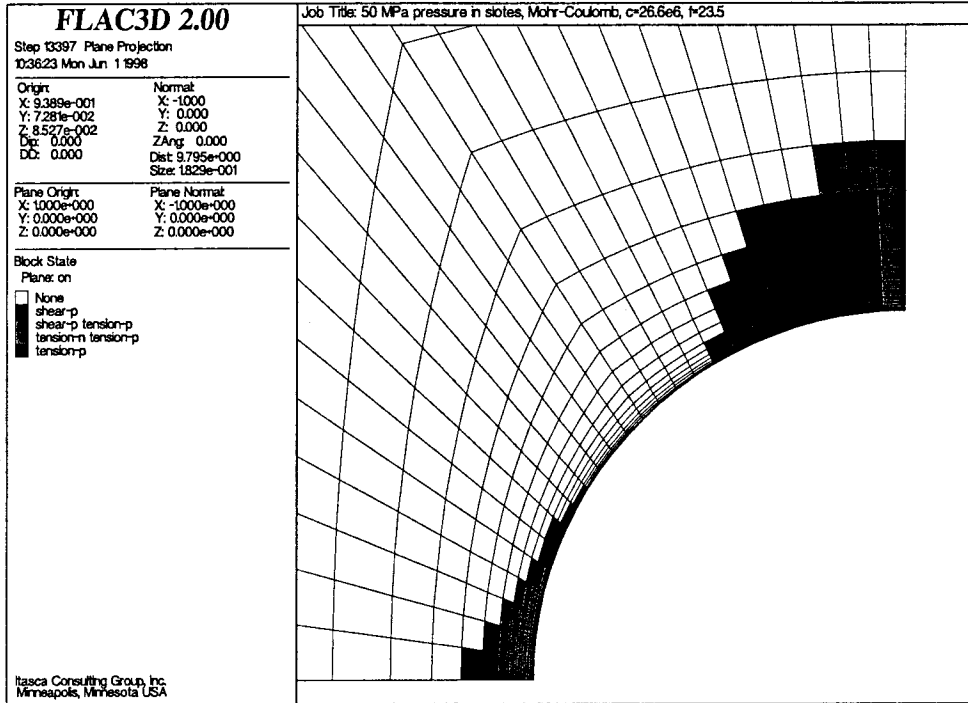


Figure 6-6. Sections 1 and 2 perpendicular to the test hole at positions shown in Figure 6-4 showing the states of failure, swelling pressure of 50 MPa with the Mohr-Coulomb material model of type 2 with cohesion 26.6 MPa and friction angle of 23.5°.

Section 3



Section 4

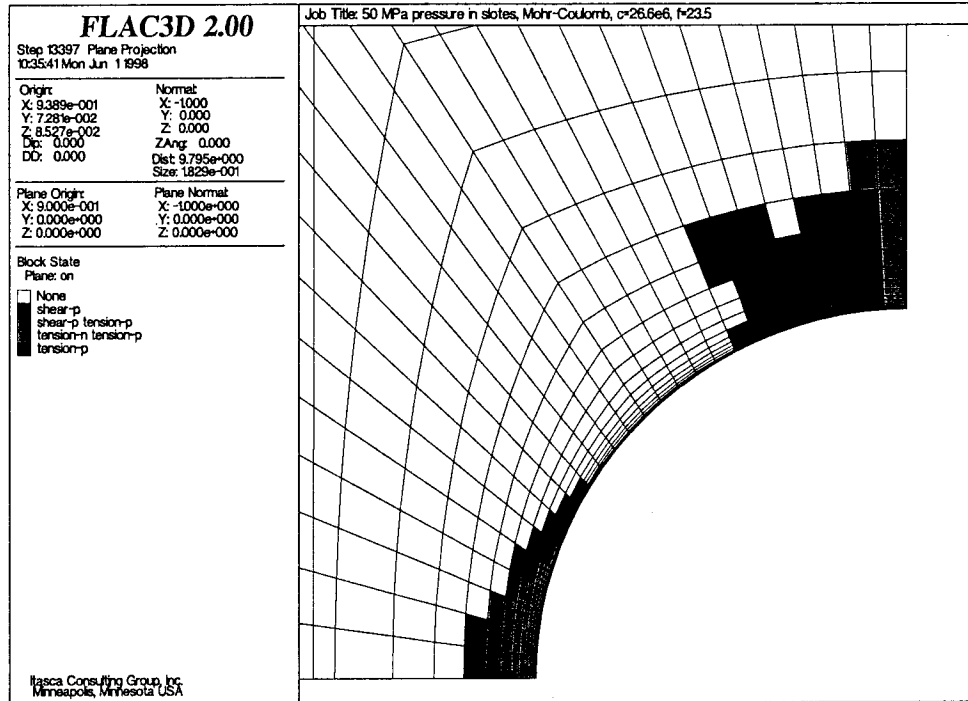


Figure 6-7. Sections 3 and 4 perpendicular to the test hole at positions shown in Figure 6-4 showing the states of failure, swelling pressure of 50 MPa with the Mohr-Coulomb material model of type 2 with cohesion 26.6 MPa and friction angle of 23.5°.

REFERENCES

- Haimson, C.B. & Song I. 1995.** A new borehole failure criterion for estimating in situ stress from breakout span. proc. of 8th Int. Congr. on Rock Mechanics. AA Balkema, Rotterdam.
- Itasca Consulting Group, 1994.** 3DEC, Three Dimensional Distinct Element Code. Version 1.5 manual. Itasca Consulting Group, Minneapolis.
- Itasca Consulting Group, 1995a.** FLAC^{2D}, Fast Lagrangian Analysis of Continua in Two Dimensions. Version 3.3-manual. Itasca Consulting Group, Minneapolis.
- Itasca Consulting Group, 1995b.** FLAC^{3D}, Fast Lagrangian Analysis of Continua in Three Dimensions. Version 1.0 manual. Itasca Consulting Group, Minneapolis.
- Johansson, E.&, Autio, J. 1993.** Rock Mechanical properties of intact rock in TVO's research tunnel. August 1993, TEKA-93-05
- Johansson, E. & Autio, J. 1995.** Properties of rock in TVO research tunnel and investigation sites. Work Report TEKA-95-10, Teollisuuden Voima Oy (TVO), Helsinki.
- Kuula, H. & Johansson, E. 1991.** Rock mechanical stability of the VLJ-repository. Helsinki, Nuclear Waste Commission of Finnish Power Companies, Report YJT-91-03. (In Finnish).
- Nykyri, M., Riekkola, R., Äikäs, K., Johansson, E. & Kuula, H. 1991.** Underground repository for low and intermediate level radioactive waste at Olkiluoto, Finland. Proc. of 7th Inr. Congr. on Rock Mechanics. AA Balkema, Rotterdam.
- Nykyri, M., Helenius, J., Johansson, E. & Nieminen, J. 1994.** Monitoring of the bedrock in the VLJ Repository in 1992. Work report VLJ 94-02. Teollisuuden Voima Oy, Helsinki (in Finnish).
- Äikäs, K. & Sacklén, N. 1993.** Fracture mapping in the Research Tunnel. Work Report 93-01, Teollisuuden Voima Oy, TVO/Research Tunnel, Helsinki.

APPENDICES

FLAC^{2D} MODELLING

1. Plasticity regions of FLAC^{2D} -model. The slots are horizontal. Friction is 55 degrees and cohesion 12.7 MPa. The width of slot is 500 mm.

3D TEST GEOMETRIES

2. First test geometry (slots are vertical).
3. Second test geometry (slots are horizontal).
4. Third test geometry (slots are horizontal, dimensions: L = 775 mm, W = 1000 mm).

FLAC^{3D} MODELLING

5. Lay-out of FLAC^{3D}-model (regions).
6. Closer lay-out of FLAC^{3D}-model (regions).
7. *In situ* principal stresses around deposition hole.
8. *In situ* principal stresses after borehole and slots are bored. Pressure is not applied for slots.
9. Principal stresses caused by 60 MPa pressure in slots. Elastic model. Slot dimensions: L = 500 mm, W = 500 mm, geometry in Appendix 1.
10. Principal stresses caused by 60 MPa pressure in slots. Elastic model. Slot dimensions: L = 500 mm, W = 1000 mm.
11. Principal stresses caused by 20 MPa pressure in slots. Elastic model. Slot dimensions: L = 775 mm, W = 1000 mm.
12. Principal stresses caused by 30 MPa pressure in slots. Elastic model. Slot dimensions: L = 775 mm, W = 1000 mm.
13. Principal stresses caused by 40 MPa pressure in slots. Elastic model. Slot dimensions: L = 775 mm, W = 1000 mm.
14. Principal stresses caused by 50 MPa pressure in slots. Elastic model. Slot dimensions: L = 775 mm, W = 1000 mm.
15. Principal stresses caused by 60 MPa pressure in slots. Elastic model. Slot dimensions: L = 775 mm, W = 1000 mm.
16. Mohr-Coulomb failure criteria of types 1, 2 and 3 used in modelling.
17. Safety factors Elastic model, M-C criterion: case-3, 30 MPa pressure in slots.
18. Safety factors, Elastic model, M-C criterion: case-3, 40 MPa pressure in slots.
19. Safety factors, Elastic model, M-C criterion: case-3, 50 MPa pressure in slots.
20. Safety factors, Elastic model, M-C criterion: case-3, 60 MPa pressure in slots.
21. Safety factors, Elastic model, M-C criterion: case-2, 30 MPa pressure in slots.
22. Safety factors, Elastic model, M-C criterion: case-2, 40 MPa pressure in slots.
23. Safety factors, Elastic model, M-C criterion: case-2, 50 MPa pressure in slots.
24. Safety factors, Elastic model, M-C criterion: case-2, 60 MPa pressure in slots.
25. Safety factors, Elastic model, M-C criterion: case-1, 30 MPa pressure in slots.
26. Safety factors, Elastic model, M-C criterion: case-1, 40 MPa pressure in slots.

27. Safety factors, Elastic model, M-C criterion: case-1, 50 MPa pressure in slots.
28. Safety factors, Elastic model, M-C criterion: case-1, 60 MPa pressure in slots.
29. Safety factors, Elastic model, Mogi's criterion, 30 MPa pressure in slots.
30. Safety factors, Elastic model, Mogi's criterion, 40 MPa pressure in slots.
31. Safety factors, Elastic model, Mogi's criterion, 50 MPa pressure in slots.
32. Safety factors, Elastic model, Mogi's criterion, 60 MPa pressure in slots.
33. Plasticity regions, Mohr-Coulomb, M-C criterion: case-1, 30 MPa pressure in slots.
34. Plasticity regions, Mohr-Coulomb, M-C criterion: case-1, 40 MPa pressure in slots.
35. Plasticity regions, Mohr-Coulomb, M-C criterion: case-1, 50 MPa pressure in slots.
36. Plasticity regions, Mohr-Coulomb, M-C criterion: case-1, 60 MPa pressure in slots.
37. Plasticity regions, Mohr-Coulomb, M-C criterion: case-3, 30 MPa pressure in slots.
38. Plasticity regions, Mohr-Coulomb, M-C criterion: case-3, 40 MPa pressure in slots.
39. Plasticity regions, Mohr-Coulomb, M-C criterion: case-3, 50 MPa pressure in slots.
40. Plasticity regions, Mohr-Coulomb, M-C criterion: case-3, 60 MPa pressure in slots.
41. Plasticity regions, Mohr-Coulomb, M-C criterion: case-2, 30 MPa pressure in slots.
42. Plasticity regions, Mohr-Coulomb, M-C criterion: case-2, 40 MPa pressure in slots.
43. Plasticity regions, Mohr-Coulomb, M-C criterion: case-2, 50 MPa pressure in slots.
44. Plasticity regions, Mohr-Coulomb, M-C criterion: case-2, 60 MPa pressure in slots.
45. Plasticity regions, Strain-softening model, 30 MPa pressure in slots.
46. Plasticity regions, Strain-softening model, 40 MPa pressure in slots.
47. Plasticity regions, Strain-softening model, 50 MPa pressure in slots.
48. Plasticity regions, Strain-softening model, 60 MPa pressure in slots.
49. Displacements around the centre hole in a perpendicular section to the hole axis at in situ stresses of 2.56-1.21-1.
50. Displacements around the centre hole in a perpendicular section to the hole axis at in situ stresses of 5.12-2.42-1 MPa.
51. Displacements around the centre hole in a perpendicular section to the hole axis at in situ stresses of 10.24-4.84-1 MPa.
52. Displacements around the centre hole at in situ stresses of 5.12-2.42-1 MPa.

JOB TITLE: (File:pyst10.dat) Crack pres. 60 MPa, M-C: f i=55, C=12.7, ten=8.4, E=58.3, v=0.25

FLAC (Version 3.30)

LEGEND

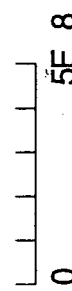
10/19/1995 14:30
 step 10025
 -5.000E-02 <x< 4.000E-01
 -5.000E-02 <y< 4.000E-01

Boundary plot



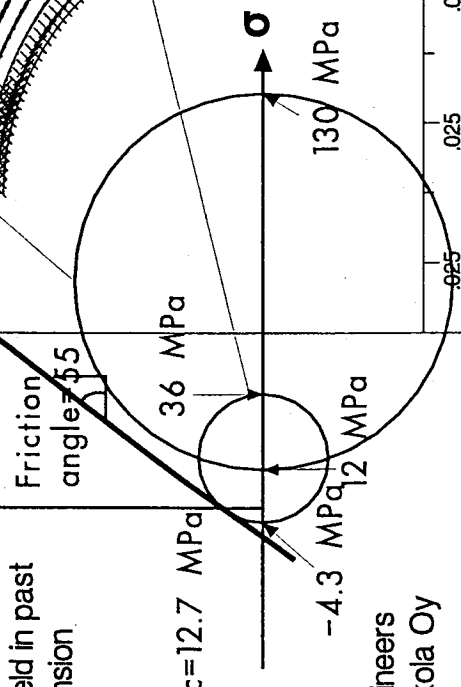
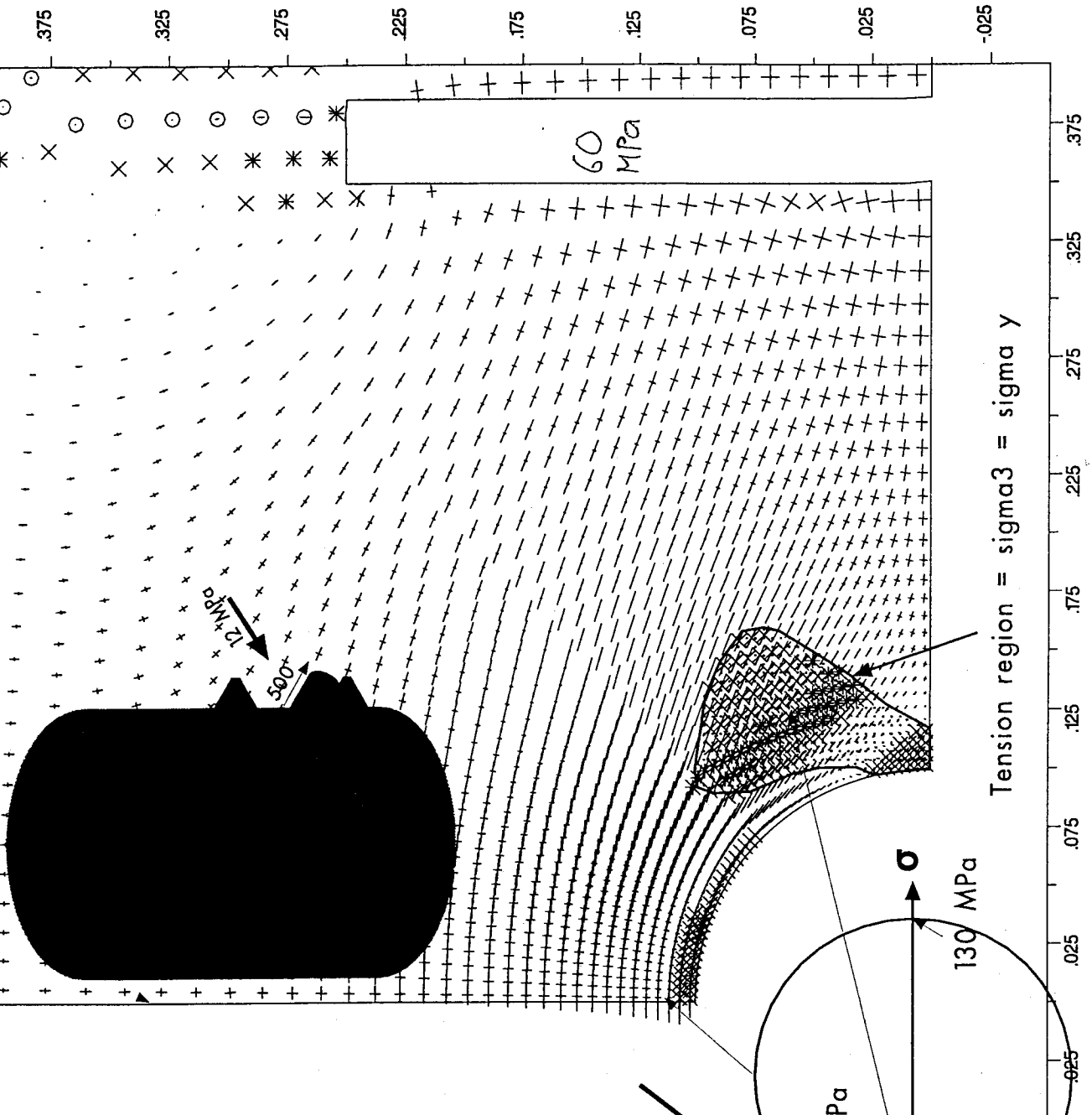
Principal stresses

Max. Value = 1.411E+08

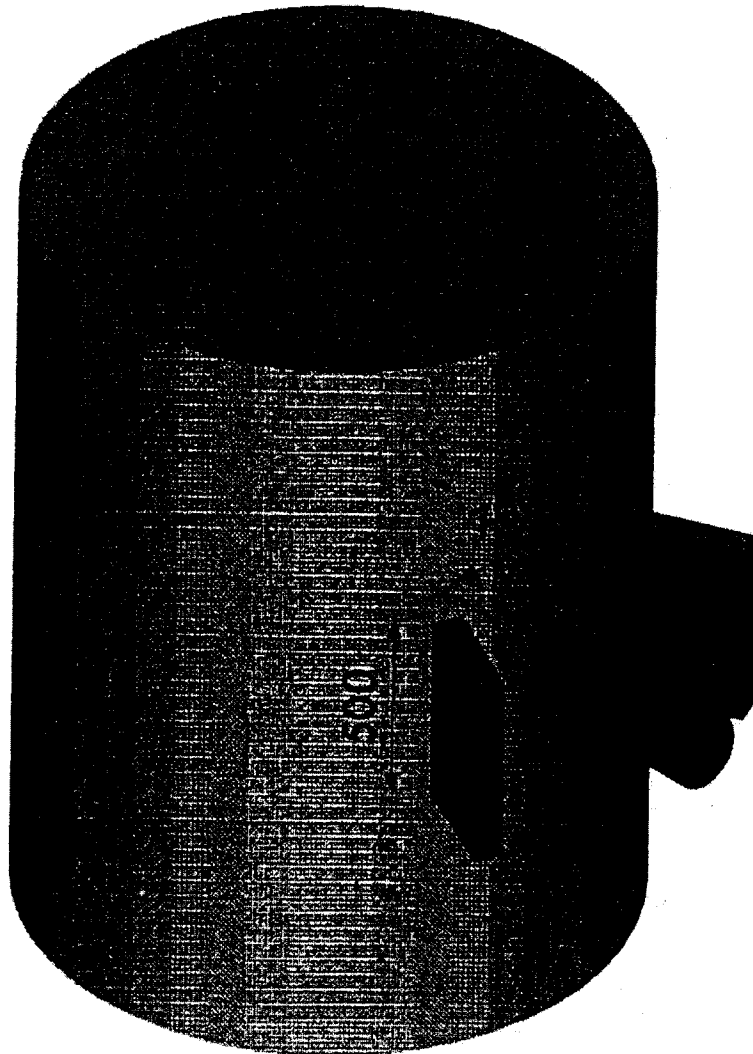
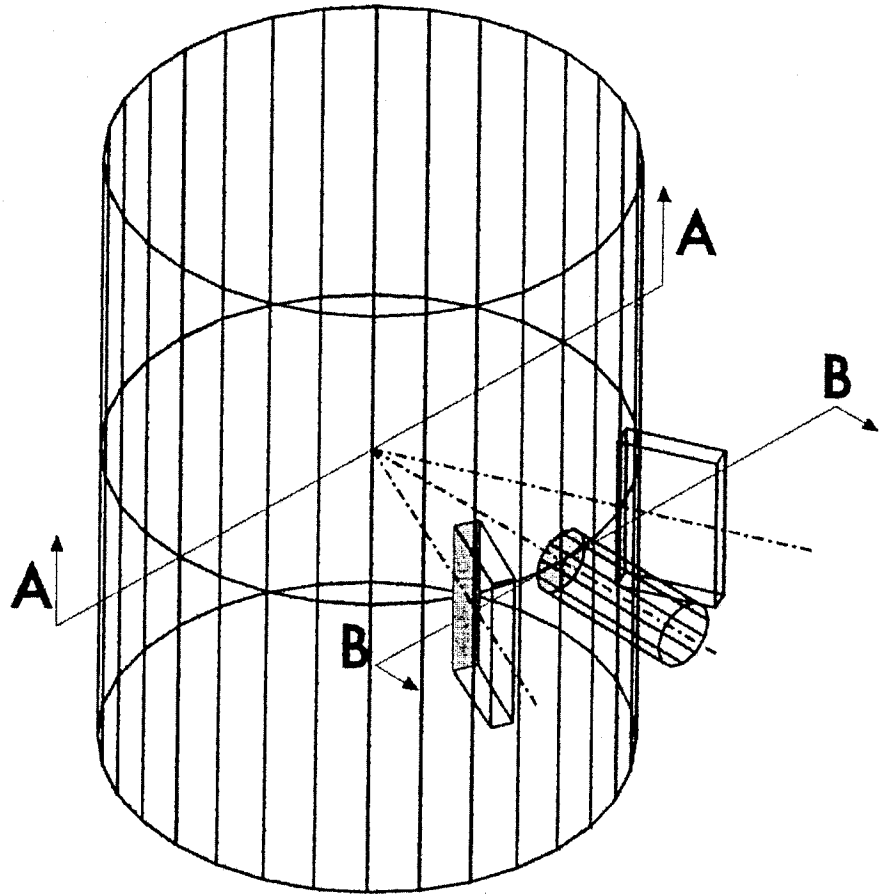


Plasticity Indicator

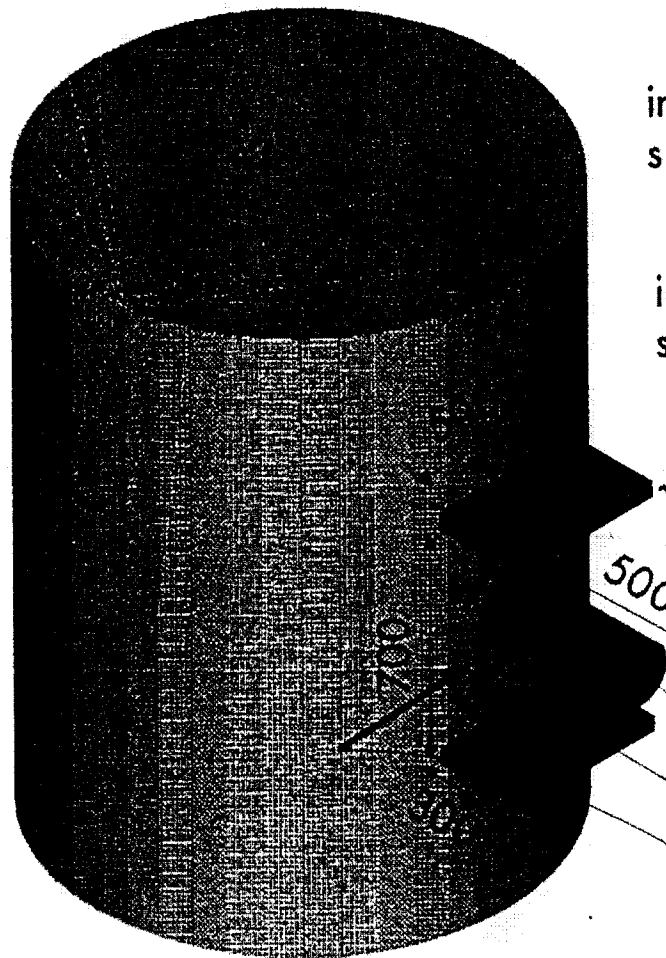
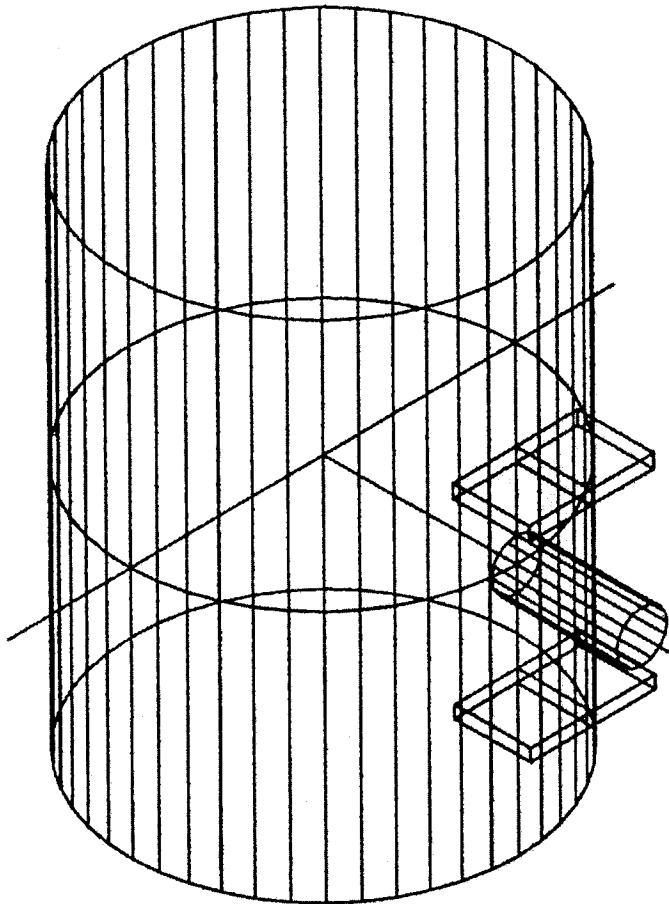
- * at yield in shear or vol.
- X elastic, at yield in past
- o at yield in tension



Consulting Engineers
 Saario & Riekkola Oy

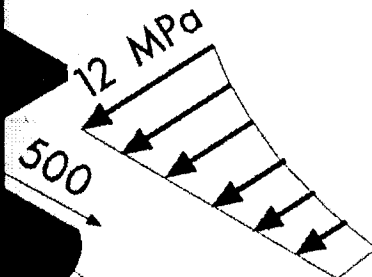


TEST GEOMETRY : 2



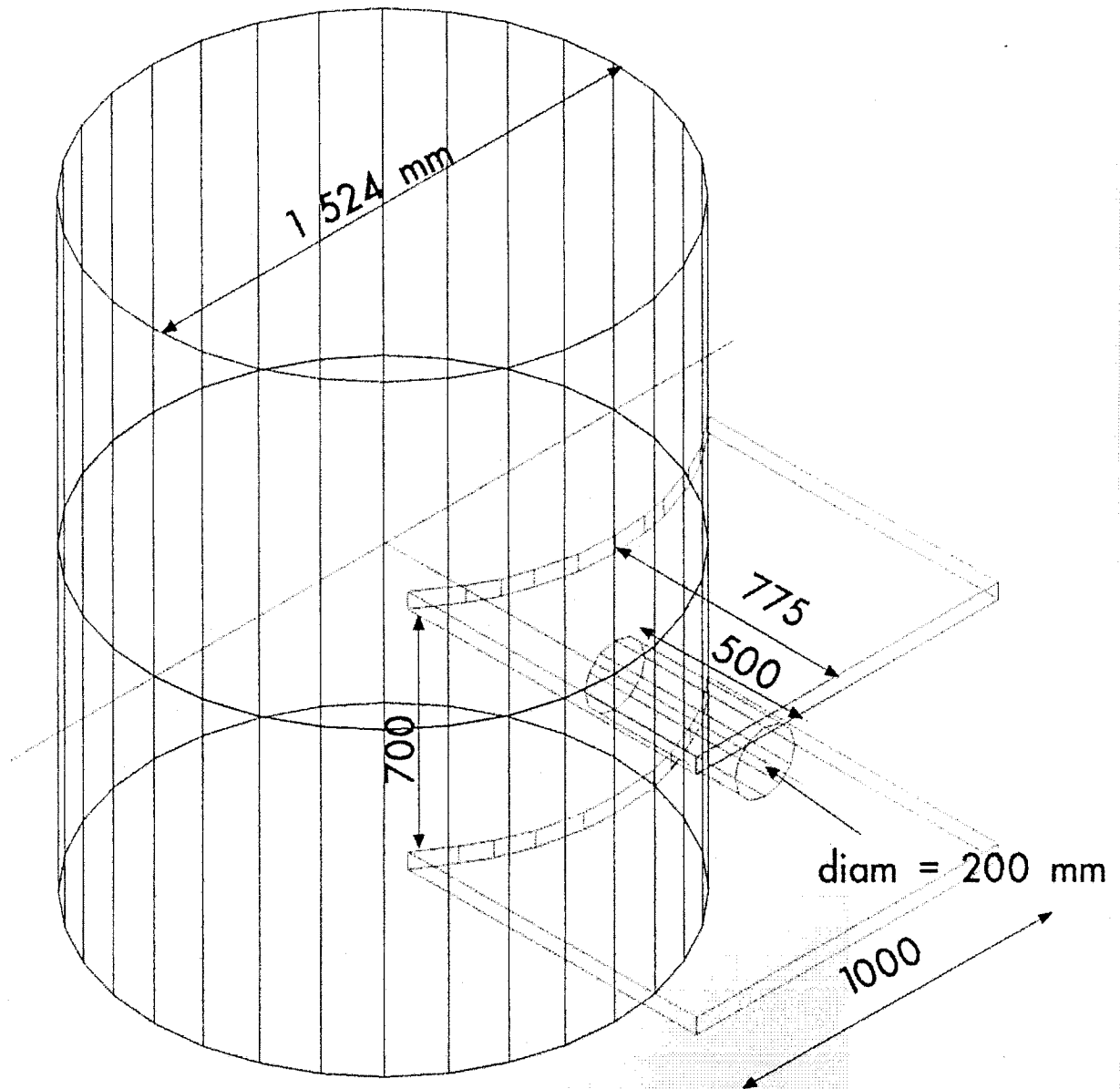
insitu primary
signal = 5.12 MPa

insitu secondary
signal max = 12 MPa



diam = 200 mm

TEST GEOMETRY : 4



Job Title: Inshu state

FLAC3D 1.00

Step 3232 Perspective

10:20:52 Fri Jan 5 1996

Rotation:

X: 330.00

Y: 0.00

Z: 40.00

Center:

X: 1264e+00

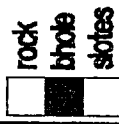
Y: 1279e+00

Z: 5.653e-01

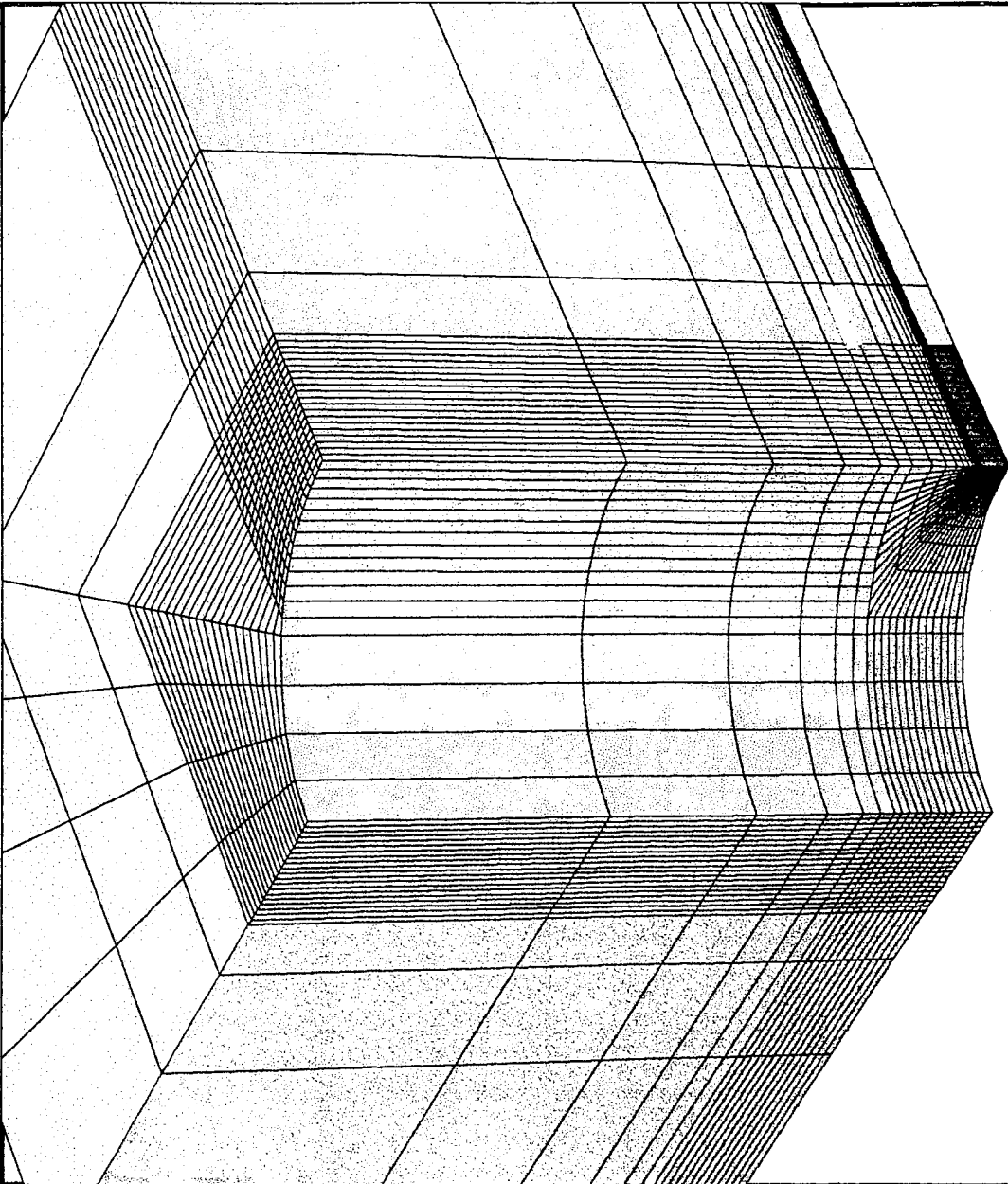
Eye Dist: 2.866e+01

Size: (1.891e+00, 2.053e+00)

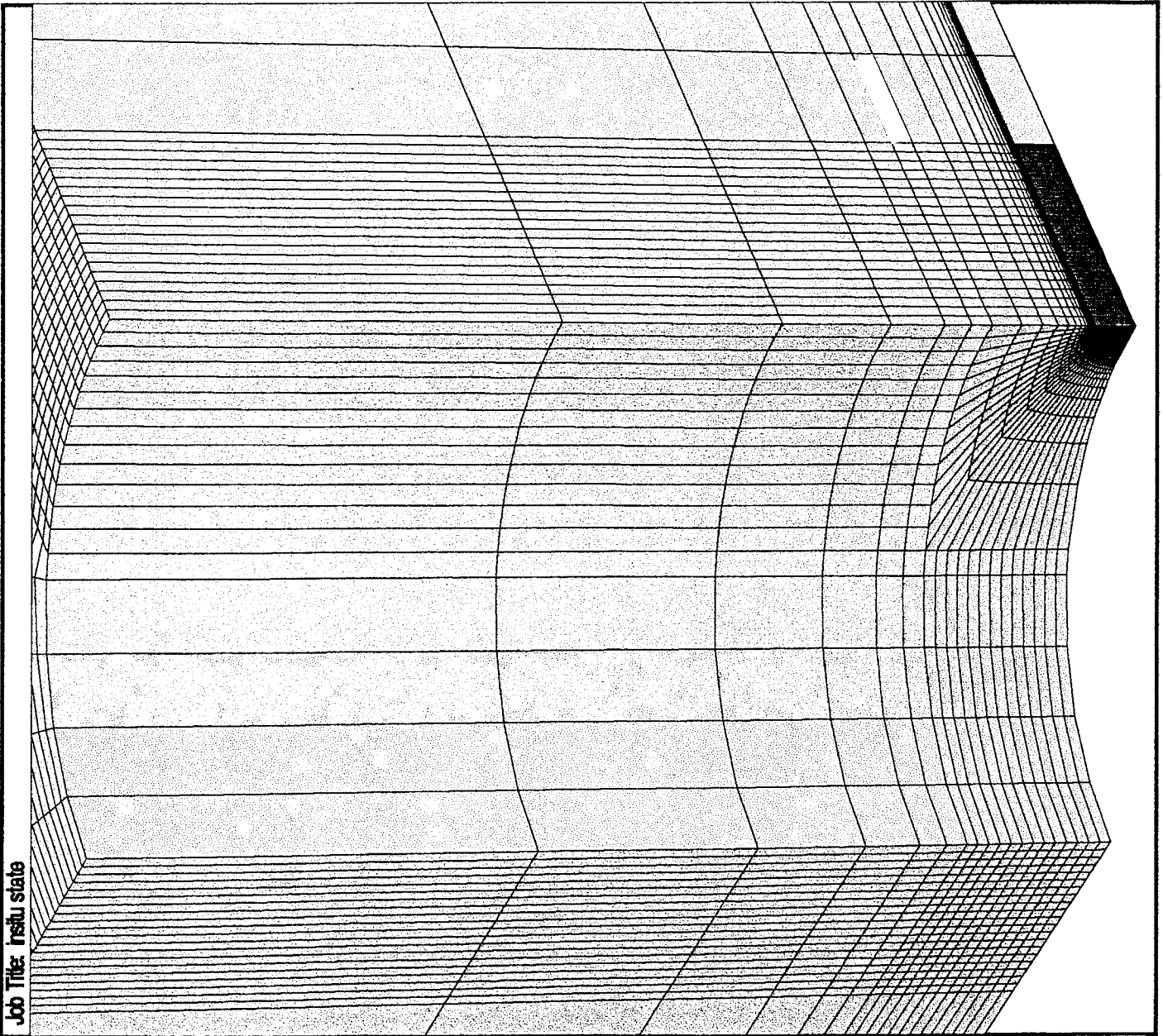
Block Plot of Region



Itasca Consulting Group, Inc.
Minneapolis, Minnesota USA



Job Title: instu state



FLAC3D 1.00

Step 3232 Perspective

103201Fri Jan 5 1996

Rotation:

X: 330.00

Y: 0.00

Z: 40.00

Center:

X: 1264e+00

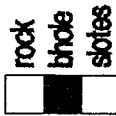
Y: 1219e+00

Z: 5.653e-01

Eye Dist: 2.886e+01

Size: (1102e+00, 1198e+00)

Block Plot of Region



Itasca Consulting Group, Inc.
Minneapolis, Minnesota USA

Job Title: insitu state

FLAC3D 1.00

Perspective

Step 3232
10:35:33 Fri Jan 5 1996

Rotation: σ_1 primary = 5.1 MPa

X: 330.00

Y: 0.00

Z: 40.00

Center:

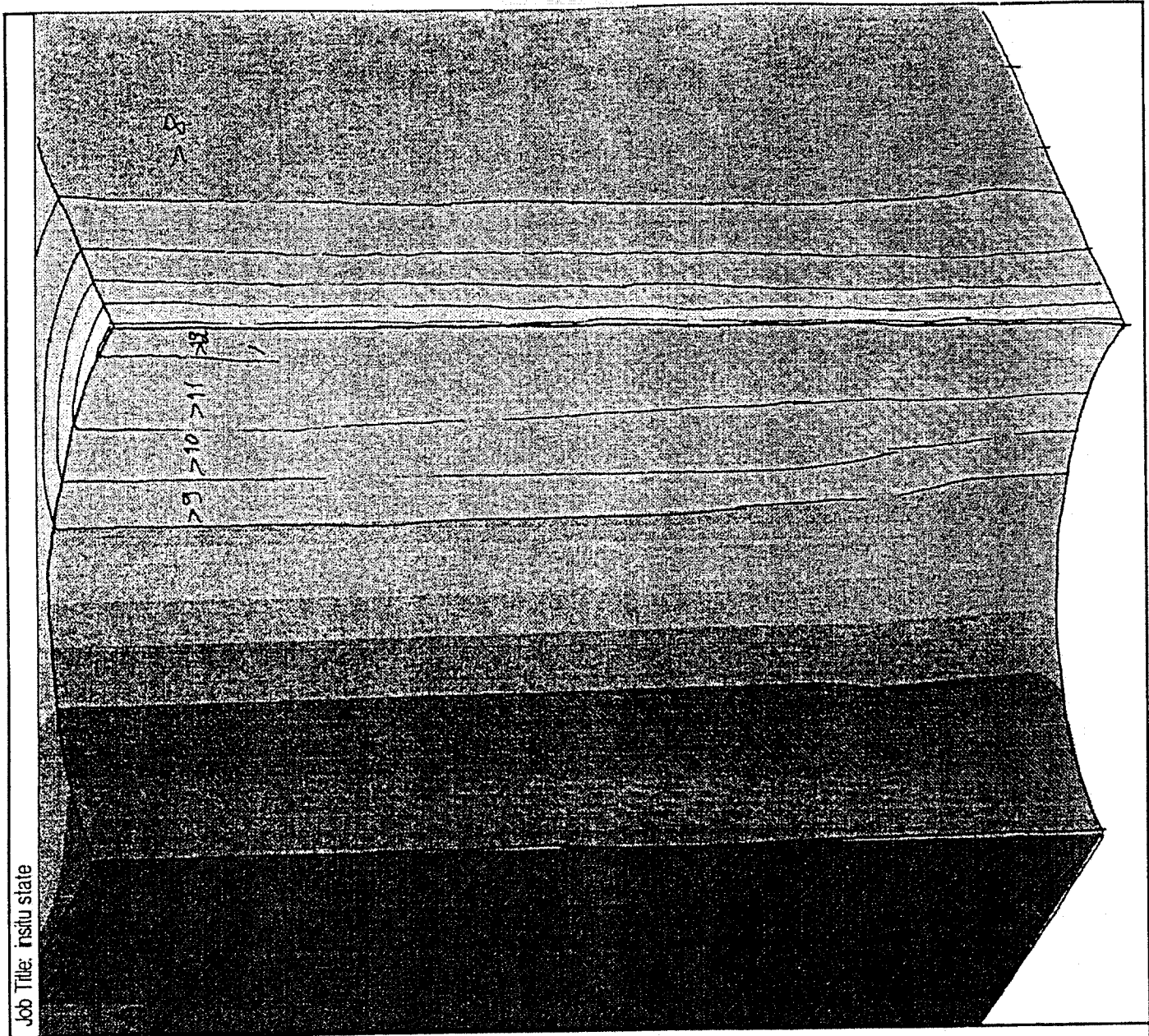
X: 1264e+00

Y: 1219e+00

Z: 5653e-01

Eye Dist: 2886e+01

Size: (102e+00, 1196e+00)



Contour of Min. Prin. Stress σ_1

	-12319e+07 to -12000e+07	> 12	MPa
	-12000e+07 to -11000e+07	> 11	MPa
	-11000e+07 to -10000e+07	> 10	MPa
	-10000e+07 to -90000e+06	> 9	MPa
	-90000e+06 to -80000e+06	> 8	MPa
	-80000e+06 to -70000e+06	> 7	MPa
	-70000e+06 to -60000e+06	> 6	
	-60000e+06 to -50000e+06		
	-50000e+06 to -40000e+06		
	-40000e+06 to -30000e+06		
	-30000e+06 to -20000e+06		
	-20000e+06 to -19863e+06		

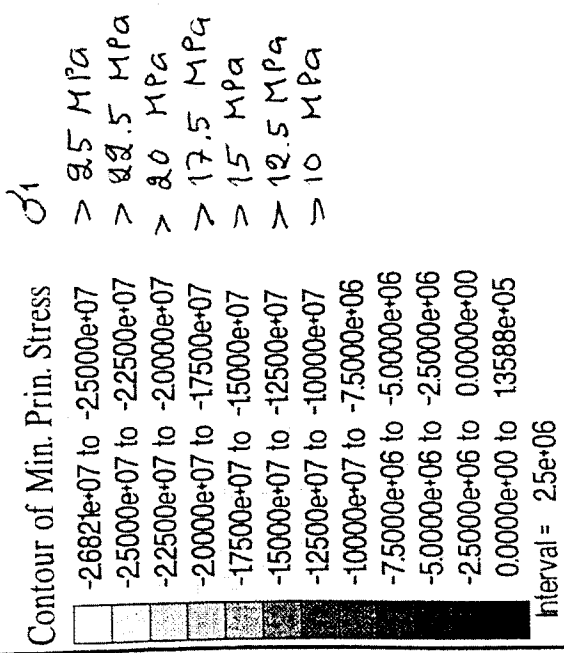
Interval = 10e+06

Job Title: slots and borehole

FLAC3D 1.00

Step 4371 Perspective
 1107:52 Fri Jan 5 1996

Rotation
 X: 38.26
 Y: 12.70
 Z: 54.42
 Center:
 X: 1749e+00
 Y: 8.866e-01
 Z: 9.921e-01
 Eye Dist: 2.986e+01
 Size: (4.302e-01, 4.670e-01)



Itasca Consulting Group, Inc.
 Minneapolis, Minnesota USA

Job Title: 60 MPa pressure in slots, elastic model

FLAC3D 1.00

Step 5752 Perspective

1100:53 Sun Dec 17 1995

Rotation:

X: 10.65

Y: 2.79

Z: 71.97

Center:

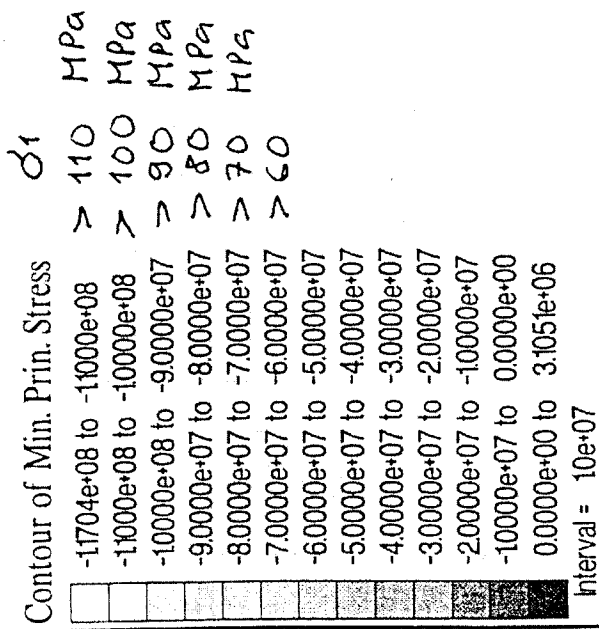
X: 1.963e+00

Y: 5.767e-01

Z: 4.355e-01

Eye Dist: 3.031e+01

Size: (4.302e-01, 4.670e-01)



Itasca Consulting Group, Inc.
 Minneapolis, Minnesota USA

FLAC3D 1.00

Step 17183 Perspective

11:45:57 Fri Dec 15 1995

Rotation:

X: 10.65

Y: 2.79

Z: 7.197

Center:

X: 1963e+00

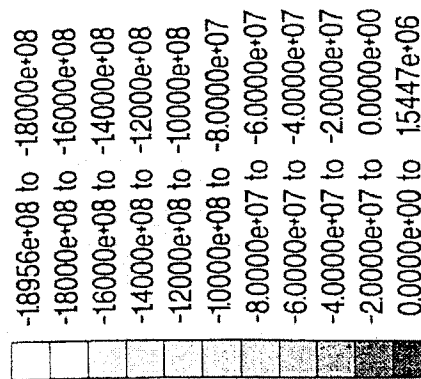
Y: 5.767e-01

Z: 4.355e-01

Eye Dist: 3.031e+01

Size: (4.302e-01, 4.670e-01)

Contour of Min. Prin. Stress

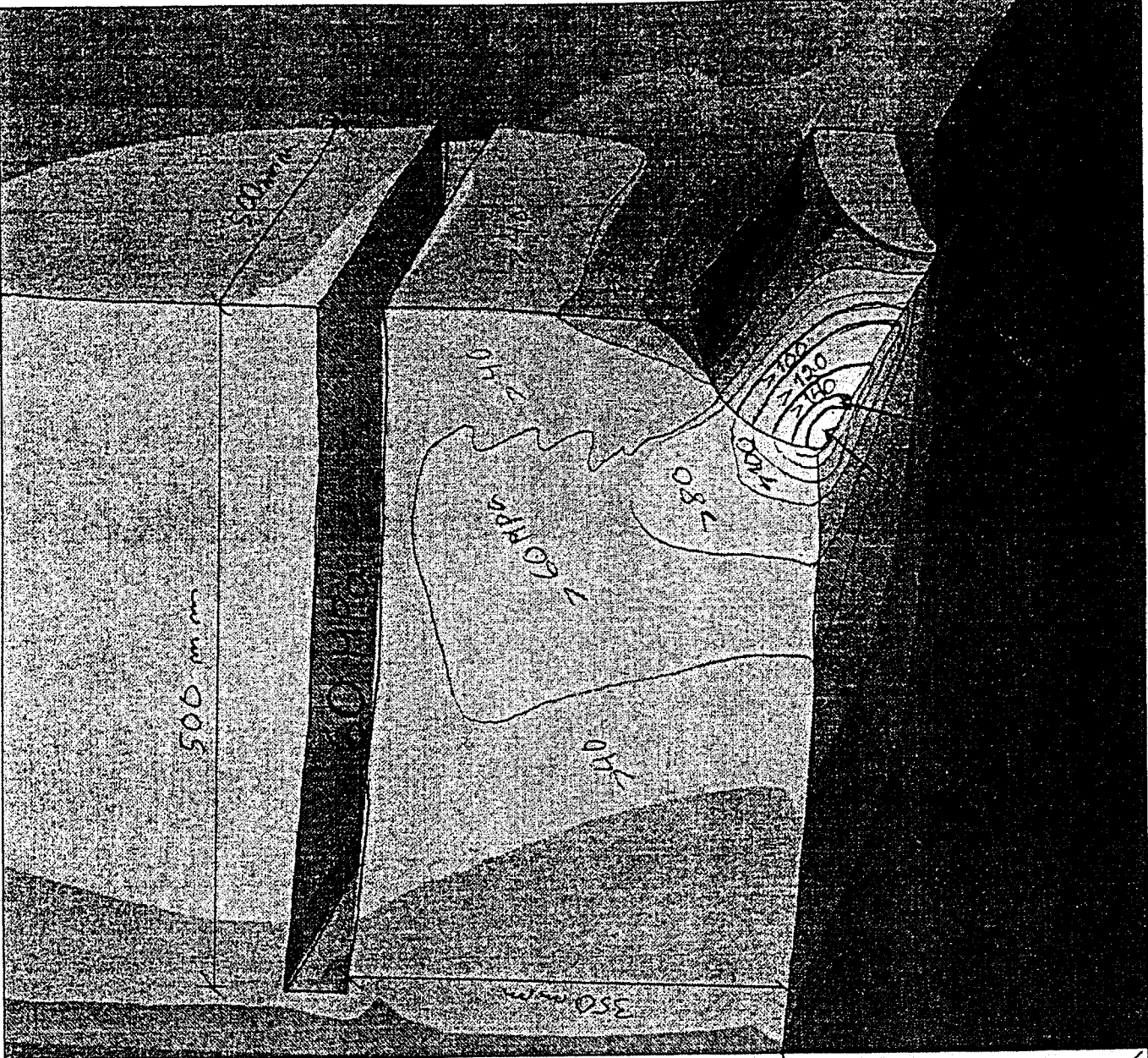


σ_1

- > 180 MPa
- > 160 MPa
- > 140 MPa
- > 120 MPa
- > 100 MPa

*max/min
pohja*

Job Title: 60 MPa pressure in slotes, elastic, file depl.dat



Job Title: 20 MPa pressure in slots, elastic, C=26.6e6, f=23.5

FLAC3D 1.00

Step 6352 Perspective
 10:52:56 Thu Dec 21 1995

Rotation
 X: 38.26
 Y: 12.70
 Z: 54.42
 Center.
 X: 1749e+00
 Y: 8866e-01
 Z: 9921e-01
 Eye Dist: 2986e+01
 Size: (4.302e-01, 4.670e-01)

Contour of Min. Prin. Stress	σ_1
-4.0418e+07 to -4.0000e+07	> 40 MPa
-3.7500e+07 to -3.5000e+07	> 35 MPa
-3.2500e+07 to -3.0000e+07	> 30 MPa
-2.7500e+07 to -2.5000e+07	> 25 MPa
-2.2500e+07 to -2.0000e+07	> 20 MPa
-1.7500e+07 to -1.5000e+07	> 15 MPa
-1.2500e+07 to -1.0000e+07	> 10 MPa
-7.5000e+06 to -5.0000e+06	> 5 MPa
-2.5000e+06 to -2.0660e+06	
Interval = 2.5e+06	

Itasca Consulting Group, Inc.
 Minneapolis, Minnesota USA

Job Title: 30 MPa pressure in slots, elastic, C=26.6e6, f=23.5

FLAC3D 1.00

Step 9156 Perspective

10:53:58 Thu Dec 21 1995

Rotation

X: 38.26

Y: 12.70

Z: 54.42

Center:

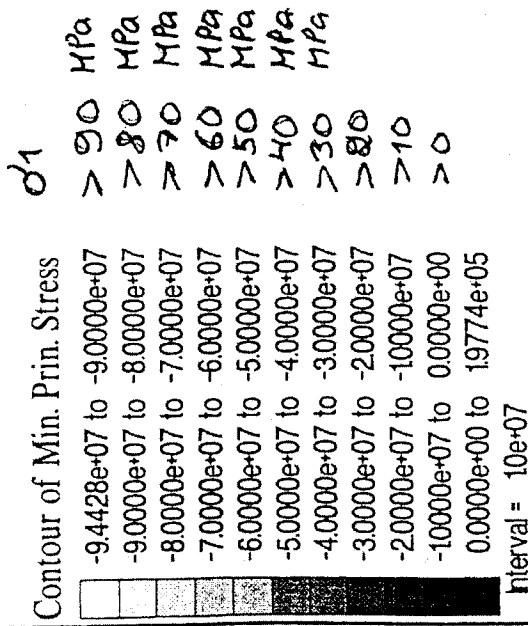
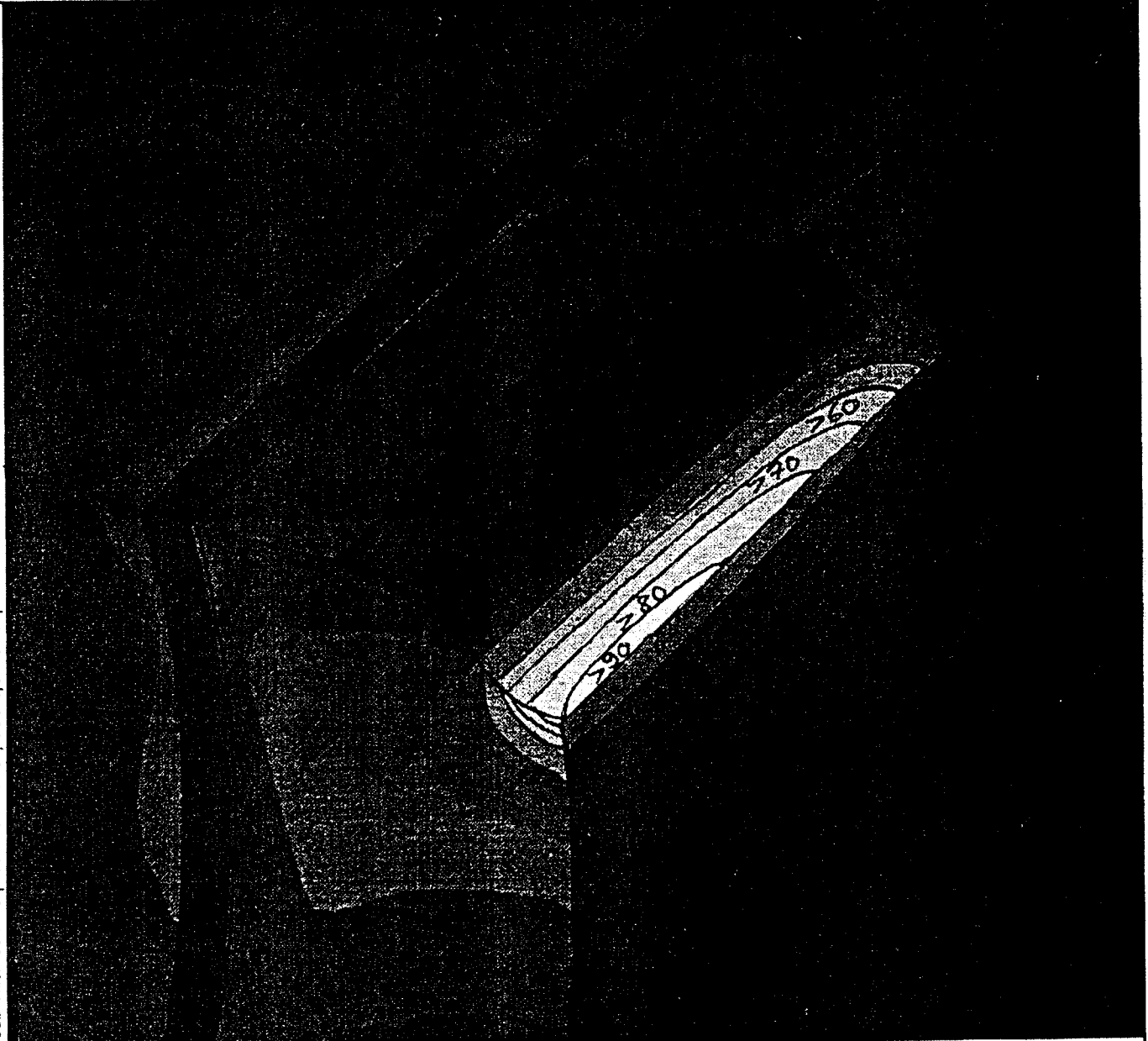
X: 1749e+00

Y: 8.866e-01

Z: 9.921e-01

Eye Dist 2986e+01

Size: (4.302e-01 4.670e-01)



Job Title: 40 MPa pressure in soles, elastic, C=26.6e6, f=23.5

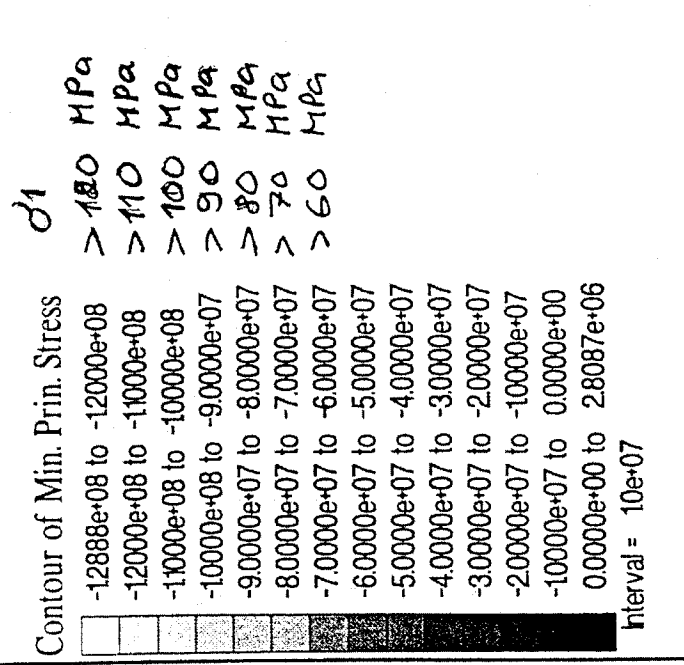
FLAC3D 1.00

Step 12324 Perspective
 10:55:03 Thu Dec 21 1995

Rotation
 X: 38.26
 Y: 12.70
 Z: 54.42

Center:
 X: 1749e+00
 Y: 8866e-01
 Z: 9921e-01

Eye Dist: 2986e+01
 Size: (4.302e-01, 4.670e-01)



Itasca Consulting Group, Inc.
 Minneapolis, Minnesota USA

Job Title: 50 MPa pressure in soles, elastic, C=266, f=23.5

FLAC3D 1.00

Step 15629 Perspective
 10:56:15 Thu Dec 21 1995

Rotation:

X: 38.26

Y: 12.70

Z: 54.42

Center:

X: 1749e+00

Y: 8.866e-01

Z: 9.921e-01

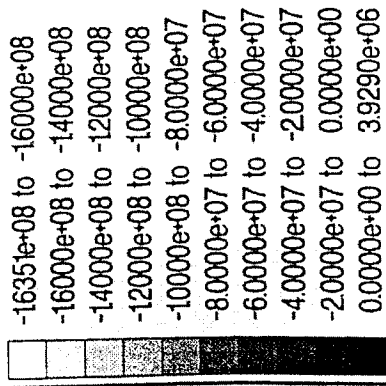
Eye Dist 2986e+01

Size: (4.302e-01, 4.670e-01)

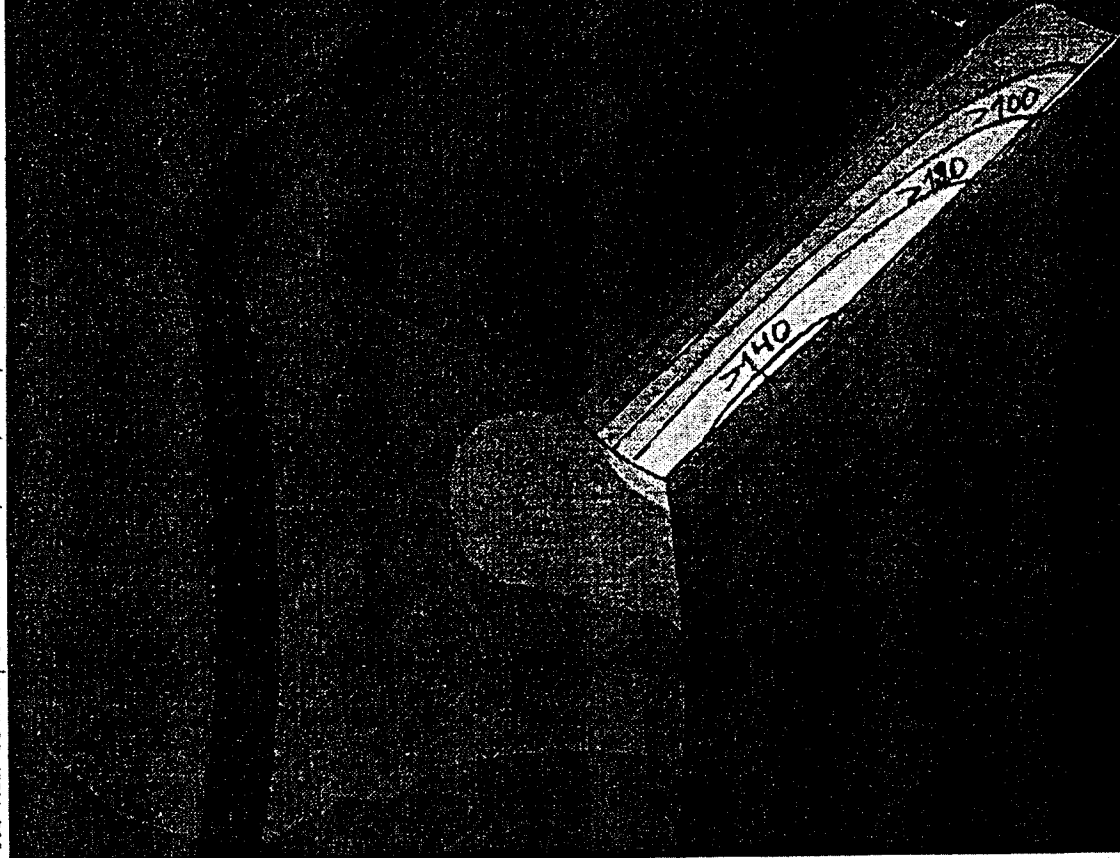
σ_1

> 160	MPa
> 140	MPa
> 120	MPa
> 100	MPa
> 80	MPa
> 60	MPa

Contour of Min. Prin. Stress



Interval = 2.0e+07



Job Title: 60 MPa pressure in slots, elastic,C=26.6e6, f=23.5

FLAC3D 1.00

Step 18853 Perspective

10:57:32 Thu Dec 21 1995

Rotation

X: 38.26

Y: 12.70

Z: 54.42

Center:

X: 1749e+00

Y: 8.866e-01

Z: 9921e-01

Eye Dist 2986e+01

Size: (4.302e-01 4.670e-01)

σ_1

>175	MPa
>150	MPa
>125	MPa
>100	MPa
>75	MPa
>50	MPa

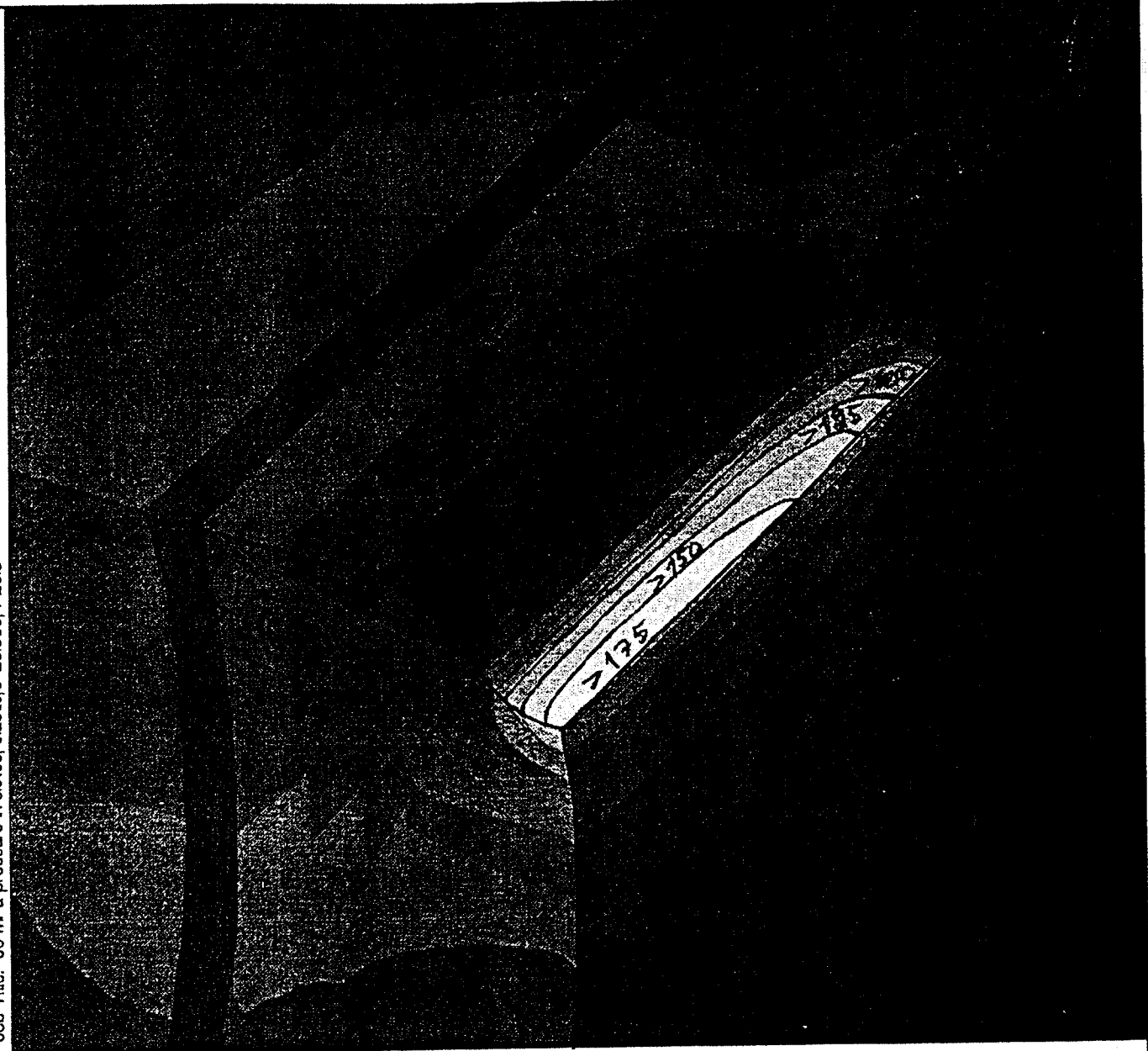
Contour of Min. Prin. Stress

- 19816e+08 to -17500e+08
- 17500e+08 to -15000e+08
- 15000e+08 to -12500e+08
- 12500e+08 to -10000e+08
- 10000e+08 to -75000e+07
- 75000e+07 to -50000e+07
- 50000e+07 to -25000e+07
- 25000e+07 to 0.0000e+00
- 0.0000e+00 to 4.7961e+06



Interval = 25e+07

Itasca Consulting Group, Inc.
 Minneapolis, Minnesota USA



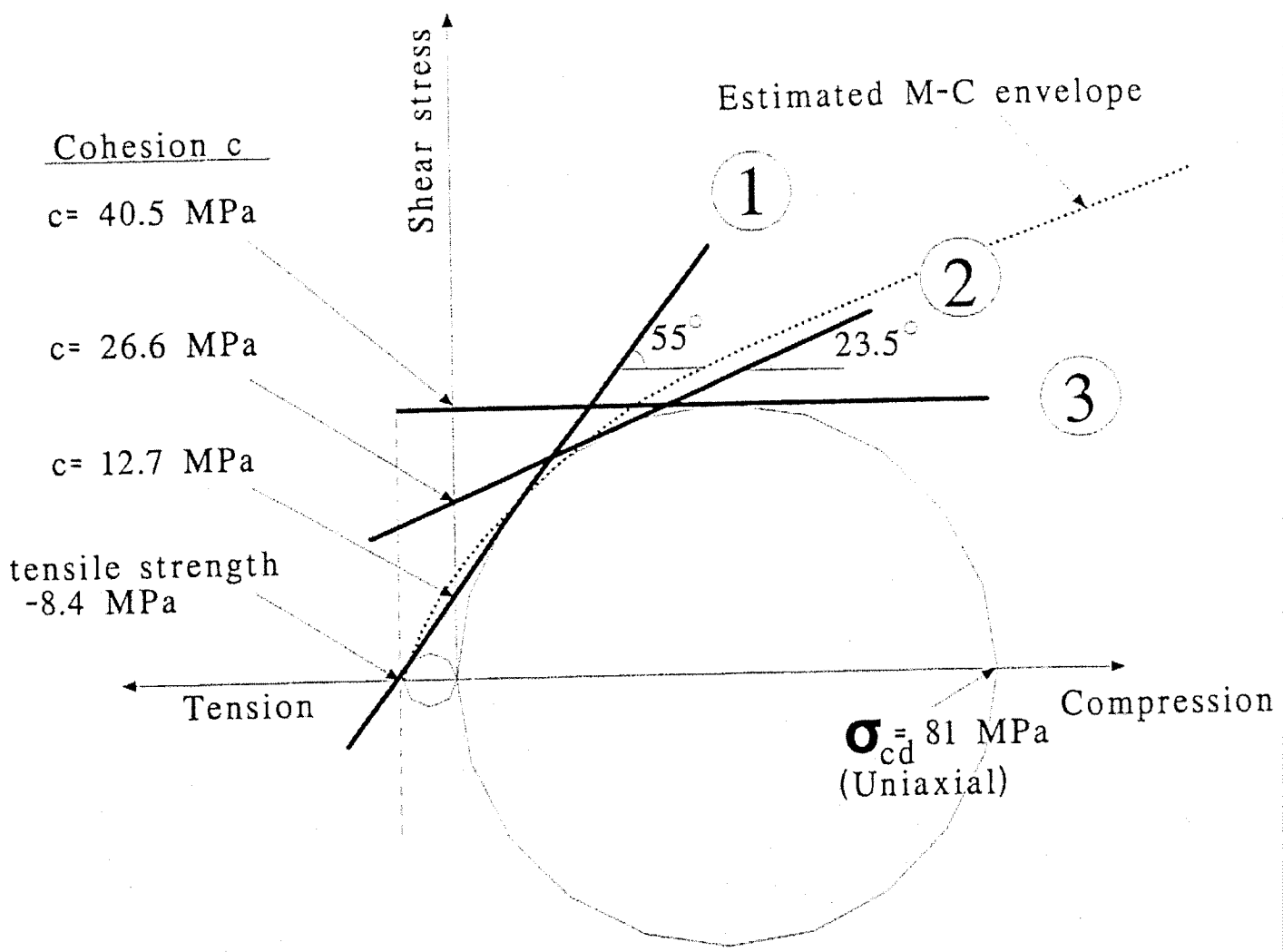


Figure 1. Mohr-Coulomb failure criterion lines

- line ① - straight approximation from uniaxial compression and tensile strength (brasilian test)
- line ② - approximation from the estimated Mohr envelope
- line ③ - mobilization of friction and cohesion (first state)

FLAC3D 1.00

Step 9156 Perspective

10:14:24 Thu Dec 21 1995

Rotation:

X: 38.26

Y: 1270

Z: 54.42

Center:

X: 1749e+00

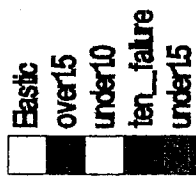
Y: 8.866e-01

Z: 9.921e-01

Eye Dist: 2.986e+01

Size: (4.302e-01, 4.670e-01)

Block Plot of Region



Job Title: 30 MPa pressure in slots, elastic, C-40.5e6, f=0



Job Title: 40 MPa pressure in slots, elastic,C-40.5e6, f=0

FLAC3D 1.00

Step 12324
10:16:31 Thu Dec 21 1995

Perspective

Rotation:

X: 38.26

Y: 12.70

Z: 54.42

Center:

X: 1749e+00

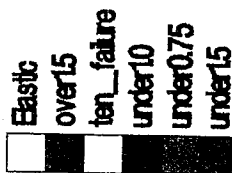
Y: 8866e-01

Z: 9.921e-01

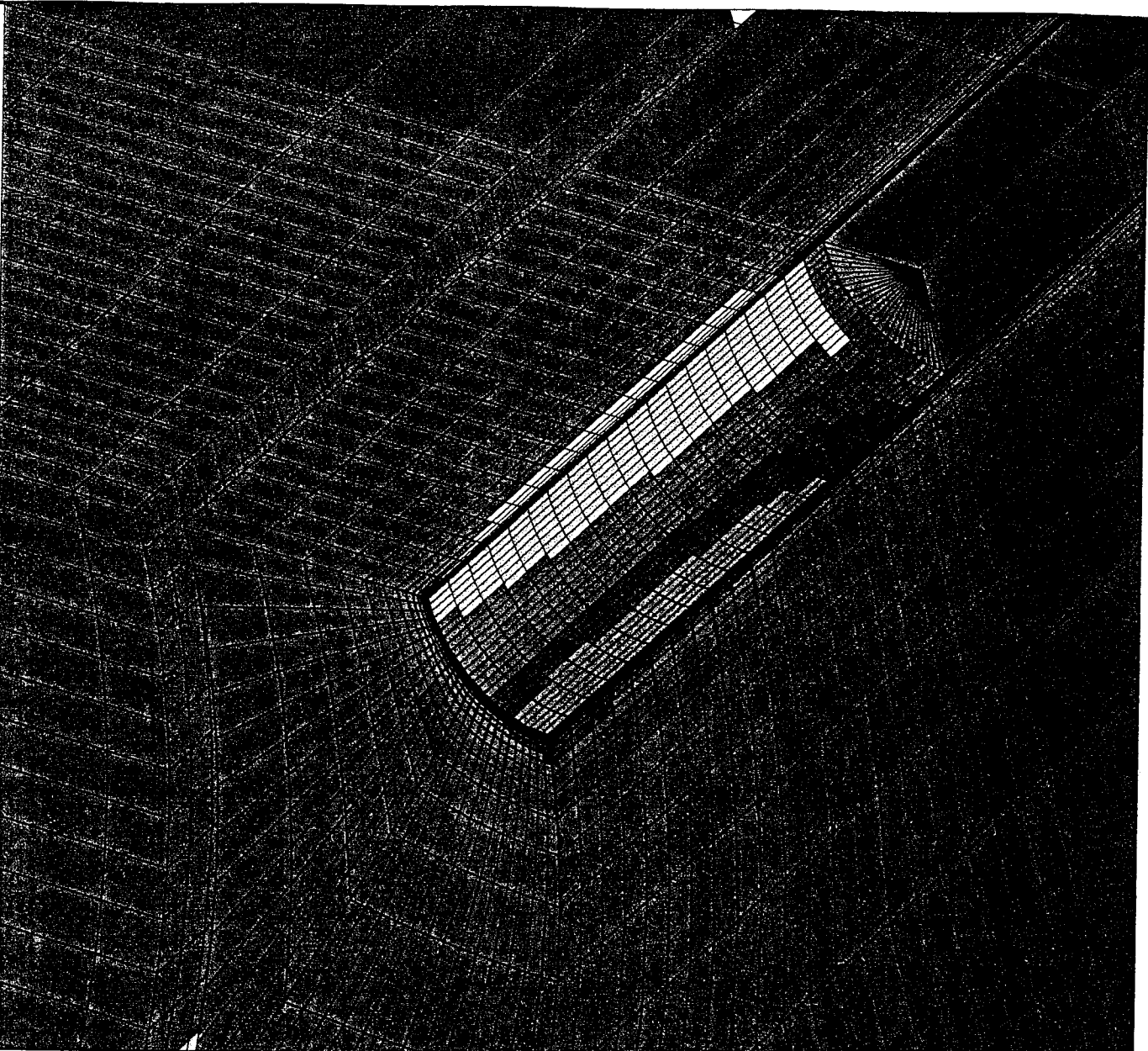
Eye Dist: 2.966e+01

Size: (4.302e-01, 4.670e-01)

Block Plot of Region



Itasca Consulting Group, Inc.
Minneapolis, Minnesota USA



Job Title: 50 MPa pressure in slots, elastic, C-40.5e6, f=0°

FLAC3D 1.00

Step 15629 Perspective

10:18:58 Thu Dec 21 1995

Rotation:

X: 38.26

Y: 12.70

Z: 54.42

Center:

X: 1.749e+00

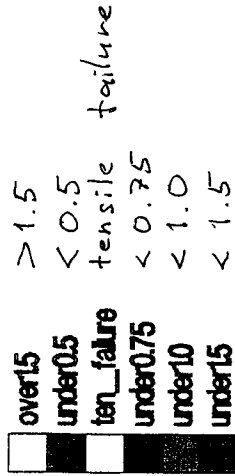
Y: 8.866e-01

Z: 9.921e-01

Eye Dist: 2.986e+01

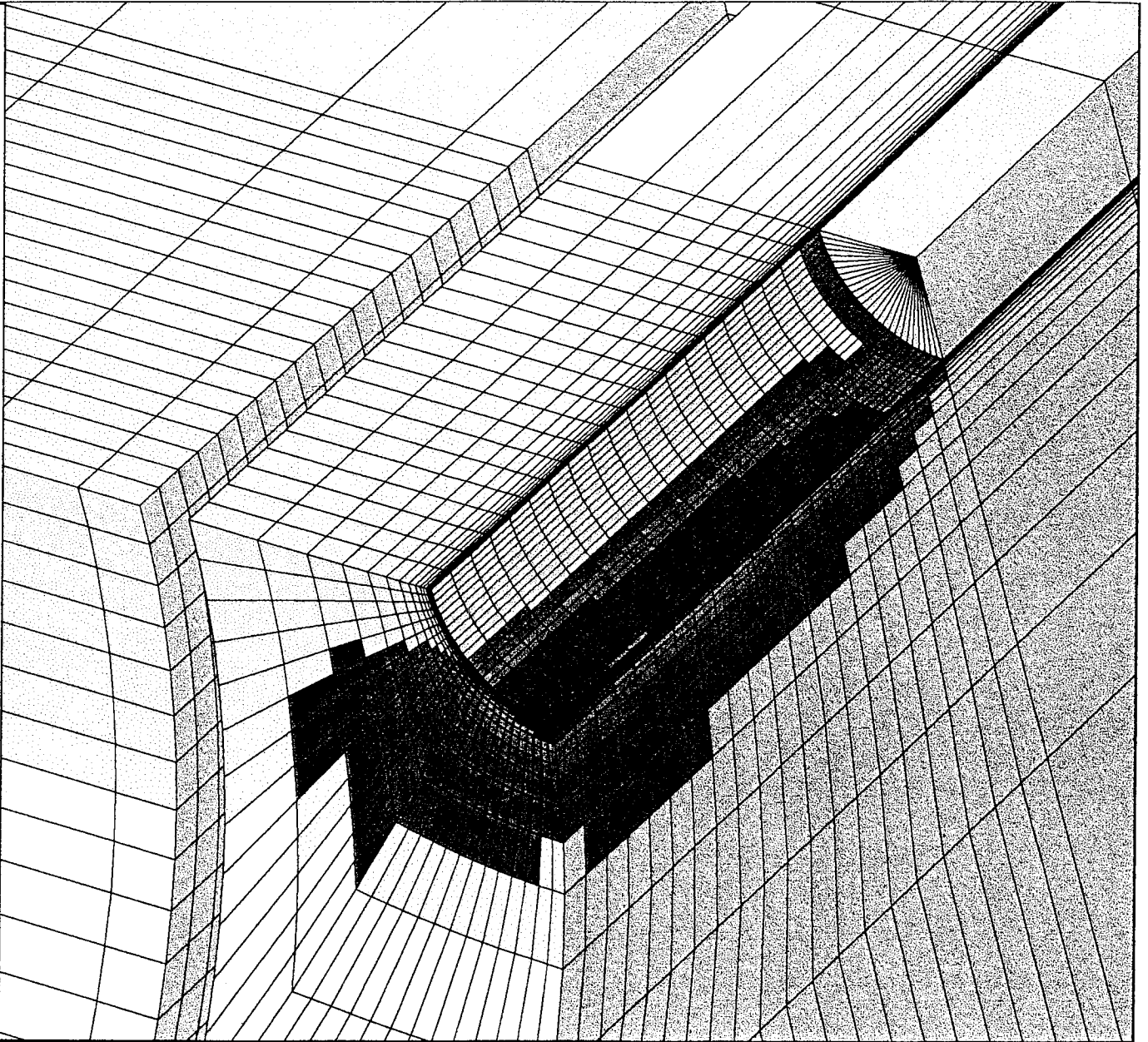
Size: (4.302e-01, 4.670e-01)

Block Plot of Region SAFETY FACTOR



3

Itasca Consulting Group, Inc.
 Minneapolis, Minnesota USA



Job Title: 60 MPa pressure in slots, elastic, C=40.5e6, f=0

FLAC3D 1.00

Step 18853 Perspective

102137 Thu Dec 21 1995

Rotation:

X: 38.26

Y: 12.70

Z: 54.42

Center:

X: 1749e+00

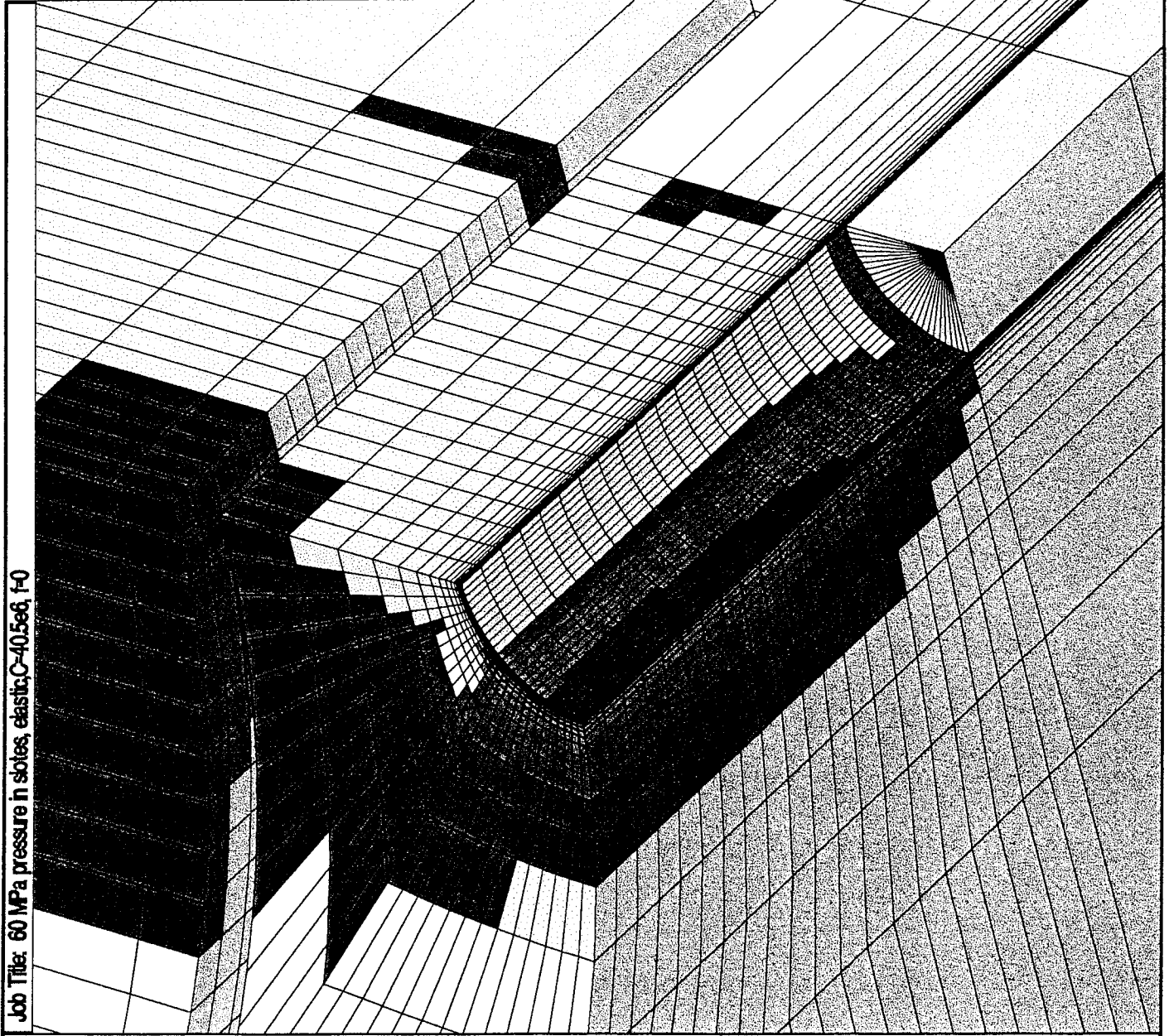
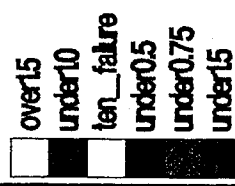
Y: 8.866e-01

Z: 9.921e-01

Eye Dist: 2.986e+01

Size: (4.302e-01, 4.670e-01)

Block Plot of Region



FLAC3D 1.00

Step 9156 Perspective
 10:13:45 Thu Dec 21 1995

Rotation

X: 38.26
 Y: 12.70
 Z: 54.42
Center.

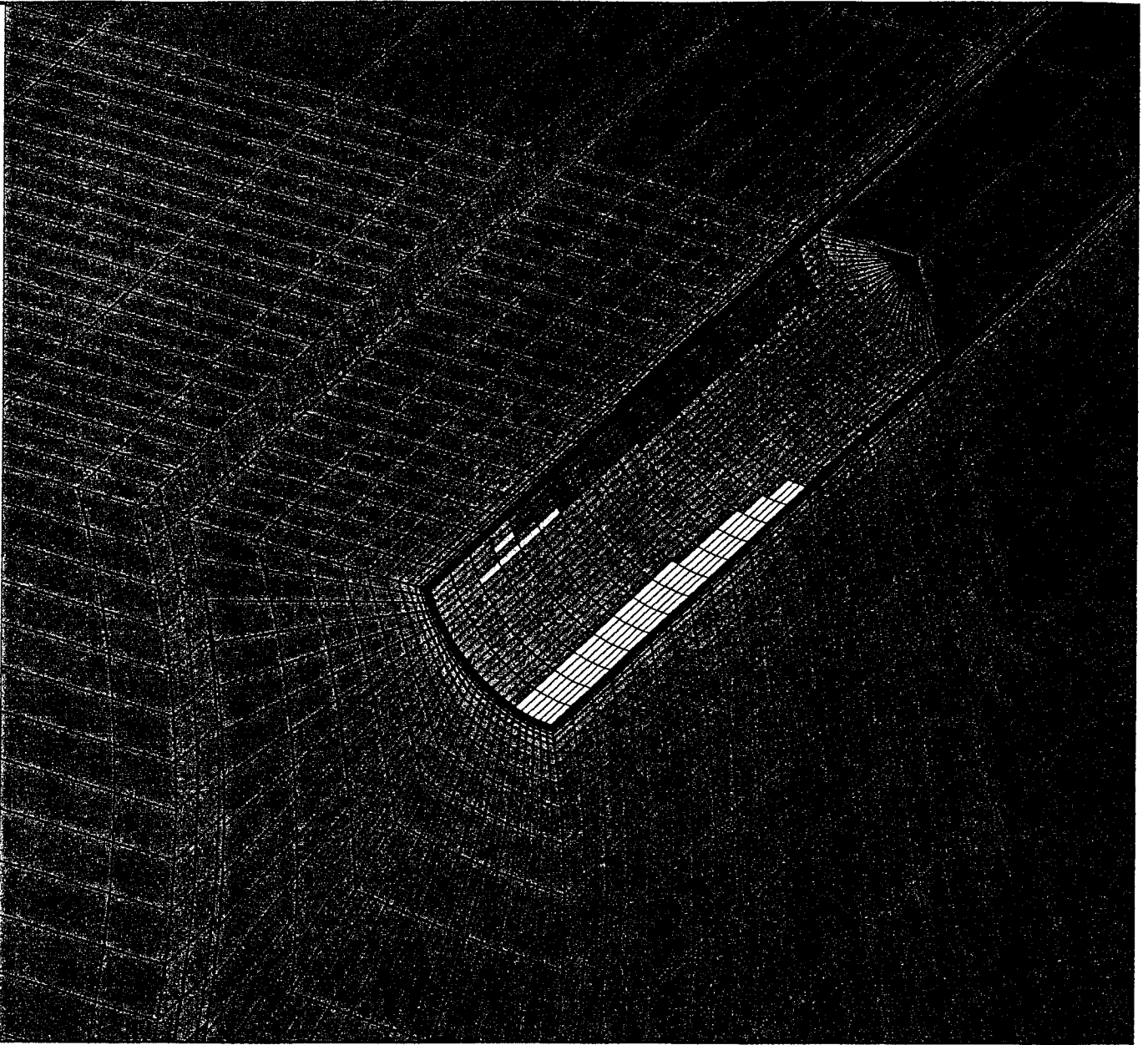
X: 1.749e+00
 Y: 8.866e-01
 Z: 9.921e-01

Eye Dist: 2.986e+01
 Size: (4.302e-01, 4.670e-01)

Block Plot of Region

█	Elastic
█	over15
█	under10
█	ten_failure
█	under15

Job Title: 30 MPa pressure in slots, elastic, C-26.6e6, f-23.5



Itasca Consulting Group, Inc.
 Minneapolis, Minnesota USA

Job Title: 40 MPa pressure in slots, elastic; C-26.6e6, f-23.5

FLAC3D 1.00

Step 12324 Perspective
 10:15:46 Thu Dec 21 1995

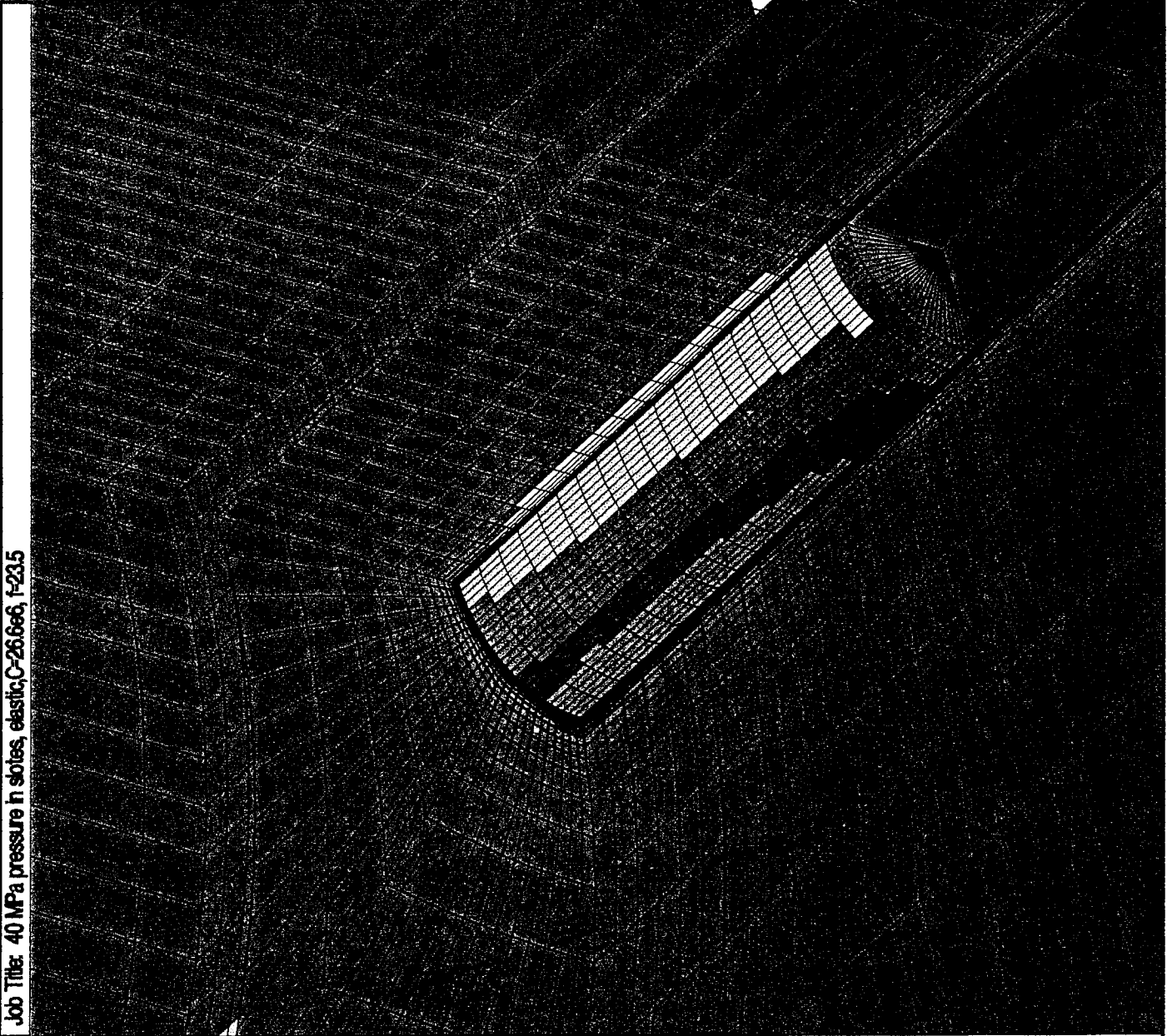
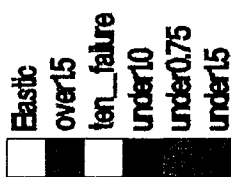
Rotation

X: 38.26
 Y: 12.70
 Z: 54.42

Center:

X: 1749e+00
 Y: 8.868e-01
 Z: 9.921e-01
 Eye Dist: 2.986e+01
 Size: (4.302e-01, 4.670e-01)

Block Plot of Region



Job Title: 50 MPa pressure in soles, elastic; C=266, f=23.5°

FLAC3D 1.00

Step 15629 Perspective

10:16:06 Thu Dec 21 1995

Rotation

X: 38.26

Y: 12.70

Z: 54.42

Center.

X: 1748e+00

Y: 8886e-01

Z: 9921e-01

Eye Dist: 2986e+01

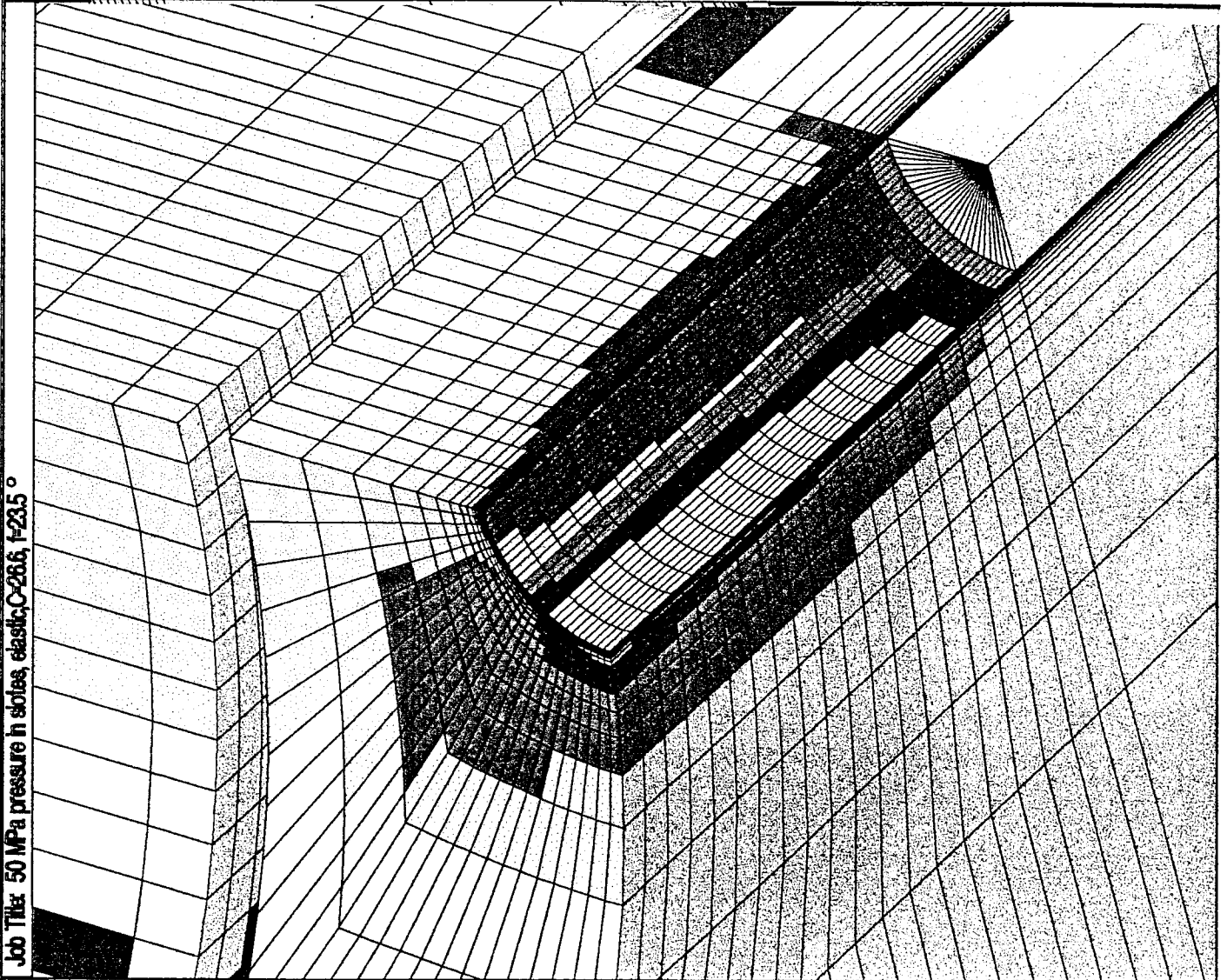
Size: (4.302e-01, 4.670e-01)

Block Plot of Region SAFETY FACTOR

Block Plot of Region	SAFETY FACTOR
over15	> 1.5
ten_failure	tensile failure
under0.75	< 0.75
under1.0	< 1.0
under1.5	< 1.5

(2.)

Iiasca Consulting Group, Inc.
 Minneapolis, Minnesota USA



Job Title: 60 MPa pressure in soles, elastic, C-26.6e6, f-23.5

FLAC3D 1.00

Step 18853
 Perspective

1020:39 Thu Dec 21 1995

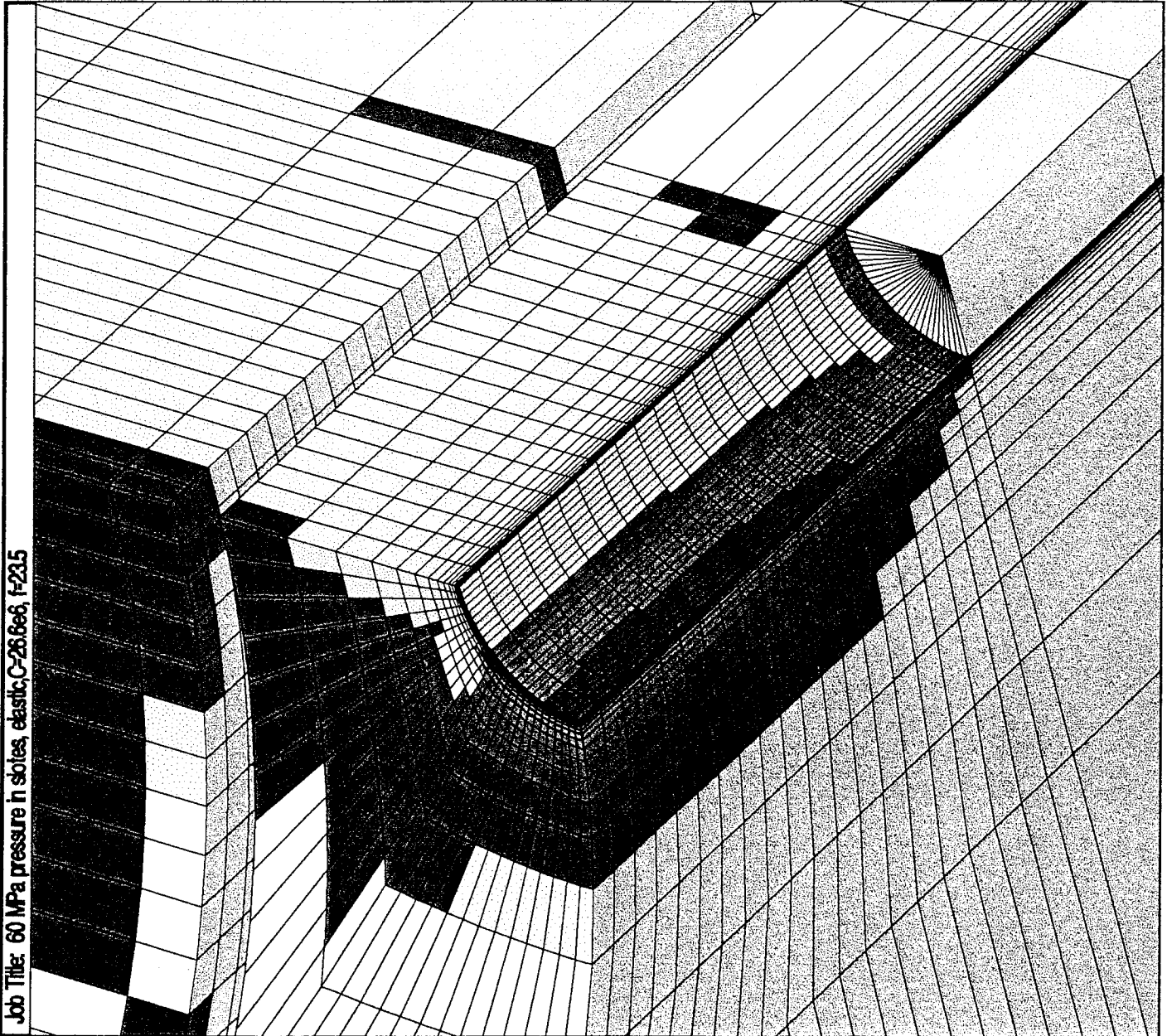
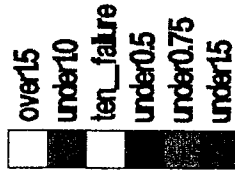
Rotation

X: 38.26
 Y: 12.70
 Z: 54.42

Center.

X: 1749e+00
 Y: 8.866e-01
 Z: 9.921e-01
 Eye Dist: 2.986e+01
 Size: (4.302e-01, 4.670e-01)

Block Plot of Region



Itasca Consulting Group, Inc.
 Minneapolis, Minnesota USA

FLAC3D 1.00

Step 9156
Perspective

10:15:04 Thu Dec 21 1985

Rotation:

X: 38.26

Y: 12.70

Z: 54.42

Center:

X: 1749e+00

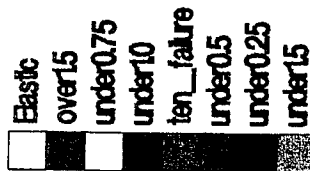
Y: 8.866e-01

Z: 9.921e-01

Eye Dist: 2.986e+01

Size: (4.302e-01 4.670e-01)

Block Plot of Region



Job Title: 30 MPa pressure in soles, elastic; C-127e6, f-55



Job Title: 40 MPa pressure in slots, elastic, C-12.7e6, 165

FLAC3D 1.00

Step 12324
Perspective

10:17:18 Thu Dec 21 1995

Rotation

X: 38.26

Y: 12.70

Z: 54.42

Center

X: 1.749e+00

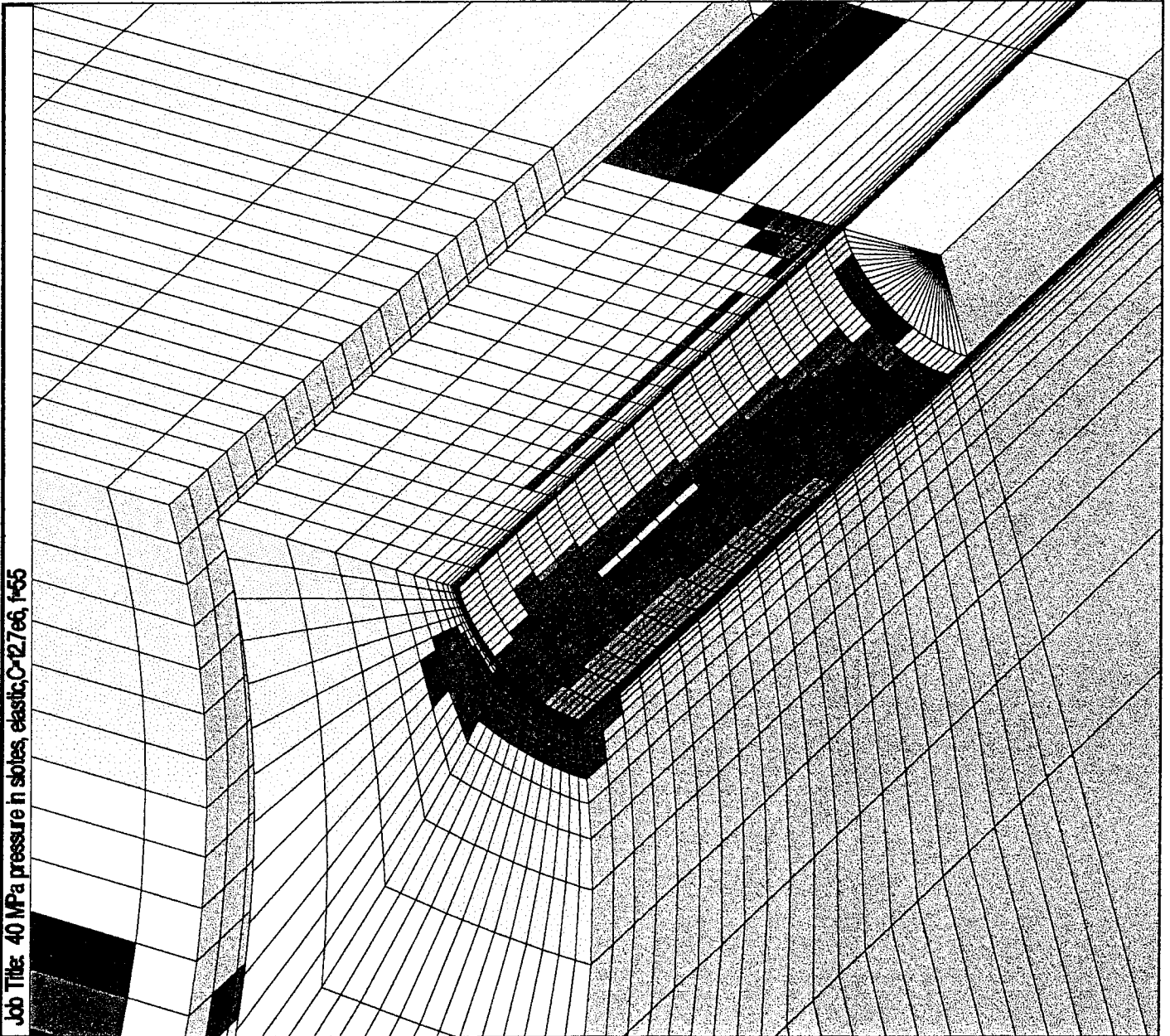
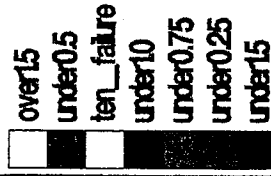
Y: 8.886e-01

Z: 9.921e-01

Eye Dist: 2.986e+01

Size: (4.302e-01, 4.670e-01)

Block Plot of Region



Itasca Consulting Group, Inc.
Minneapolis, Minnesota USA

Job Title: 50 MPa pressure in slots, elastic; C-127e6, f-55

FLAC3D 1.00

Step 15629
10:19:46 Thu Dec 21 1995

Perspective

Rotation:

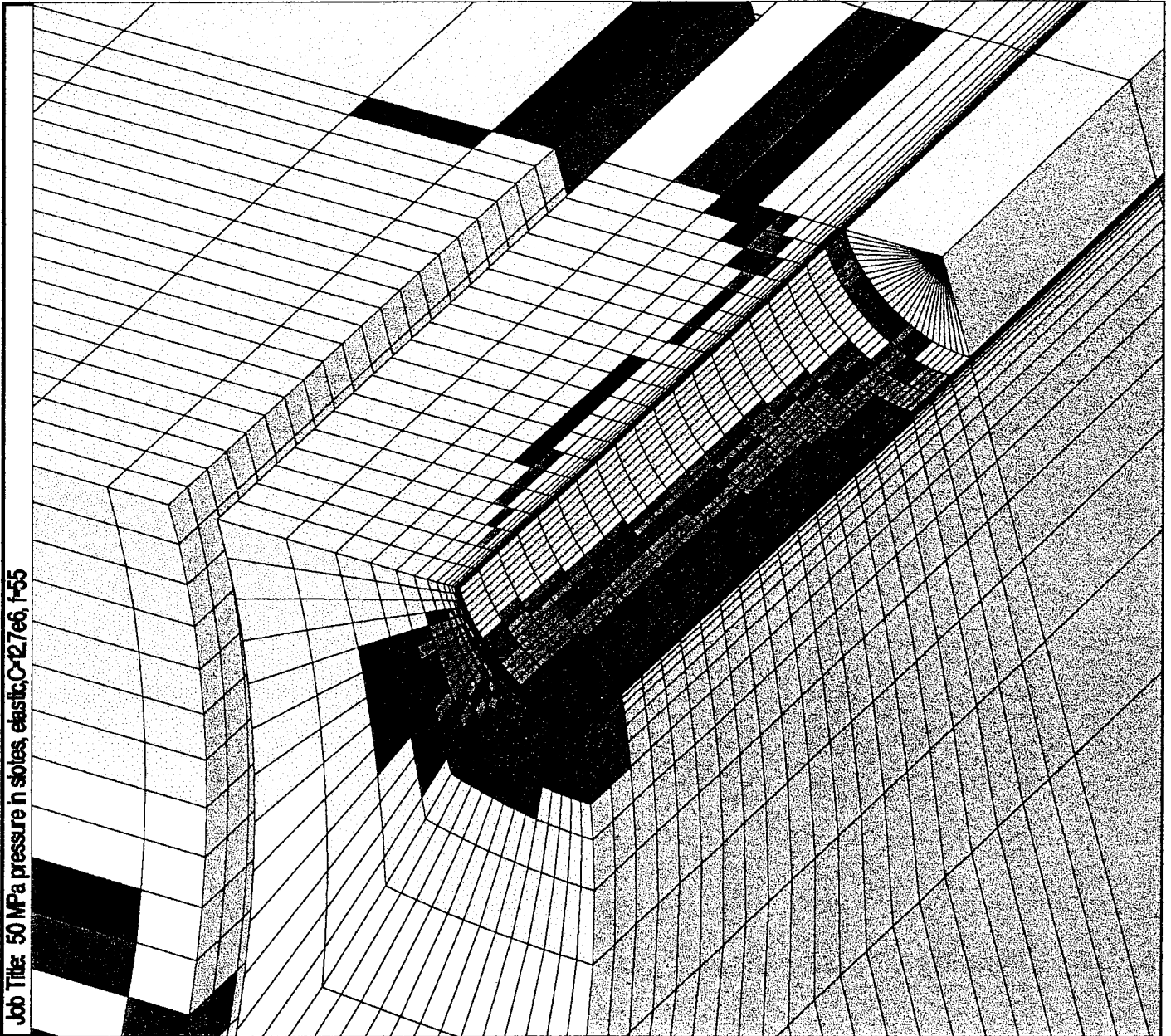
X: 38.26
Y: 12.70
Z: 54.42

Center:

X: 1749e+00
Y: 8.866e-01
Z: 9.921e-01
Eye Dist: 2.986e+01
Size: (4.302e-01, 4.670e-01)

Block Plot of Region

- over15
- under05
- ten_failure
- under075
- under10
- under025
- under15



Job Title: 60 MPa pressure in soles, elastic, C-127e6, f-55

FLAC3D 1.00

Step 18853
Perspective

10:22:29 Thu Dec 21 1995

Rotation:

X: 38.26

Y: 12.70

Z: 54.42

Center:

X: 1749e+00

Y: 8.866e-01

Z: 9.921e-01

Eye Dist: 2.986e+01

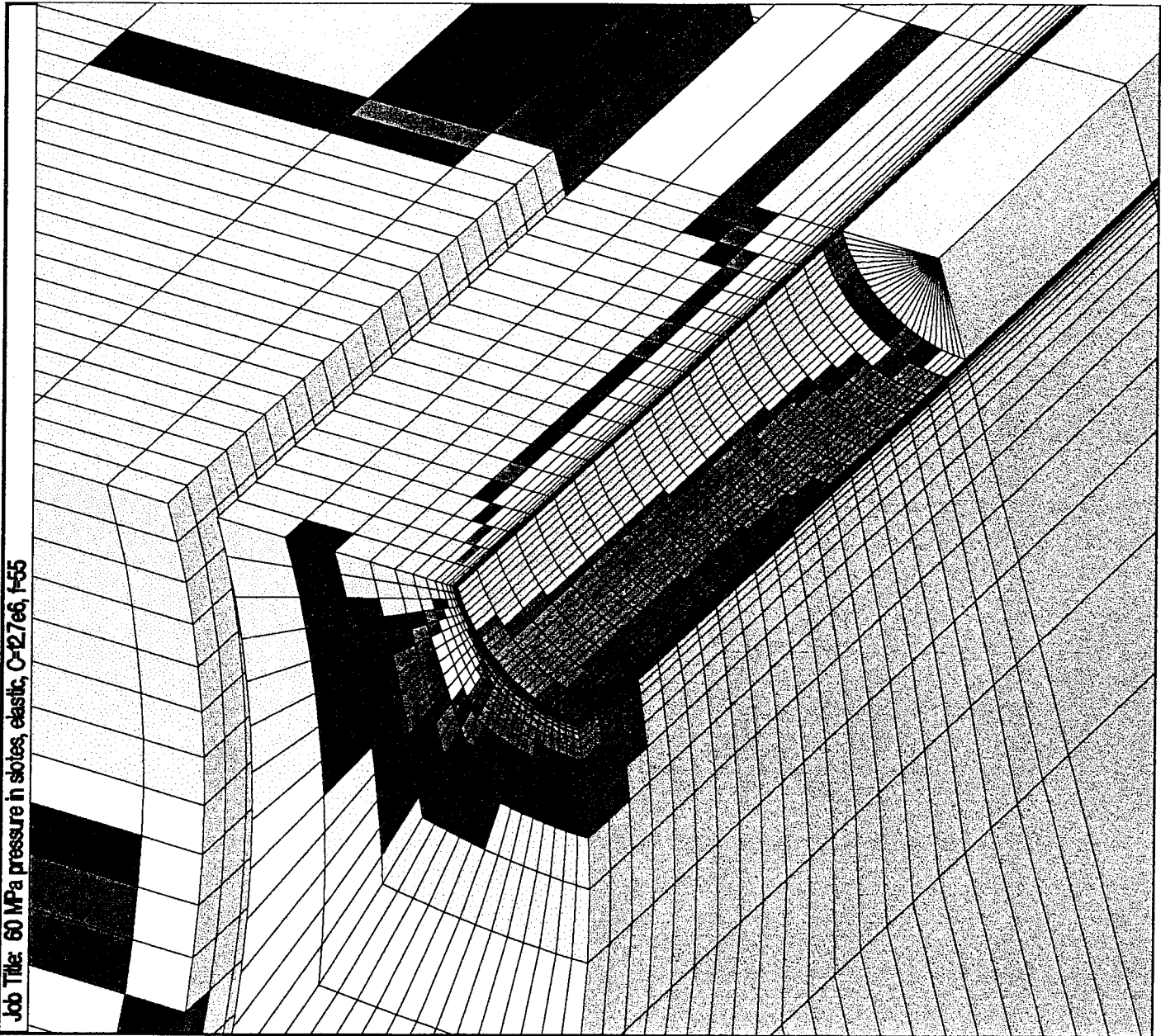
Size: (4.302e-01, 4.670e-01)

Block Plot of Region SAFETY FACTOR

Block Plot of Region	SAFETY FACTOR
over15	> 1.5
under10	< 1.0
ten_failure	tensile failure
under0.5	< 0.5
under0.75	< 0.75
under0.25	< 0.25
under15	< 1.5

4.

Itasca Consulting Group, Inc.
Minneapolis, Minnesota USA



Job Title: 30 MPa pressure in soles, elastic, mops (C-127e6, f-55)

FLAC3D 1.00

Step 9156
Perspective

09:03:23 Mon Jan 8 1996

Rotation:

X: 38.26

Y: 12.70

Z: 54.42

Center:

X: 1749e+00

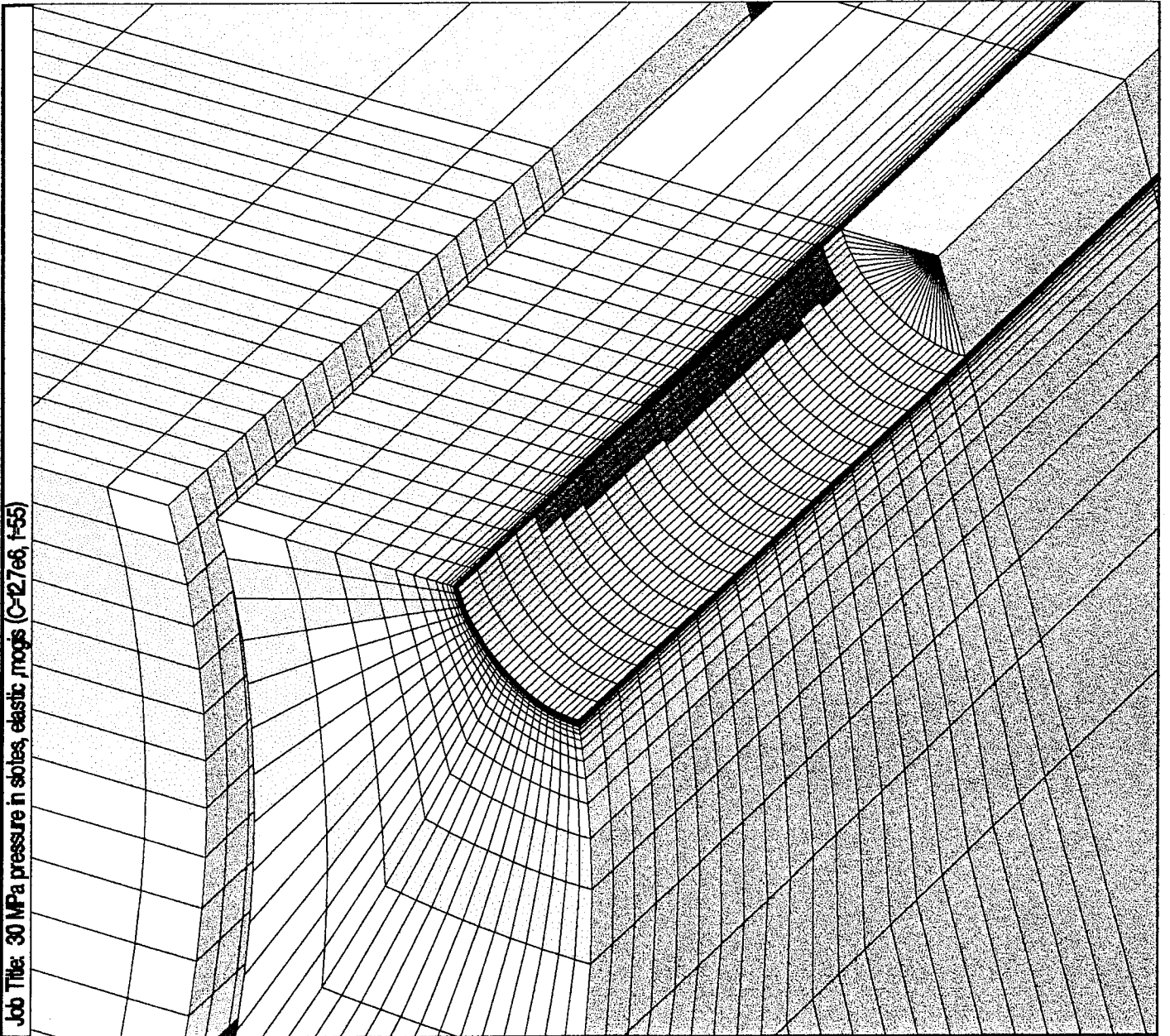
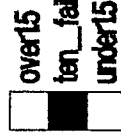
Y: 8.866e-01

Z: 9.921e-01

Eye Dist: 2.986e+01

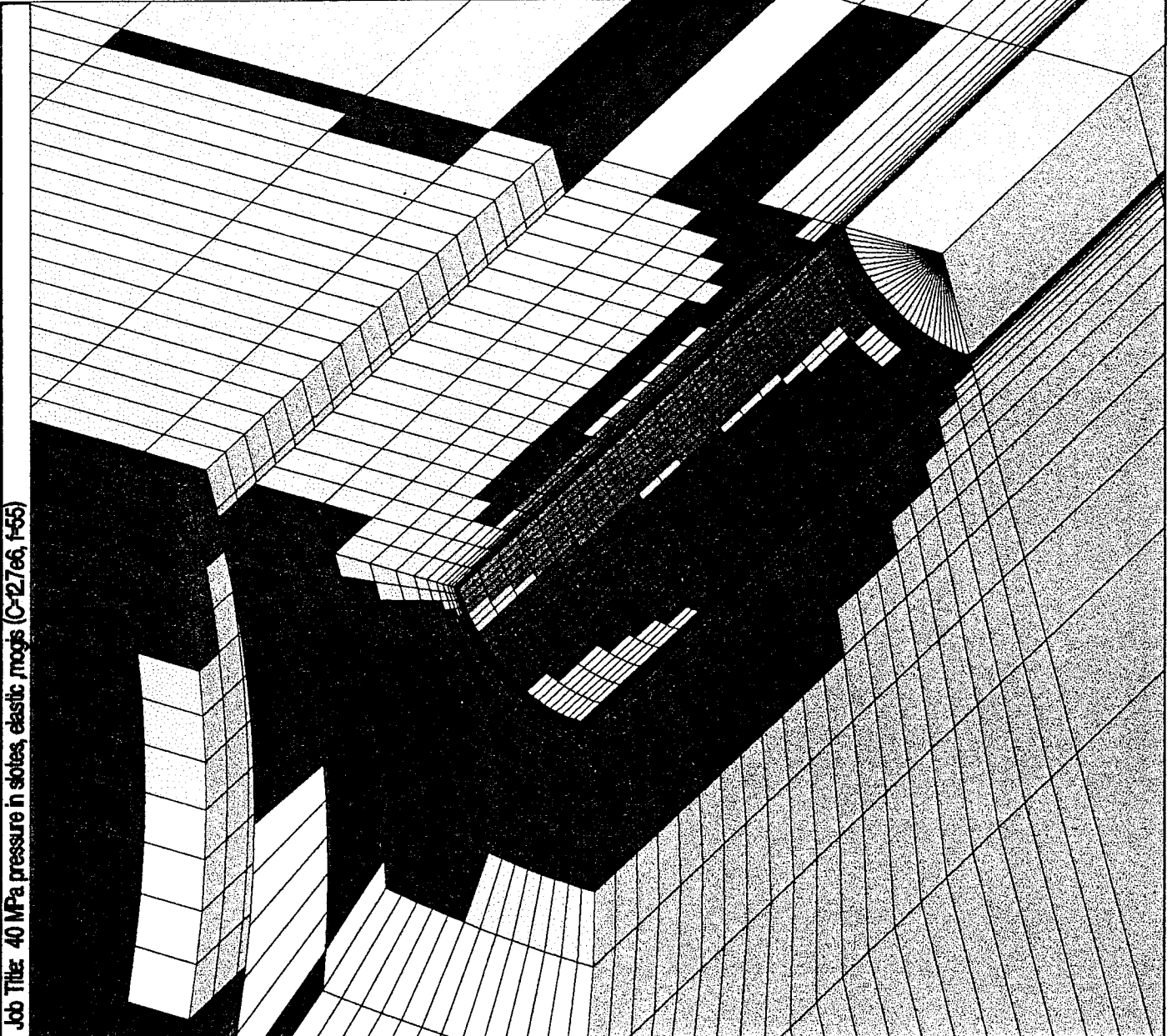
Size: (4.302e-01, 4.670e-01)

Block Plot of Region



Itasca Consulting Group, Inc.
Minneapolis, Minnesota USA

Job Title: 40 MPa pressure in slots, elastic, moogs (C-12.7e6, f-55)



FLAC3D 1.00

Step 12324 Perspective

09:03:59 Mon Jan 8 1996

Rotation:

X: 38.26

Y: 12.70

Z: 54.42

Center:

X: 1749e+00

Y: 8.866e-01

Z: 9.927e-01

Eye Dist: 2.986e+01

Size: (4.302e-01, 4.670e-01)

Block Plot of Region

over15

ten_failure

under10

under15

Itasca Consulting Group, Inc.
 Minneapolis, Minnesota USA

Job Title: 50 MPa pressure in stiles, elastic ,mogs (C-127e6, f-55)

FLAC3D 1.00

Step 15629 Perspective

09:04:41 Mon Jan 8 1996

Rotation:

X: 38.26

Y: 12.70

Z: 54.42

Center:

X: 1749e+00

Y: 8.866e-01

Z: 9.921e-01

Eye Dist: 2986e-01

Size: (4.302e-01, 4.670e-01)

Block Plot of Region

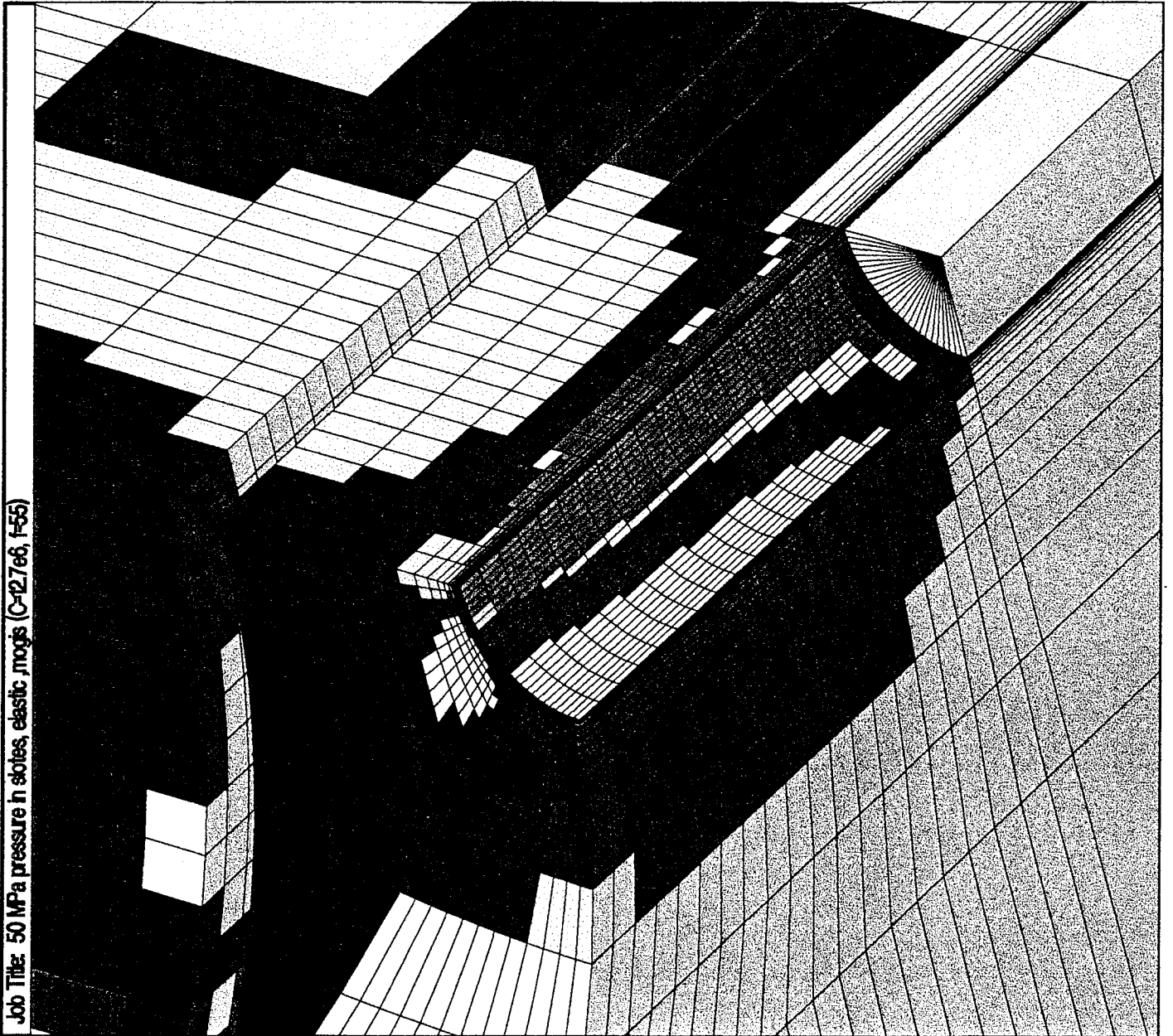
over15

ten_failure

under10

under15

Itasca Consulting Group, Inc.
 Minneapolis, Minnesota USA



Job Title: 60 MPa pressure in slots, elastic, mogs (C-127e6, f-55)

FLAC3D 1.00

Step 18853 Perspective

09:05:27 Mon Jan 8 1996

Rotation:

X: 38.26

Y: 12.70

Z: 54.42

Center:

X: 1749e+00

Y: 8.866e-01

Z: 9.921e-01

Eye Dist: 2.986e+01

Size: (4.302e-01, 4.670e-01)

Block Plot of Region

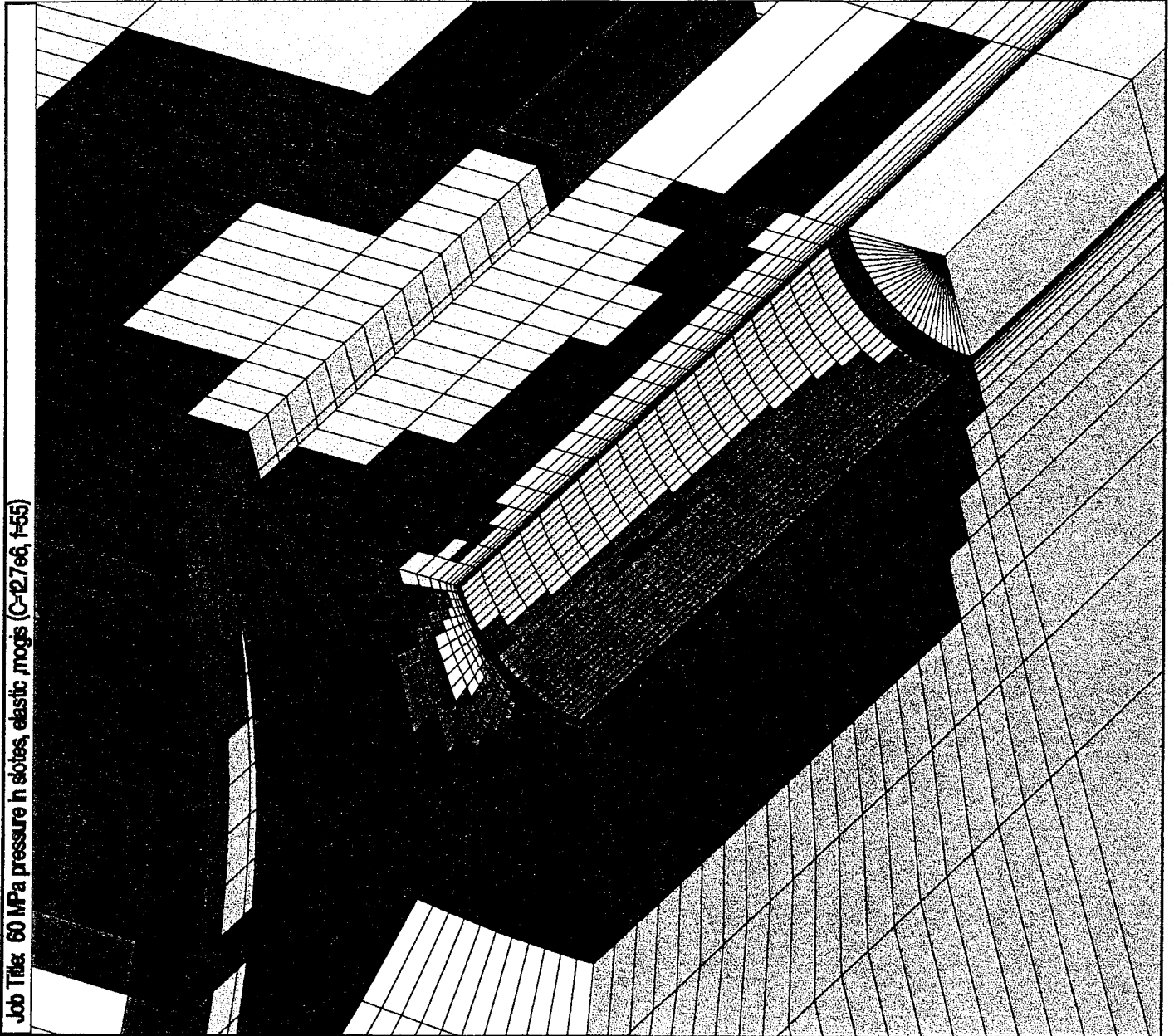
over15

under10

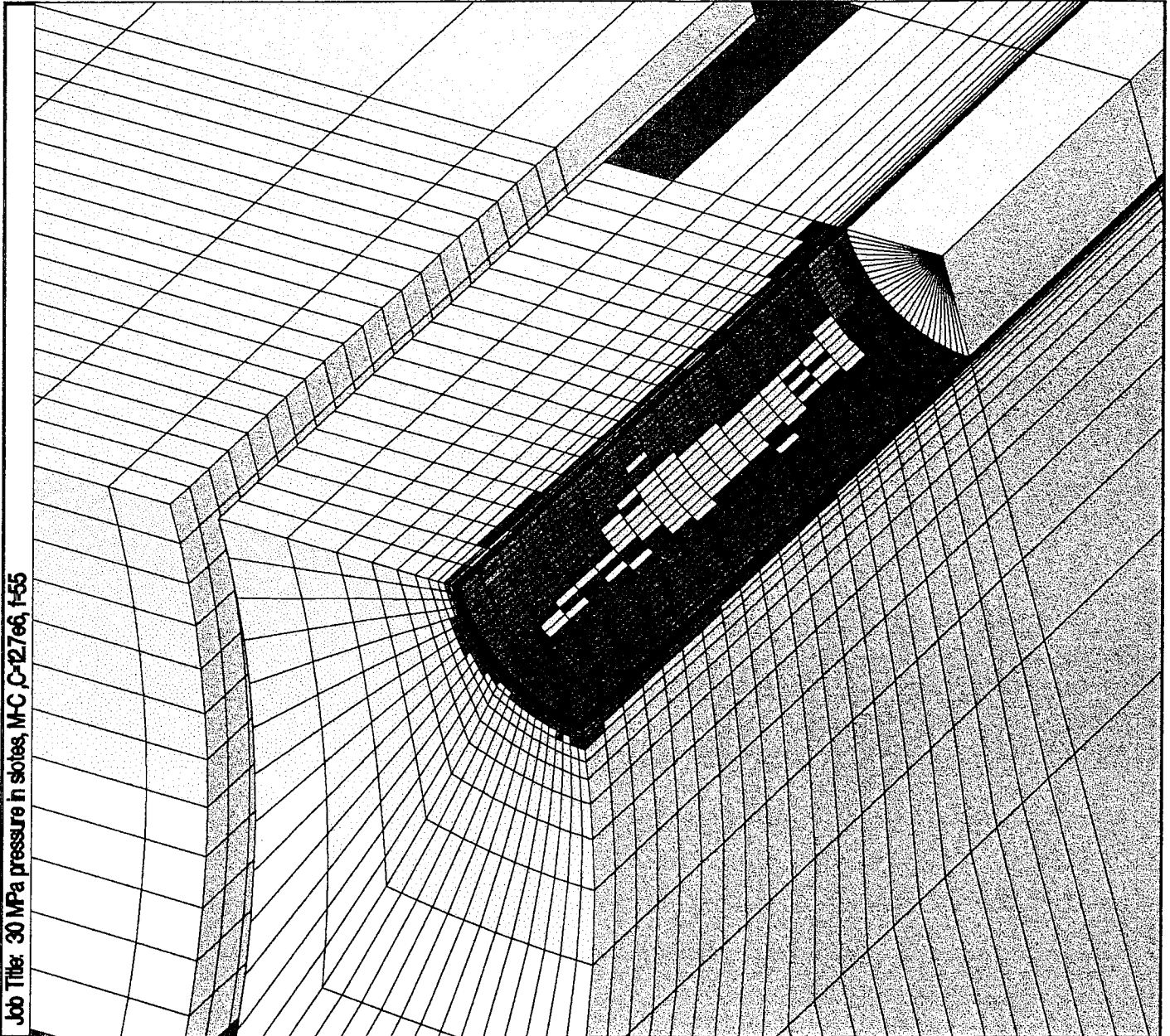
ten_failure

under15

Itasca Consulting Group, Inc.
 Minneapolis, Minnesota USA



Job Title: 30 MPa pressure in slates, M-C C-12.7e6, f-55



FLAC3D 1.00

Step 9057 Perspective

09:17:53 Fri Dec 22 1995

Rotation:

X: 38.26

Y: 12.70

Z: 54.42

Center:

X: 1749e+00

Y: 8.868e-01

Z: 9.921e-01

Eye Dist: 2.988e+01

Size: (4.302e-01, 4.670e-01)

Block Plot of State

None

shear-n shear-p

shear-n shear-p tension-p

shear-p

shear-p tension-p

tension-n shear-p tension-p

Itasca Consulting Group, Inc.
 Minneapolis, Minnesota USA

Job Title: 40 MPa pressure in slates, M-C, C-127e6, F-55

FLAC3D 1.00

Perspective

Step 12841

09:19:17 Fri Dec 22 1995

Rotation:

X: 38.26

Y: 12.70

Z: 54.42

Center:

X: 1.749e+00

Y: 8.866e-01

Z: 9.921e-01

Eye Dist: 2.986e+01

Size: (4.302e-01, 4.670e-01)

Block Plot of State

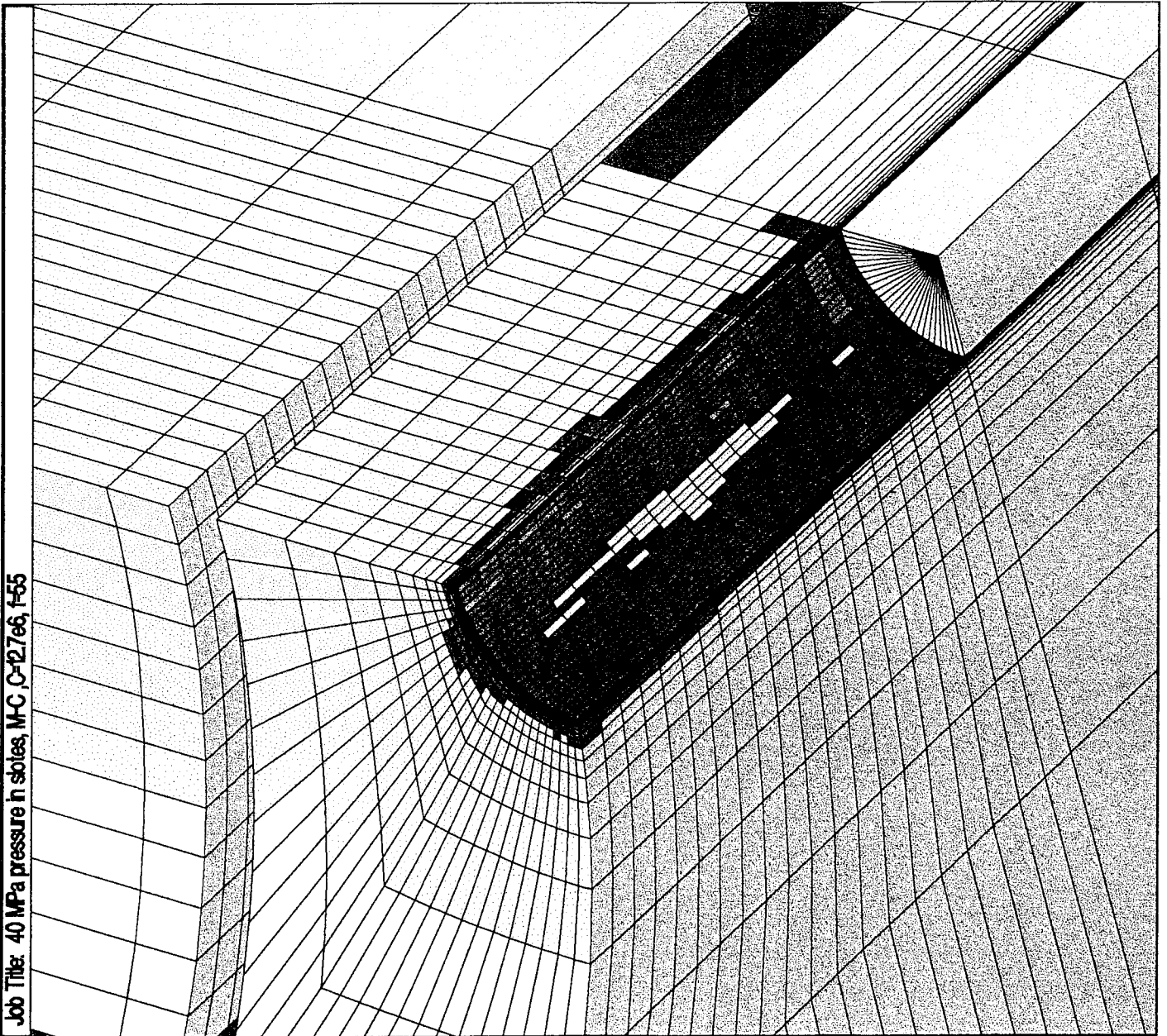
None

shear-n shear-p

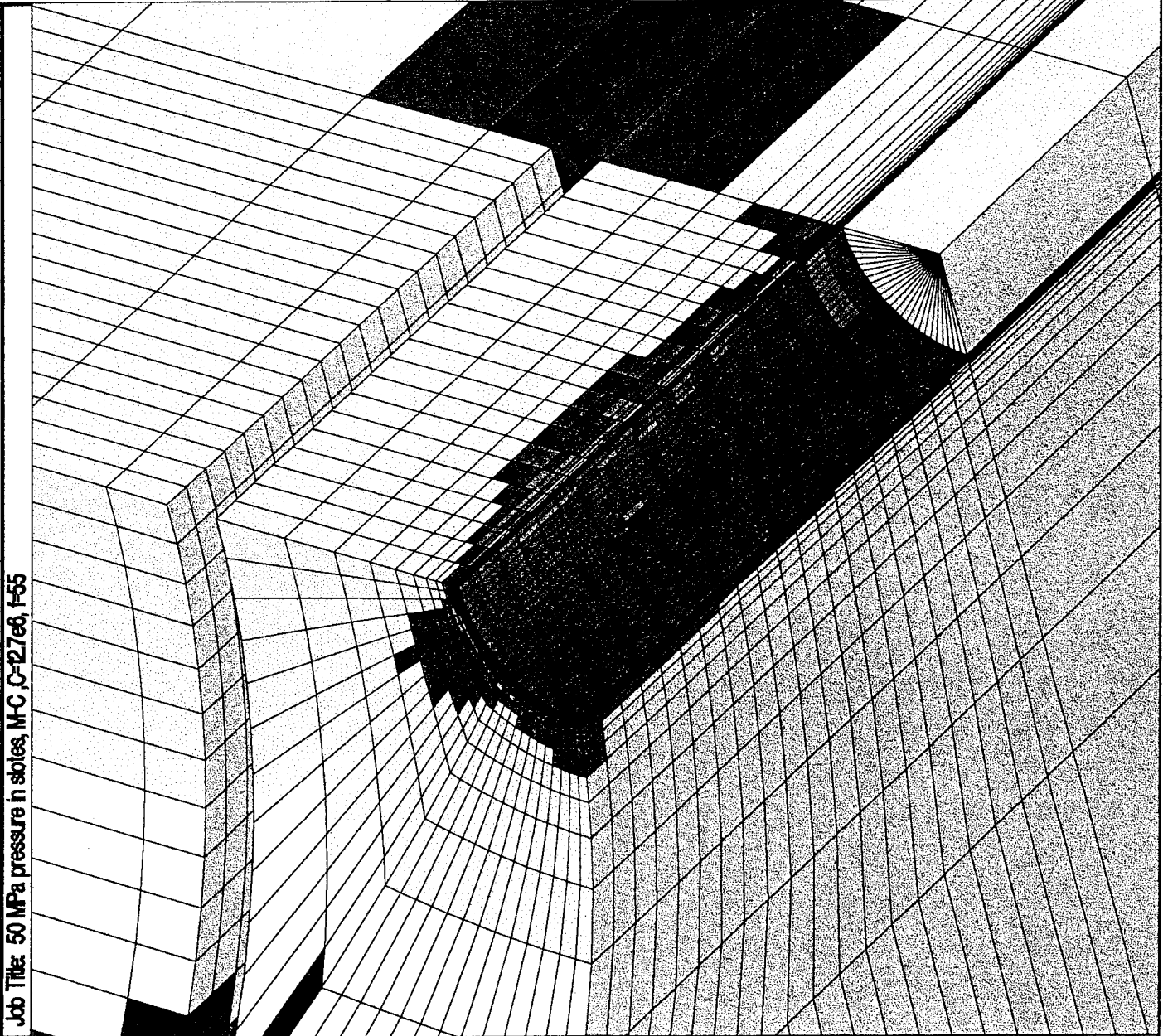
shear-n shear-p tension-p

shear-p

shear-p tension-p



Job Title: 50 MPa pressure in slots, M-C, C-27e6, f-55



FLAC3D 1.00

Perspective

Step 16659
08:15:59 Fri Dec 22 1995

Rotation:

X: 38.26

Y: 12.70

Z: 54.42

Center:

X: 1.749e+00

Y: 8.866e-01

Z: 9.921e-01

Eye Dist: 2.986e+01

Size: (4.302e-01, 4.670e-01)

Block Plot of State

None

shear-n shear-p

shear-n shear-p tension-p

shear-p

shear-p tension-p

tension-n shear-p tension-p

Itasca Consulting Group, Inc.
Minneapolis, Minnesota USA

Job Title: 60 MPa pressure in slots, M-C, C-12.7e6, r55



FLAC3D 1.00

Step 18041 Perspective

09:12:47 Fri Dec 22 1995

Rotation:

X: 38.26

Y: 12.70

Z: 54.42

Center:

X: 1749e+00

Y: 8.866e-01

Z: 9.921e-01

Eye Dist: 2.986e+01

Size: (4.302e-01, 4.670e-01)

Block Plot of State

- None
- shear-n shear-p
- shear-n shear-p tensior-p
- shear-p
- shear-p tensior-p
- tensior-n shear-p tensior-p

Itasca Consulting Group, Inc.
 Minneapolis, Minnesota USA

FLAC3D 1.00

Step 10018
Perspective

152305 Thu Dec 28 1995

Rotation:

X: 38.26

Y: 12.70

Z: 54.42

Center:

X: 1749e+00

Y: 8.868e-01

Z: 9.927e-01

Eye Dist: 2.988e+01

Size: (4.302e-01, 4.670e-01)

Block Plot of State

None

shear-n shear-p

shear-p

shear-p tension-p

tension-n tension-p

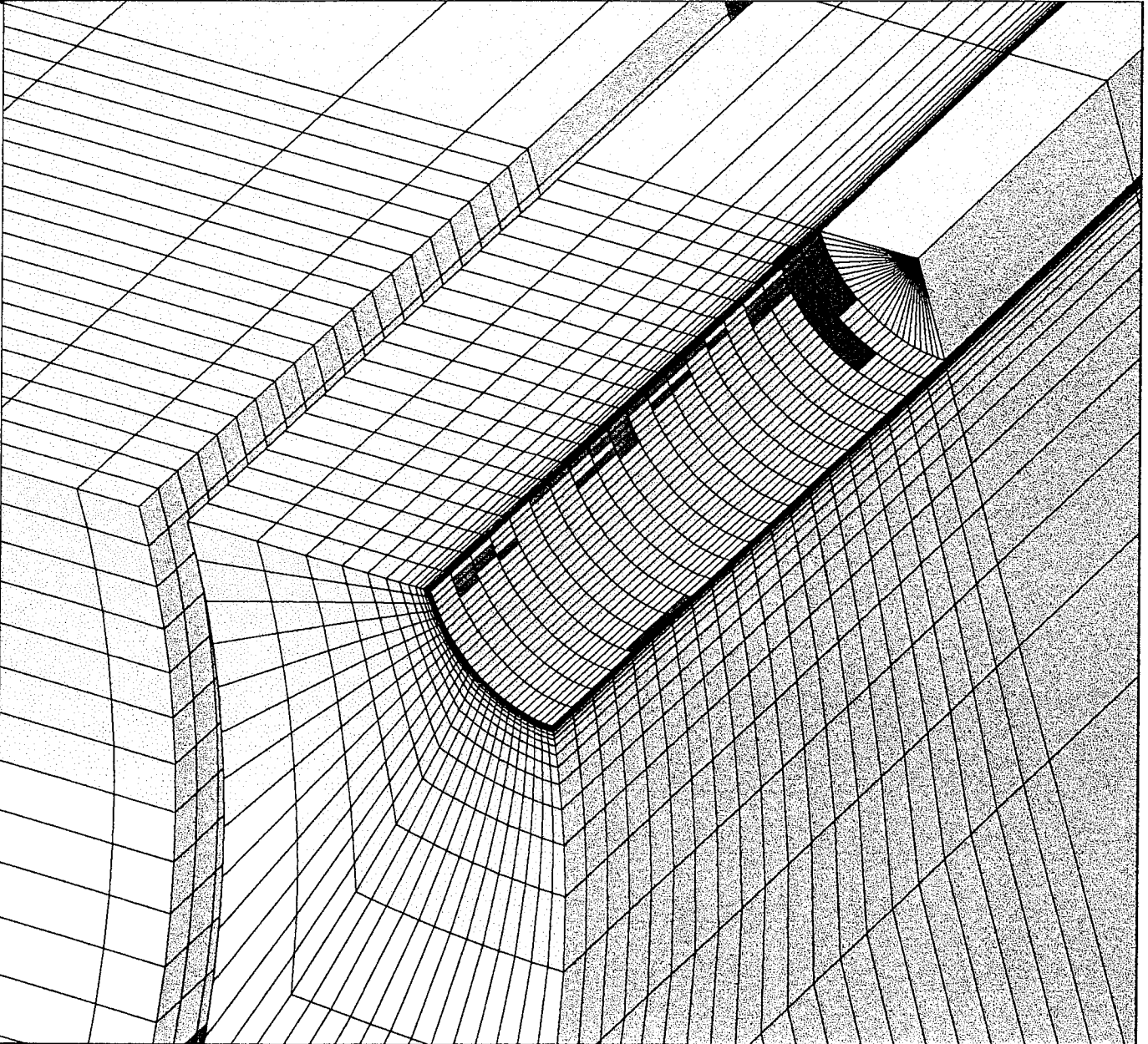
tension-p

Axes

Linestyle

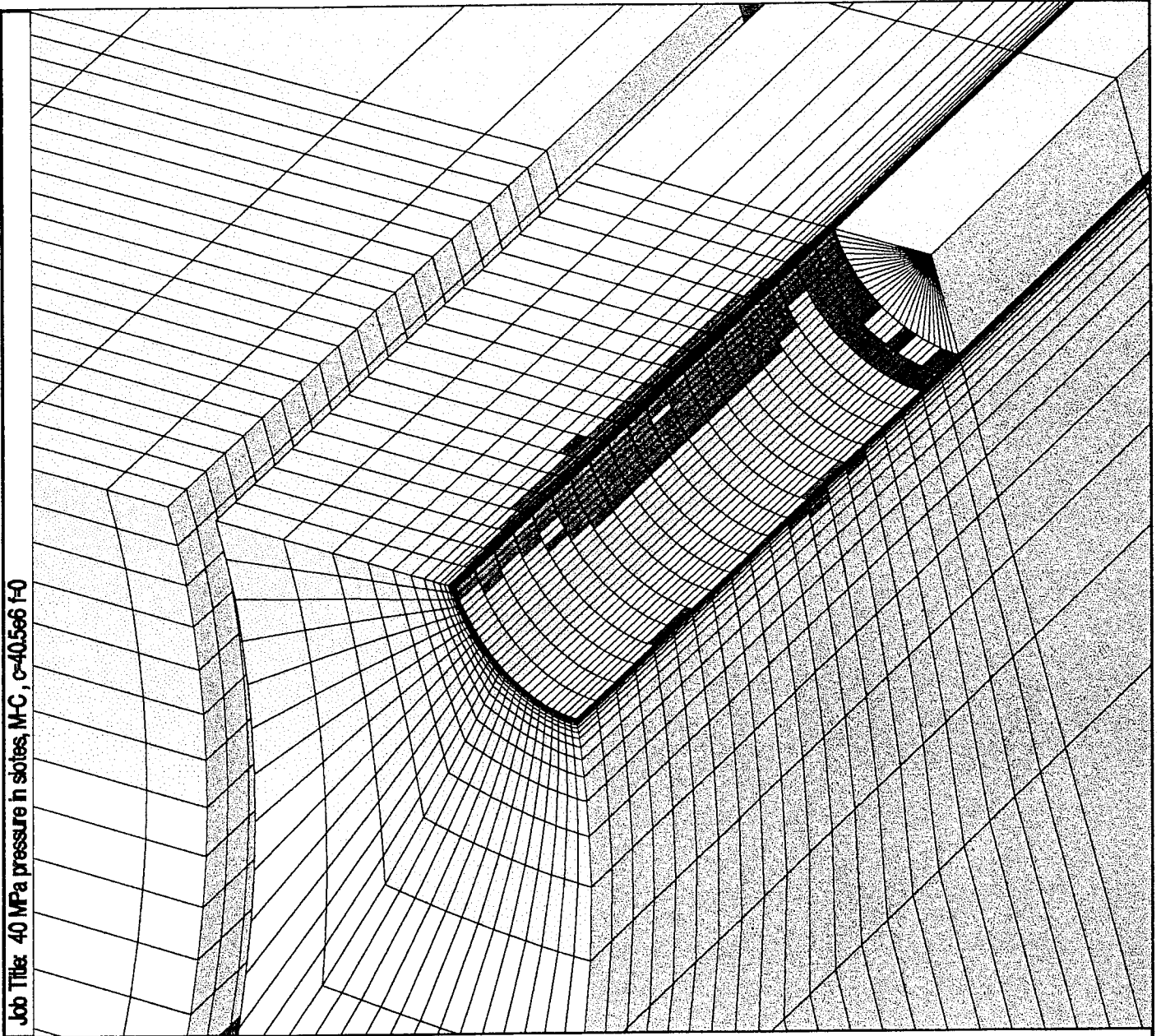
Block Plot of State

Job Title: 30 MPa pressure in slates, M-C, c=40.5e6 f=0



Consulting Engineers
Saario & Pekkola Ltd.

Job Title: 40 MPa pressure in slots, M-C, c-40.566 f-0



FLAC3D 1.00

Step 12784 Perspective

152407 Thu Dec 28 1995

Rotation

X: 38.26

Y: 12.70

Z: 54.42

Center:

X: 1749e+00

Y: 8.866e-01

Z: 9.921e-01

Eye Dist 2.986e+01

Size: (4.302e-01, 4.670e-01)

Block Plot of State

None

shear-n shear-p

shear-p

shear-p tension-p

tension-n tension-p

tension-p

Axes

Linestyle

Block Plot of State

Consulting Engineers
Saario & Pekkola Ltd.

Job Title: 50 MPa pressure in slots, M-C, c-40.566 t-0

FLAC3D 1.00

Step 15667 Perspective

152513 Thu Dec 28 1995

Rotation:

X: 38.26

Y: 12.70

Z: 54.42

Center:

X: 1749e+00

Y: 8.666e-01

Z: 9.921e-01

Eye Dist: 2.986e+01

Size: (4.302e-01 4.670e-01)

Block Plot of State

None

shear-n shear-p

shear-p

shear-p tension-p

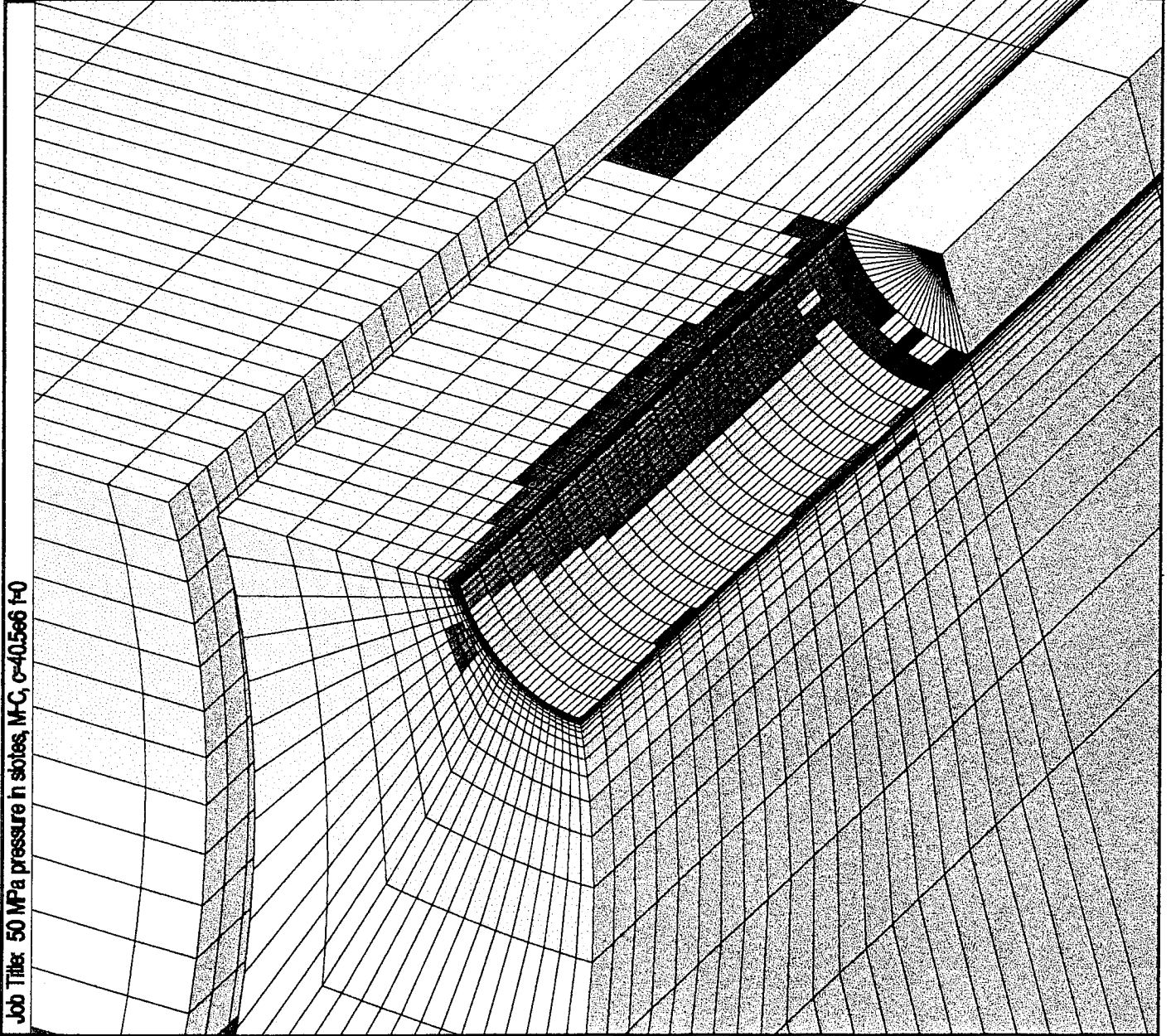
tension-n tension-p

tension-p

Axes

Linestyle

Block Plot of State



Consulting Engineers
Saarto & Piekola Ltd.

FLAC3D 1.00

Step 18740 Perspective

15:26:22 Thu Dec 28 1995

Rotation:

X: 38.26

Y: 12.70

Z: 54.42

Center:

X: 1749e+00

Y: 8.866e-01

Z: 9.921e-01

Eye Dist: 2.986e+01

Size: (4.302e-01, 4.670e-01)

Block Plot of State

- None
- shear-n shear-p
- shear-n shear-p tension-p
- shear-p
- shear-p tension-p
- tension-n tension-p
- tension-p

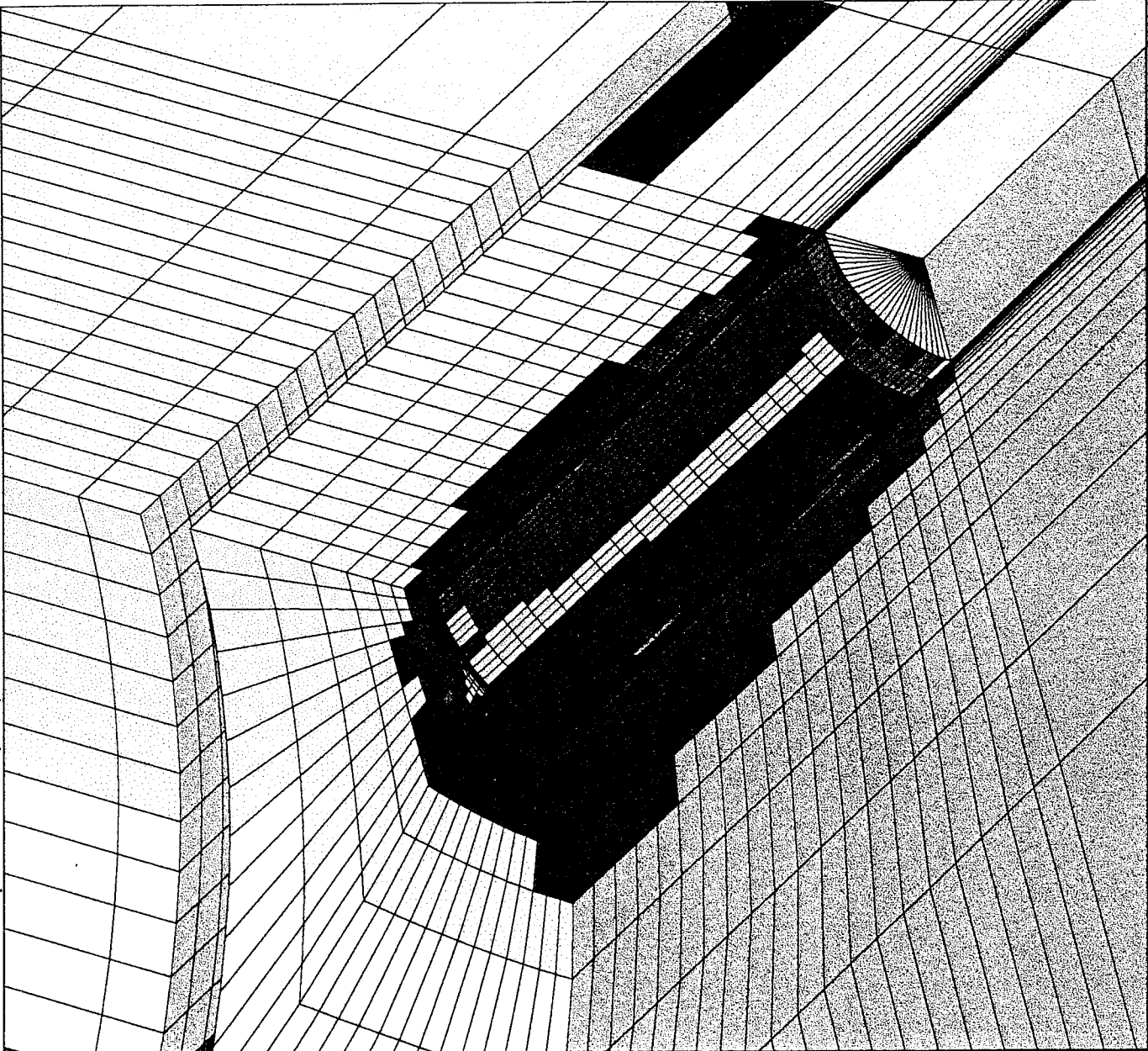
Axes

LineStyle

Block Plot of State

Consulting Engineers
Saario & Flekkola Ltd.

Job Title: 60 MPa pressure in shales, M-C, c=40.5e6 Pa



Job Title: 30 MPa pressure in slates, MC, c=26.6e6 f=23.5

FLAC3D 1.00

Step 9826
Perspective

152245 Thu Dec 28 1995

Rotation

X: 38.26

Y: 12.70

Z: 54.42

Center:

X: 1749e+00

Y: 8888e-01

Z: 9921e-01

Eye Dist: 2986e+01

Size: (4.302e-01, 4.670e-01)

Block Plot of State

None

shear-n shear-p

shear-p

shear-p tension-p

tension-n tension-p

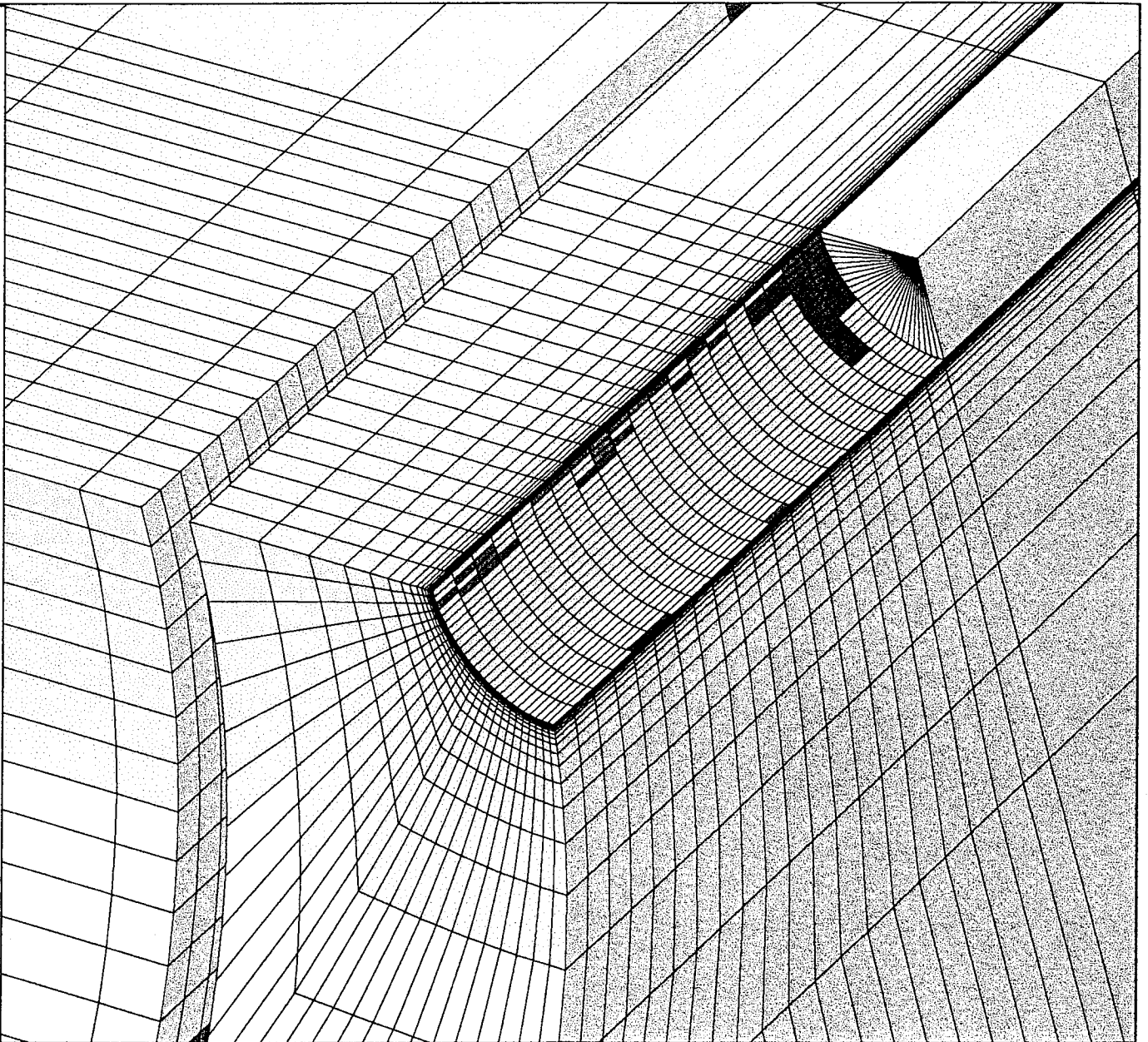
tension-p

Axes

LineStyle

Block Plot of State

Consulting Engineers
Saario & Pekkola Ltd.



Job Title: 40 MPa pressure in sbles, M-C, c-26.666 f-23.5

FLAC3D 1.00

Step 12600 Perspective

15:23:47 Thu Dec 28 1995

Rotation:

X: 38.26

Y: 12.70

Z: 54.42

Center:

X: 1749e+00

Y: 8.866e-01

Z: 9.921e-01

Eye Dist: 2.986e+01

Size: (4.302e-01, 4.670e-01)

Block Plot of State

None

shear-n shear-p

shear-p

shear-p tension-p

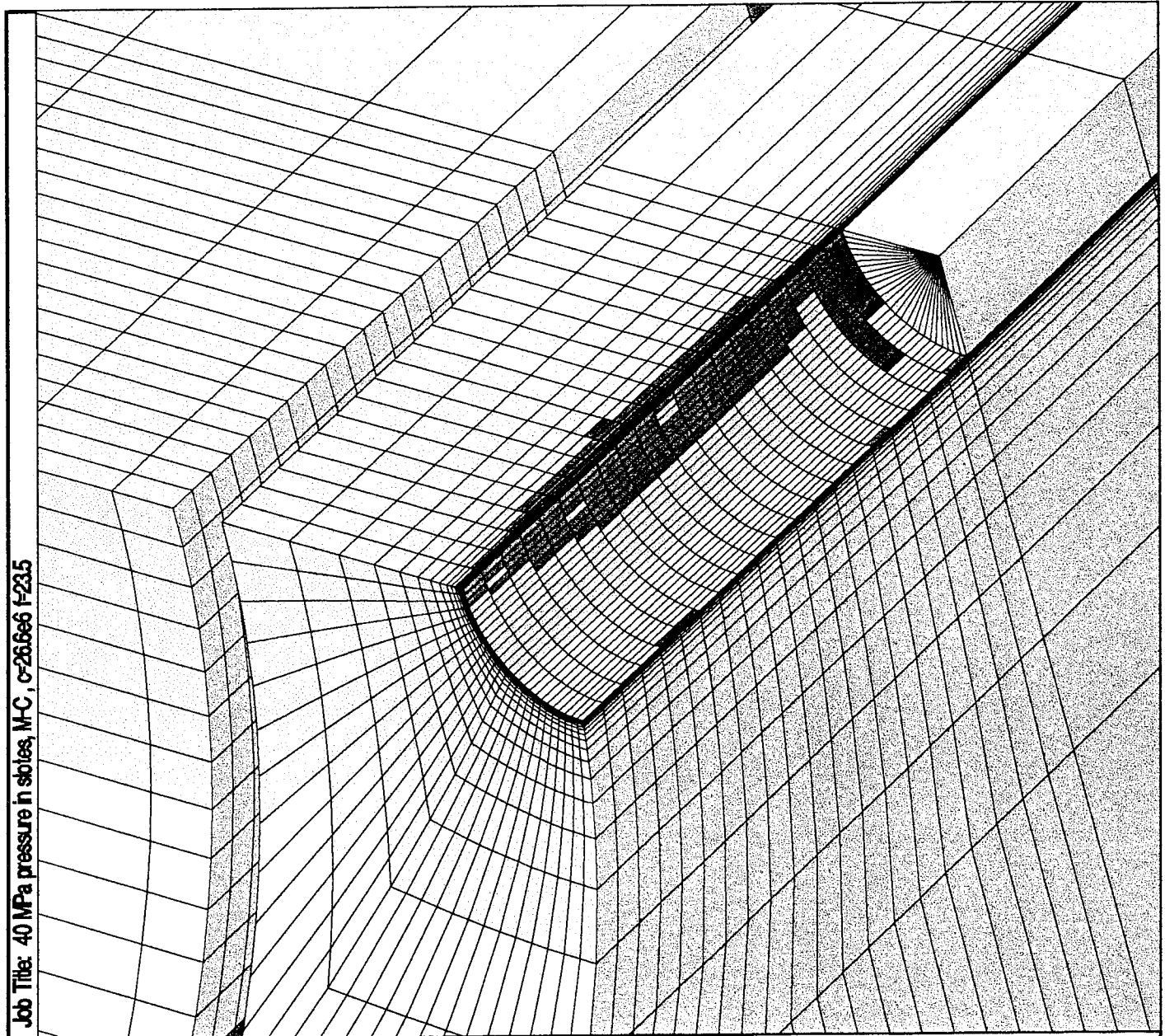
tension-n tension-p

tension-p

AXES

Lifestyle

Block Plot of State



Consulting Engineers
Saario & Flekkola Ltd.

Job Title: 50 MPa pressure in slots, M-C, c=26.6e6 f=23.5

FLAC3D 1.00

Step 15395 Perspective

1524:51 Thu Dec 28 1995

Rotation:

X: 38.26

Y: 12.70

Z: 54.42

Center:

X: 1749e+00

Y: 8.866e-01

Z: 9.927e-01

Eye Dist: 2.986e+01

Size: (4.302e-01, 4.670e-01)

Block Plot of State

None

shear-n shear-p

shear-p

shear-p tension-p

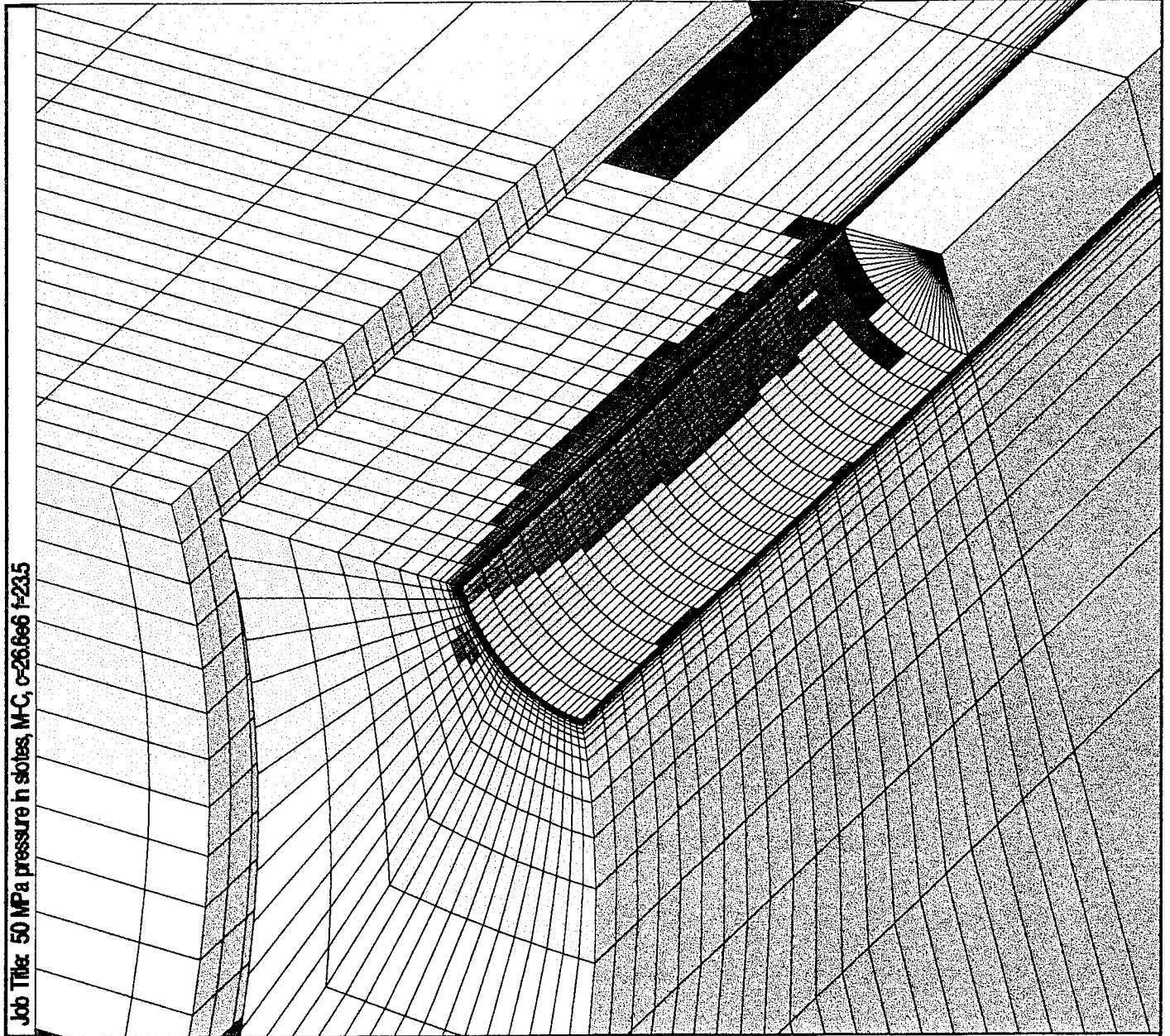
tension-n tension-p

tension-p

AXES

Linestyle

Block Plot of State



Consulting Engineers
Saario & Flekkola Ltd.

Job Title: 60 MPa pressure in slots, M-C, c=26.6e6 f=23.5

FLAC3D 1.00

Step 18501 Perspective

15:25:59 Thu Dec 28 1995

Rotation:

X: 38.26

Y: 12.70

Z: 54.42

Center:

X: 1.749e+00

Y: 8.866e-01

Z: 9.921e-01

Eye Dist: 2.986e+01

Size: (4.302e-01, 4.670e-01)

Block Plot of State

None

shear-n shear-p

shear-p

shear-p tension-p

tension-n shear-p tension-p

tension-n tension-p

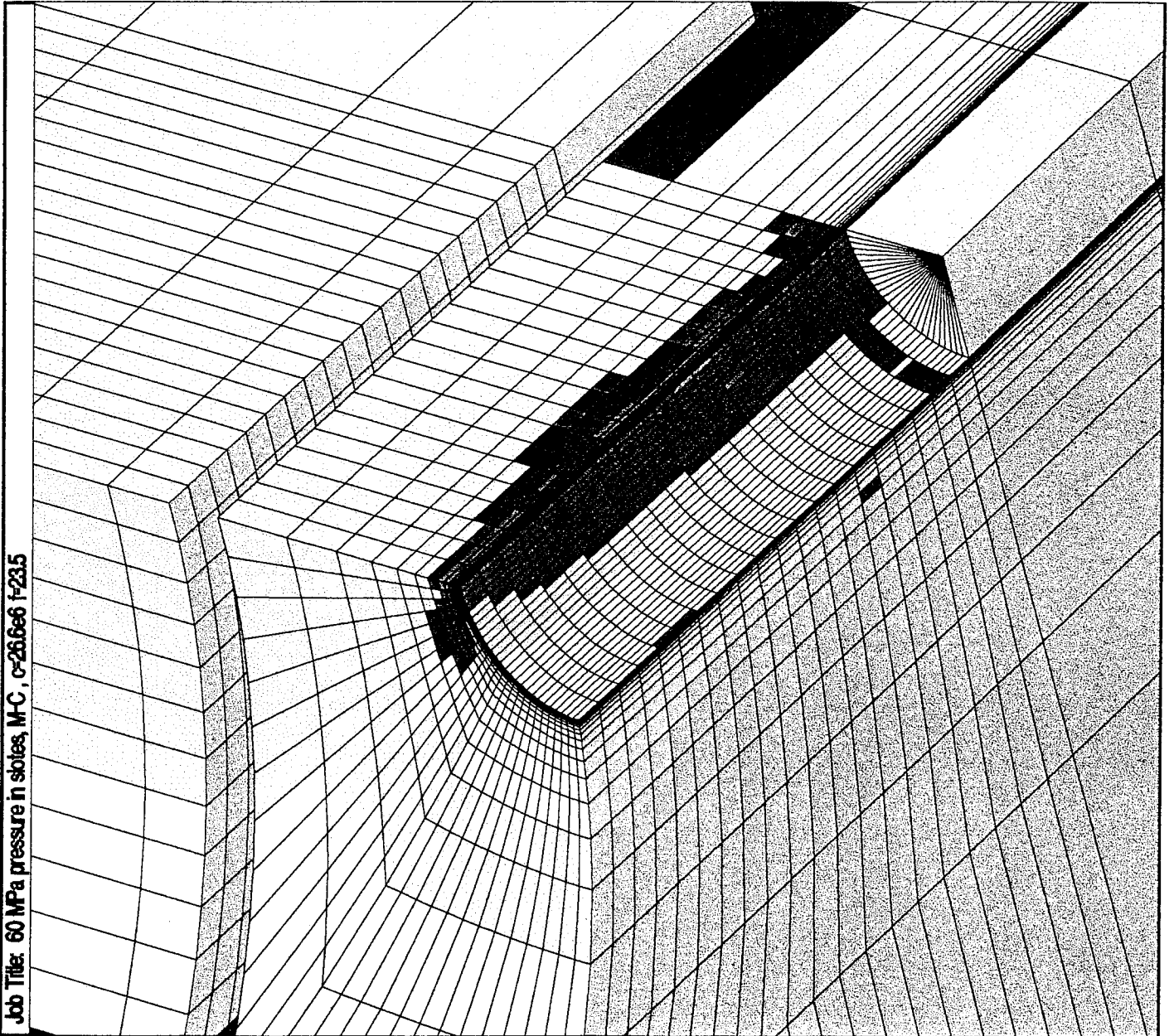
tension-p

Axes

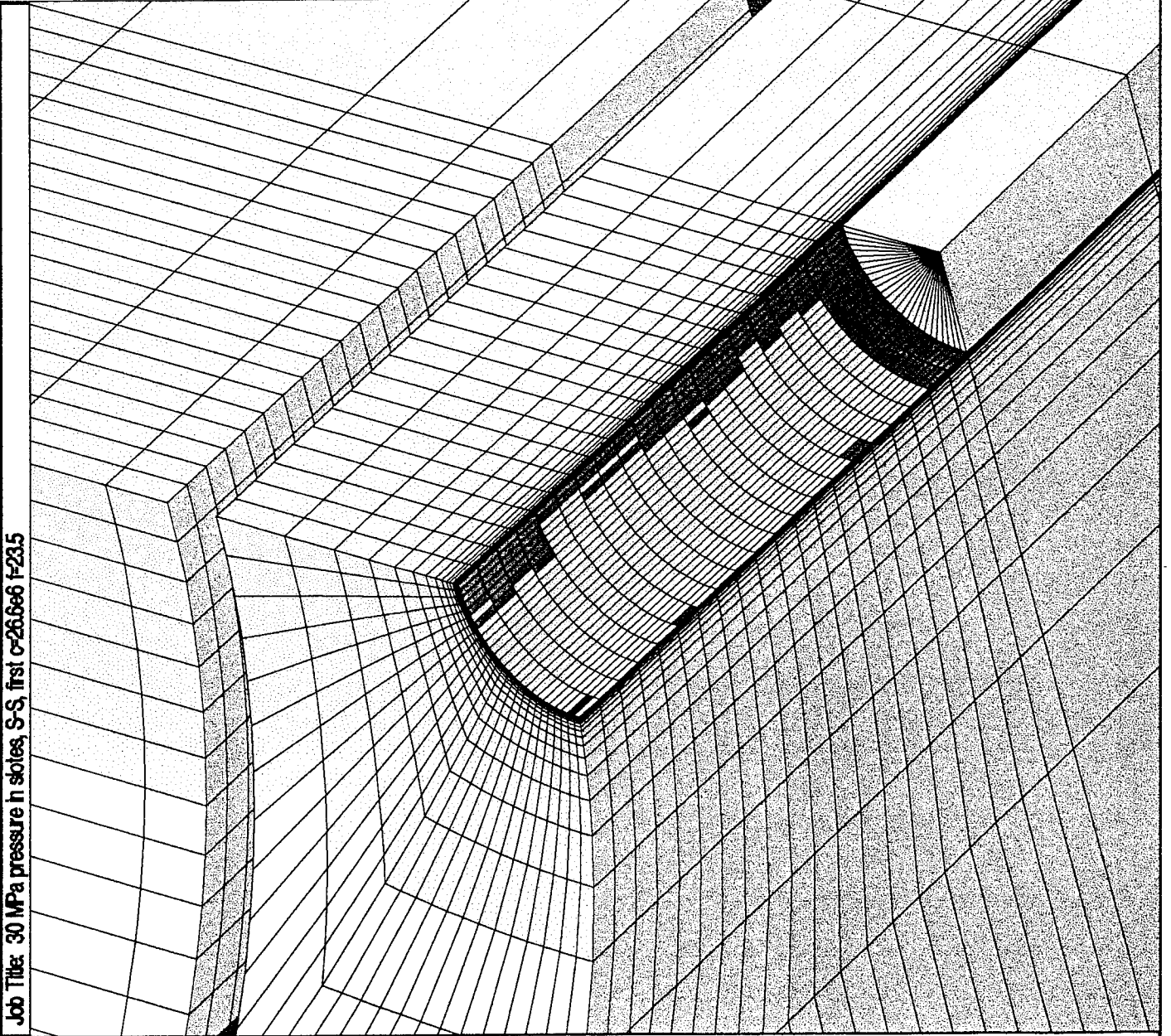
LineStyle

Block Plot of State

Consulting Engineers
Saarto & Flekkola Ltd



Job Title: 30 MPa pressure in slots, S-S, first c=26.6e6 f=23.5



FLAC3D 1.00

Step 10085 Perspective

152327 Thu Dec 28 1995

Rotation:

X: 38.26

Y: 12.70

Z: 54.42

Center:

X: 1749e+00

Y: 8.868e-01

Z: 9.921e-01

Eye Dist: 2.986e+01

Size: (4.302e-01, 4.670e-01)

Block Plot of State

None

shear-n shear-p

shear-p

shear-p tension-p

tension-n tension-p

tension-p



















AXES

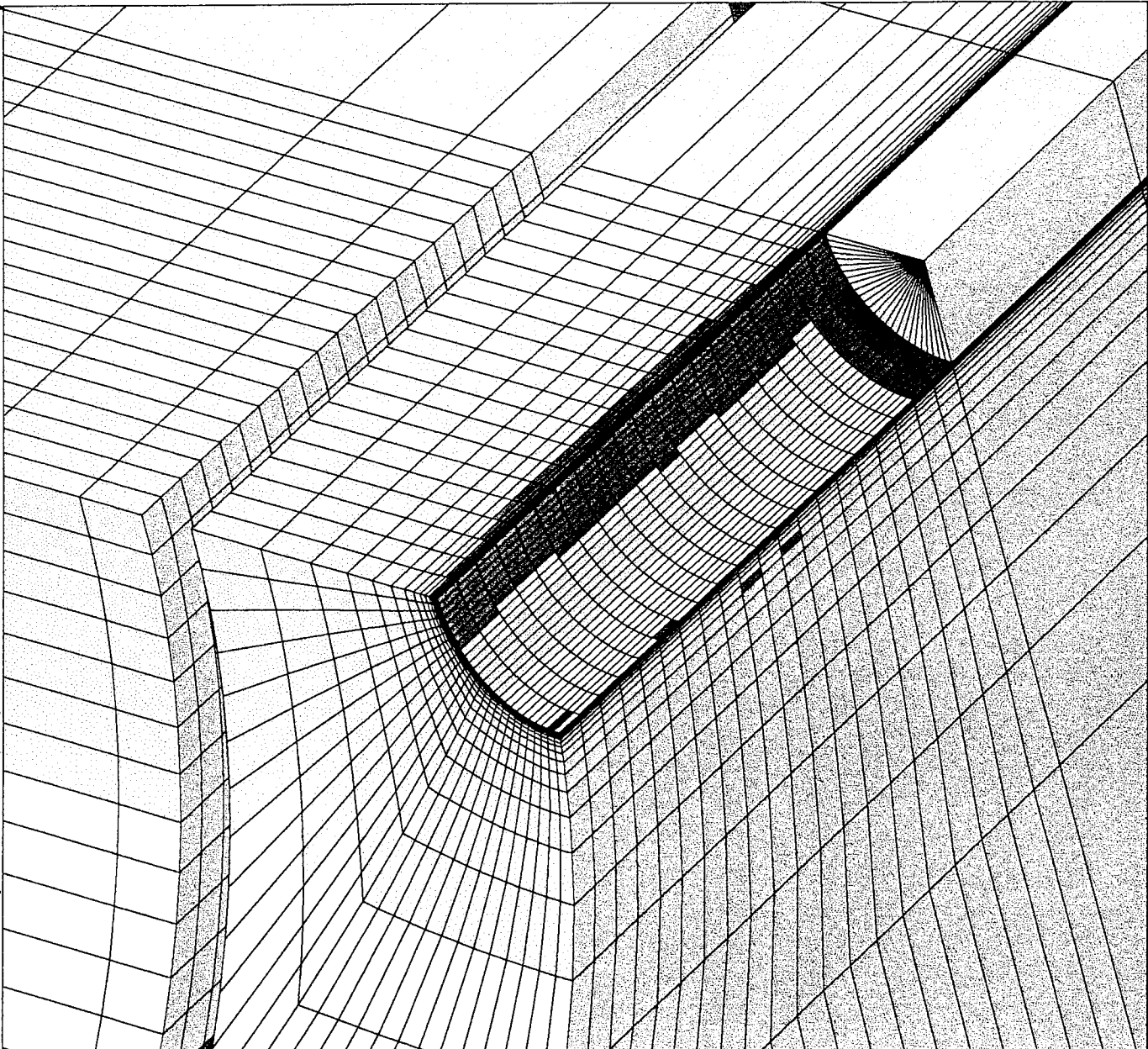
Linestyle

Block Plot of State

Consulting Engineers
Saario & Piekola Ltd.

Job Title: 40 MPa pressure in slots, S-S, first c=26.6e6 f=23.5

<p>FLAC3D 1.00</p> <p>Step 12700 Perspective 15:24:30 Thu Dec 28 1995</p>	<p>Rotation: X: 38.26 Y: 12.70 Z: 54.42</p> <p>Center: X: 1749e+00 Y: 8.866e-01 Z: 9.921e-01</p> <p>Eye Dist: 2.986e+01 Size: (4.302e-01, 4.670e-01)</p>	<p>Block Plot of State</p> <table border="0"> <tr> <td></td> <td>None</td> </tr> <tr> <td></td> <td>shear-n shear-p</td> </tr> <tr> <td></td> <td>shear-p</td> </tr> <tr> <td></td> <td>shear-p tension-p</td> </tr> <tr> <td></td> <td>tension-n tension-p</td> </tr> <tr> <td></td> <td>tension-p</td> </tr> </table> <p>AXES Lifestyle</p>		None		shear-n shear-p		shear-p		shear-p tension-p		tension-n tension-p		tension-p	<p>Block Plot of State</p> <p>Consulting Engineers Saario & Pekkola Ltd.</p>
	None														
	shear-n shear-p														
	shear-p														
	shear-p tension-p														
	tension-n tension-p														
	tension-p														



Job Title: 50 MPa pressure in slates, S-S, first c=26.6e6 f=23.5

FLAC3D 1.00

Perspective

Step 15611
152536 Thu Dec 28 1995

Rotator:

X: 38.26

Y: 12.70

Z: 54.42

Center:

X: 1749e+00

Y: 8.668e-01

Z: 9.921e-01

Eye Dist: 2.986e+01

Size: (4.302e-01, 4.670e-01)

Block Plot of State

None

shear-n shear-p

shear-p

shear-p tension-p

tension-n tension-p

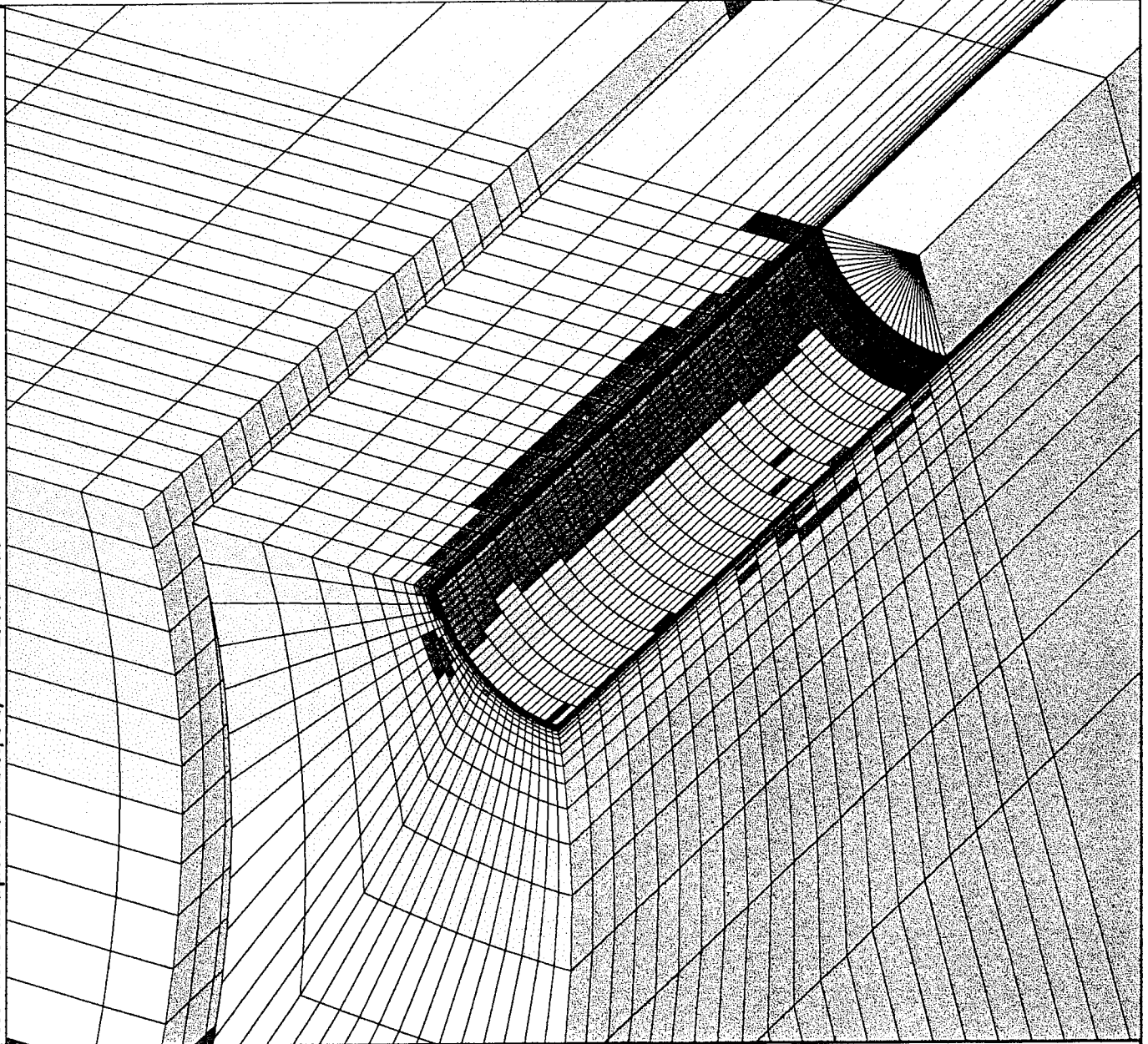
tension-p

AXES

Linestyle

Block Plot of State

Consulting Engineers
Saario & Fiekkola Ltd.



Job Title: 60 MPa pressure in slots, S-S, first c-26.6e6 f-23.5

FLAC3D 1.00

Step 18871 Perspective

15:26:45 Thu Dec 28 1995

Rotation:

X: 38.26

Y: 12.70

Z: 54.42

Center:

X: 1749e+00

Y: 8.868e-01

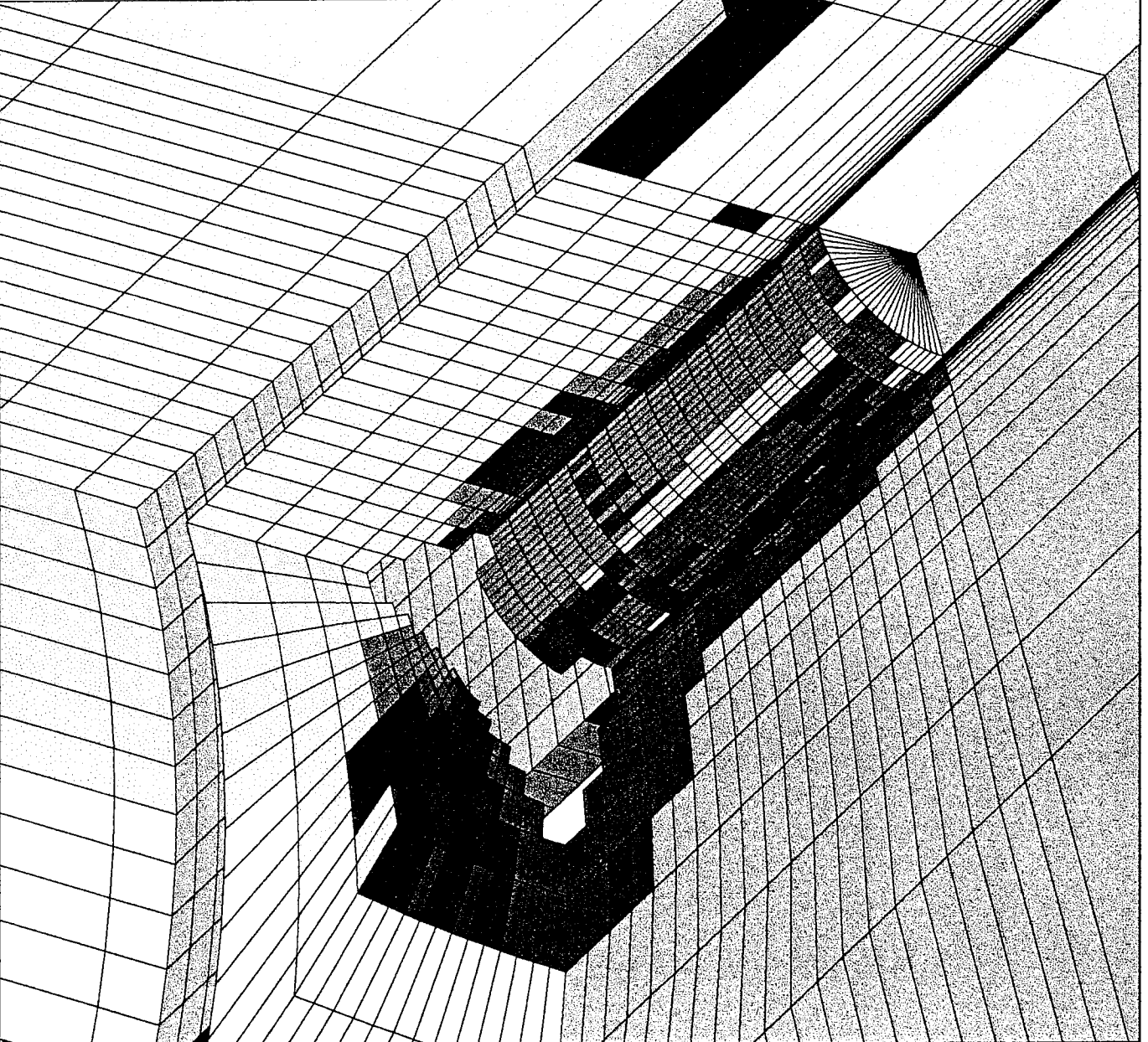
Z: 9.921e-01

Eye Dist: 2.986e+01

Size: (4.302e-01, 4.670e-01)

Block Plot of State

Consulting Engineers
Saario & Piekola Ltd.



Job Title: Displacement, elastic, E = 58.3 GPa v=0.25, stress 2.56/1.21/1 MPa

FLAC3D 1.00

Step 4373 Perspective
 16:06:07 Thu Apr 18 1996

Rotation:

X: 0.00
 Y: 0.00
 Z: 90.00

Center:

X: 1.481e+00
 Y: 5.112e-02
 Z: 4.268e-02

Eye Dist: 3.113e+01

Size: (6.728e-02, 7.304e-02)

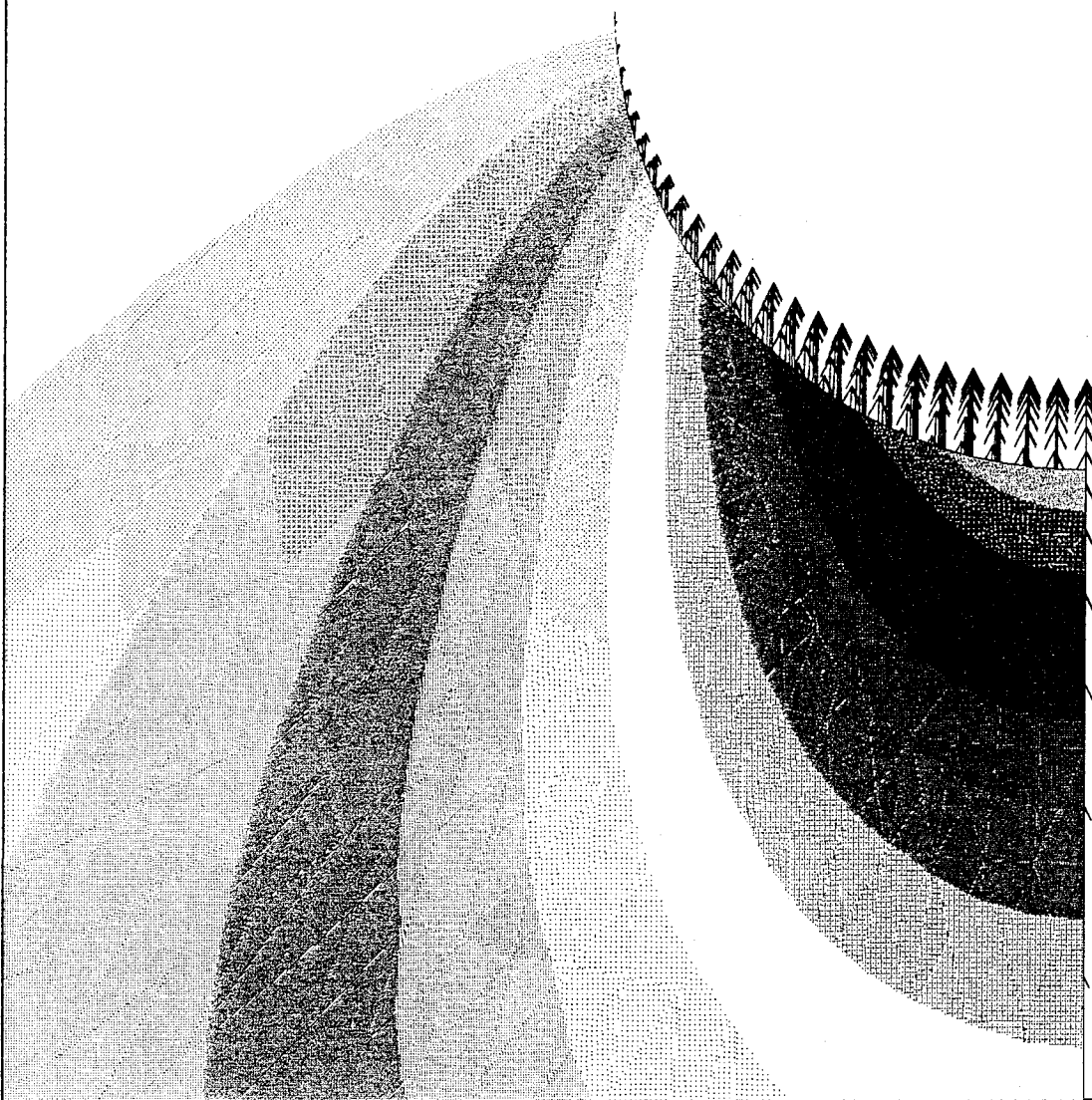
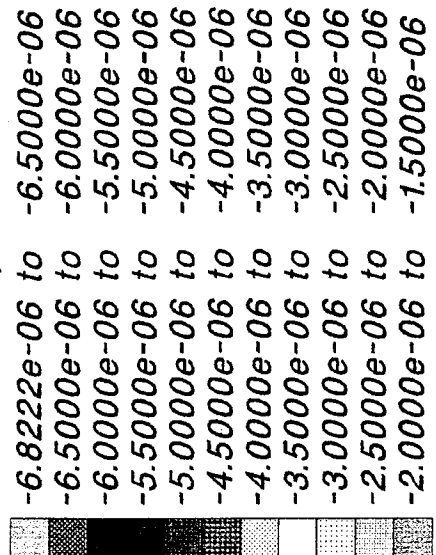
Sketch

Displacement

Maximum = 7.048e-06

LineStyle _____

Contour of Y-Displacement (m)



Job Title: Displacements, elastic, E = 58.3 GPa v=0.25, stress 5.12/2.42/1 MPa

FLAC3D 1.00

Step 5581 Perspective
 16:03:57 Thu Apr 18 1996

Rotation:

X: 0.00
 Y: 0.00
 Z: 90.00

Center:

X: 1.481e+00
 Y: 5.112e-02
 Z: 4.268e-02
 Eye Dist: 3.113e+01
 Size: (6.728e-02, 7.304e-02)

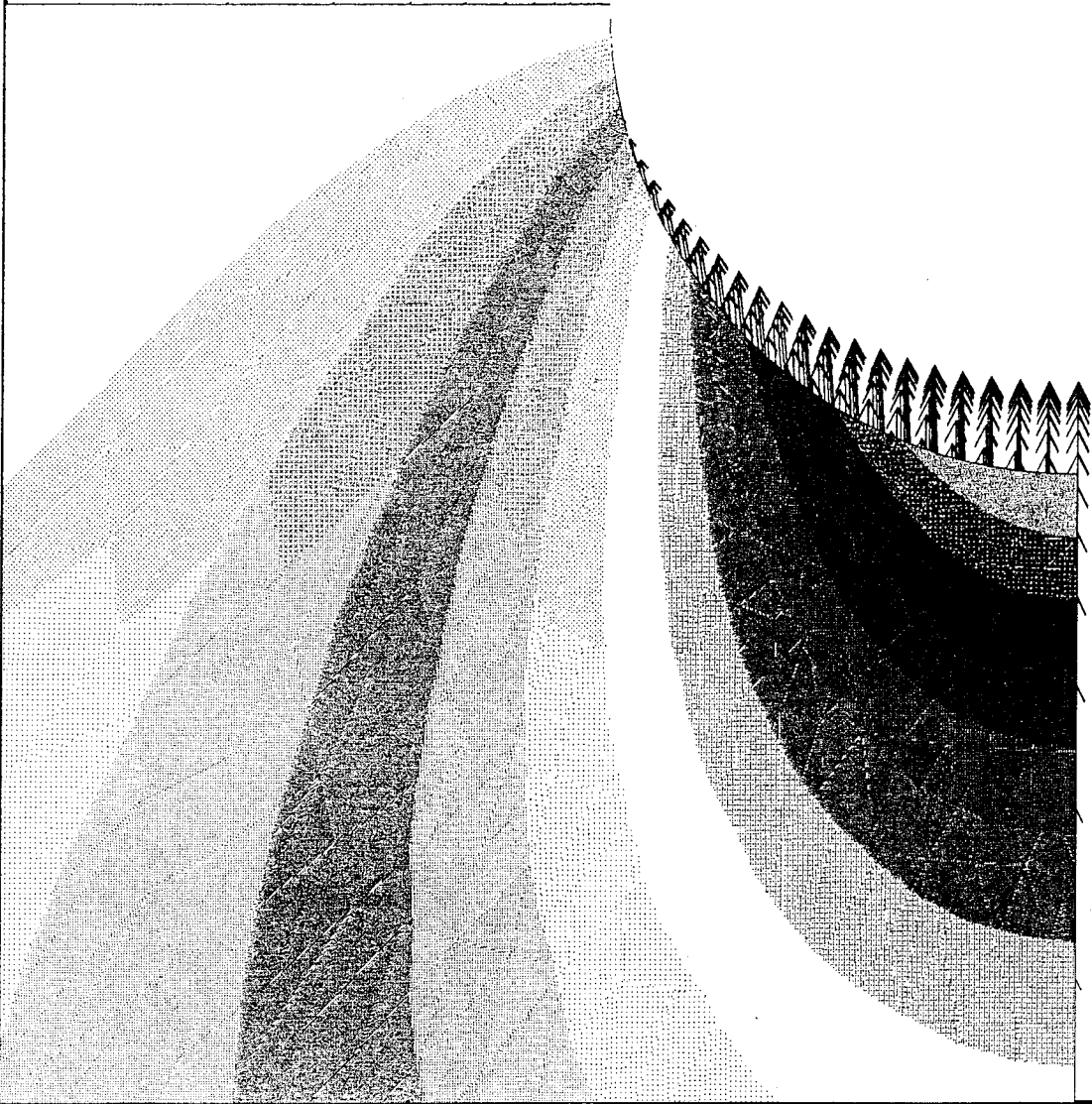
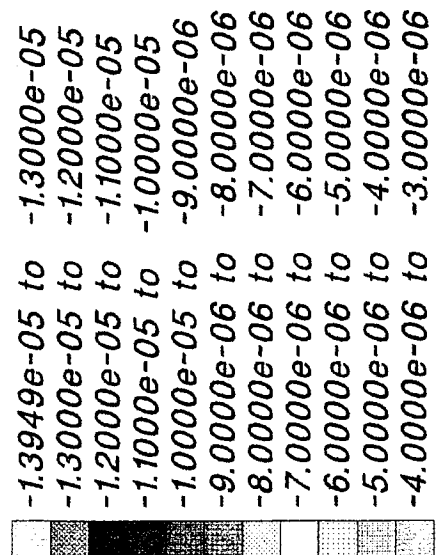
Sketch

Displacement

Maximum = 1.416e-05

Linestyle _____

Contour of Y-Displacement (m)



Job Title: Displacement, elastic, E = 58.3 GPa v=0.25, stress 10.24/4.84/1 MPa

FLAC3D 1.00

Step 7129 Perspective
 16:05:26 Thu Apr 18 1996

Rotation:

X: 0.00

Y: 0.00

Z: 90.00

Center:

X: 1.481e+00

Y: 5.112e-02

Z: 4.268e-02

Eye Dist: 3.113e+01

Size: (6.728e-02, 7.304e-02)

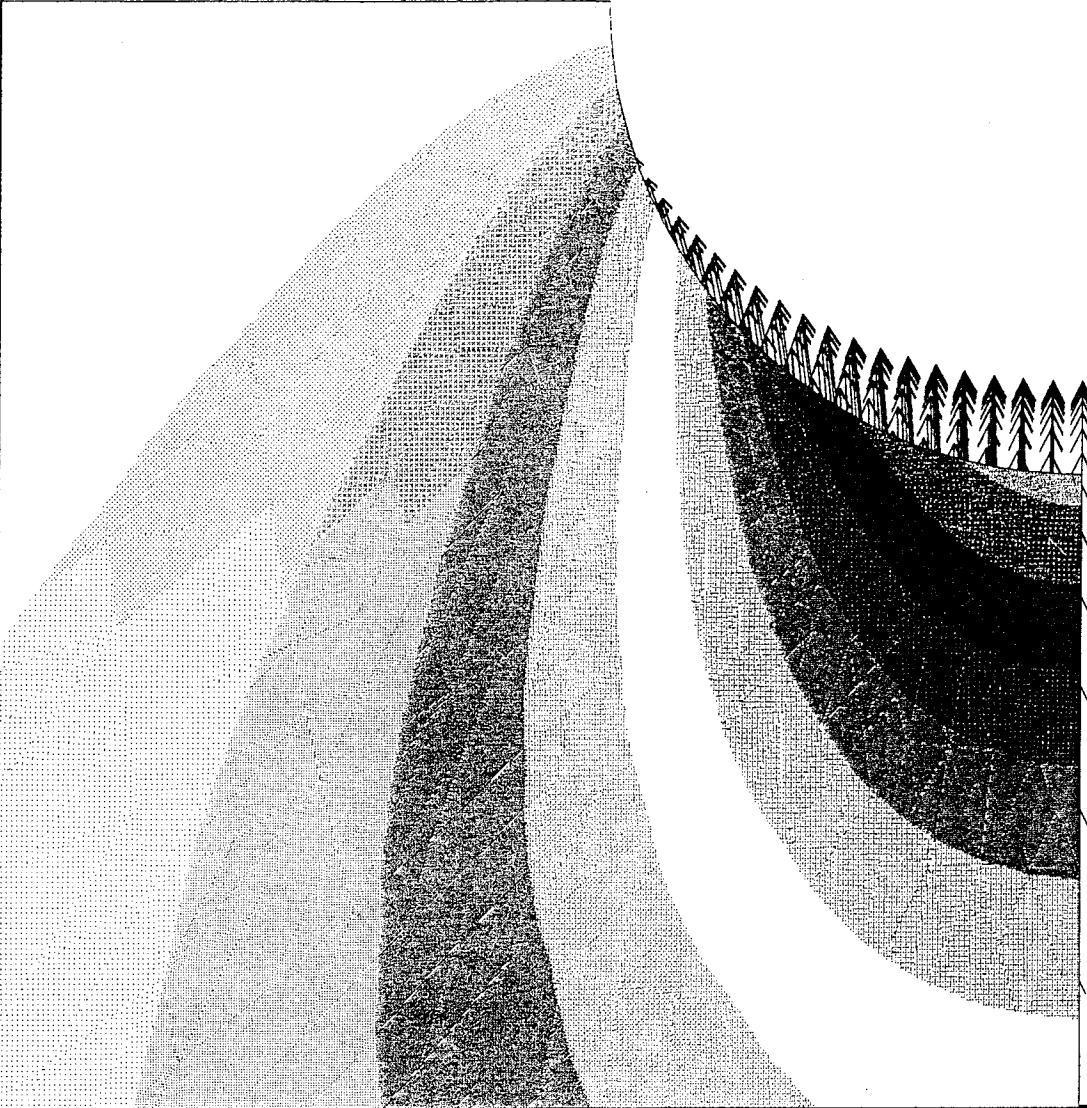
Sketch

Displacement

Maximum = 2.874e-05

LineStyle

Contour of Y-Displacement (m)	
-2.8395e-05 to -2.7500e-05	-2.7500e-05 to -2.5000e-05
-2.5000e-05 to -2.2500e-05	-2.2500e-05 to -2.0000e-05
-2.0000e-05 to -1.7500e-05	-1.7500e-05 to -1.5000e-05
-1.5000e-05 to -1.2500e-05	-1.2500e-05 to -1.0000e-05
-1.0000e-05 to -7.5000e-06	-7.5000e-06 to -5.0000e-06
-5.0000e-06 to -2.5000e-06	



Job Title: Displacements, elastic, E = 58.3 GPa v=0.25, stress 5.12/2.42/1 MPa

FLAC3D 1.00

Step 5581 Perspective
 16:04:21 Thu Apr 18 1996

Rotation:

X: 38.26

Y: 12.70

Z: 54.42

Center:

X: 1.749e+00

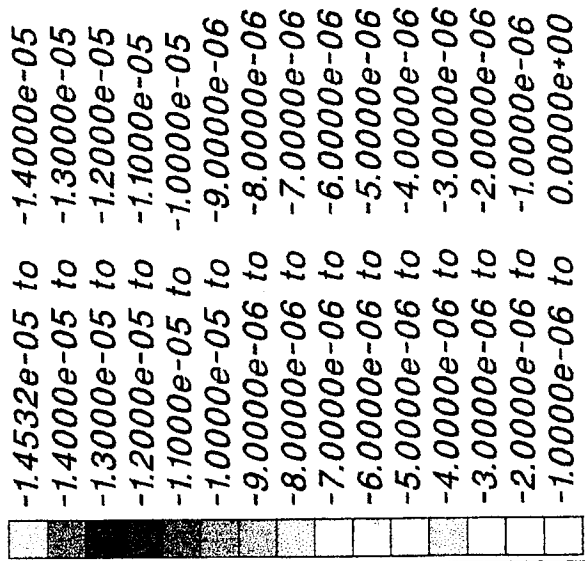
Y: 8.866e-01

Z: 9.921e-01

Eye Dist: 2.986e+01

Size: (2.671e-01, 2.900e-01)

Contour of Y-Displacement (m)



Interval = 1.0e-06

